Electronic and spatial characteristics of the retinylidene chromophore in rhodopsin

Verhoeven, M.A.

Electronic and Spatial Characteristics of the Retinylidene Chromophore of Rhodopsin

PROEFSCHRIFT

ter verkrijging van
de graad van Doctor aan de Universiteit Leiden,
op gezag van de Rector Magnificus Dr. D.D. Breimer,
hoogleraar in de faculteit der Wiskunde en
Natuurwetenschappen en die der Geneeskunde,
volgens besluit van het College voor Promoties
te verdedigen op dinsdag 15 november 2005
klokke 14.15 uur

door

Michiel Adriaan VERHOEVEN

geboren te Malden
in 1972

Promotiecommissie

Promotores:	Prof. dr. H.J.M. de Groot
	Prof. dr. W.J. de Grip
Referent:	Prof. dr. J. Reedijk
Overige leden:	Prof. dr. L.W. Jenneskens
	Prof. dr. A.P. IJzerman
	Prof. dr. H.S. Overkleeft
	Prof. dr. J. Brouwer

Table of contents

Chapter 1

General Introduction

1.1 Introduction

Rhodopsin is the protein in the retina of vertebrates responsible for dim light or black and white vision. The protein functions as a light-driven molecular switch that initiates a cascade of biochemical reactions, ultimately leading to a nerve pulse to the brain. Approximately seventy years ago George Wald discovered that retinas from frog eyes bleached from purple to orange releasing a compound resembling vitamin A.[1] To explain the chemistry of vision, he proposed a cycle in which the vitamin A derivative binds to a protein in the dark and was released in contact with light. In 1952 Wald and his co-workers demonstrated that it is in fact 11-Z retinal that binds to opsin, the apoprotein of rhodopsin.[2] At the end of the 1960s it was established that light isomerises 11-Z retinal that is bound to the protein and is released as all-E retinal.[3] A wealth of information is available on the biological, chemical, physical aspects that are related to the processes of vision. In this chapter the details of the machinery of the process of vision are introduced, going from the level of the molecular switch to its function at the macroscopic level in the eye. In addition, the ultrafast and efficient isomerisation properties of the retinylidene chromophore are discussed, followed by the scope and outline of this thesis.

1.2 Rhodopsin

Rhodopsin is a 40 kDa integral membrane protein that consists of 348 amino acid residues. Recently, the X-ray structure of rhodopsin was published.[4] A schematic representation of this structure is depicted in Figure 1.1. Like many proteins in the class of G-protein coupled receptors (GPCRs), it has 7-transmembrane α-helices. An eighth helix is found parallel to the membrane at the intradiscal interface of the membrane.[4] For its function the rhodopsin protein relies on the co-factor retinal (vitamin-A aldehyde) that is covalently bound to the ε–amino group of lysine residue 296 *via* a protonated Schiff base (PSB) linkage.[5,6] In the dark the retinylidene chromophore has the 11-Z configuration and the ligand serves as an inverse agonist that efficiently stabilises the protein in the inactive form. This produces an extremely efficient suppression of G-protein activation. Upon capture of a photon the *cis* C11=C12 bond of the retinylidene chromophore isomerises to a *trans* configuration leading to the transformation of rhodopsin to the photoproduct Bathorhodopsin (Figure 1.2).

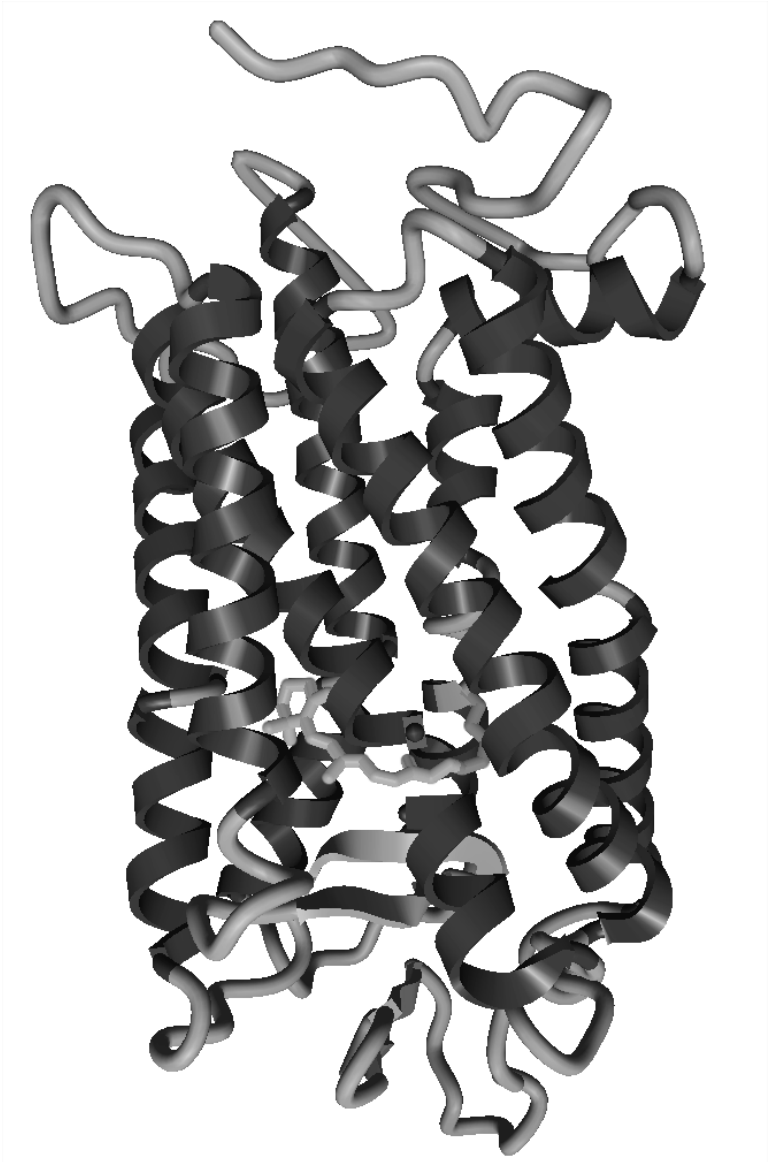

Figure 1.1 Schematic representation of the crystal structure of rhodopsin. The protein backbone and the retinylidene ligand are shown. Residue Phe115 is omitted to show the chromophore attached to the ε-NH_2 of Lys296.

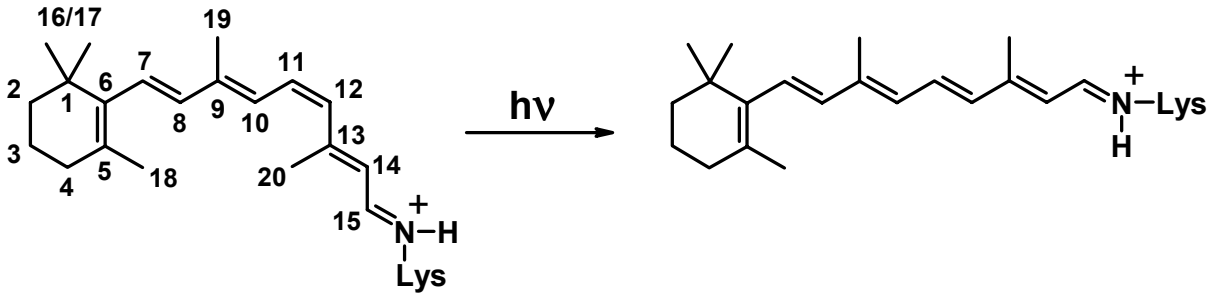

Figure 1.2 The photochemistry of rhodopsin involves the isomerisation of the 11-Z retinylidene chromophore to all-E. The numbering of the ligand follows the IUPAC numbering scheme for retinal.

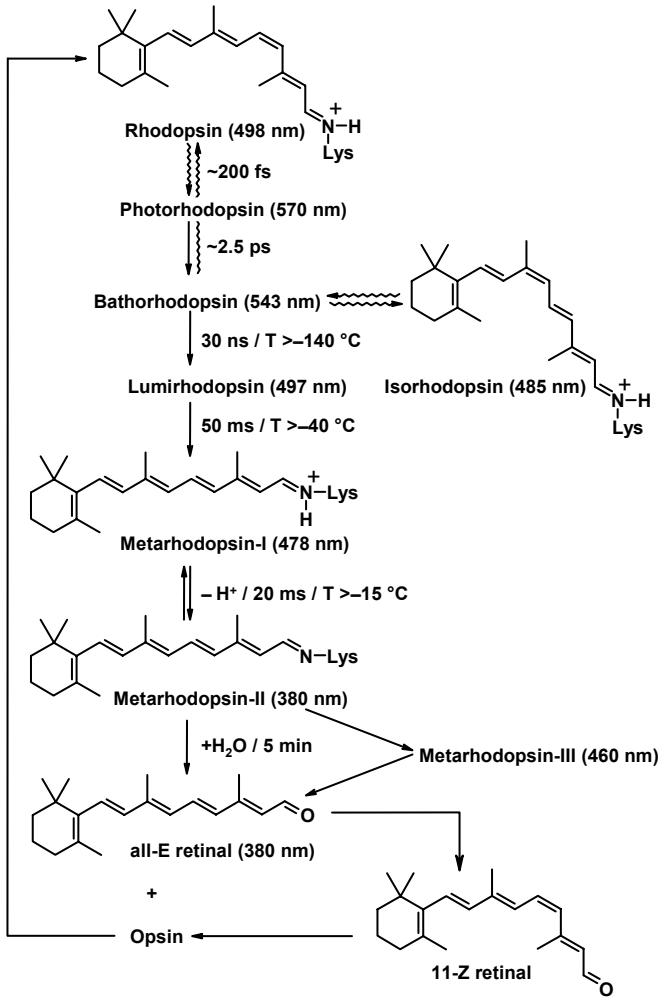

Figure 1.3 Schematic representation of the photosequence of rhodopsin

The photosequence of rhodopsin including its intermediates is depicted in Figure 1.3, which emphasises the configurations and protonation-states of the retinylidene ligand during the various steps.[7] The trapping temperatures and wavelengths of maximum absorption of the intermediates are also given in Figure 1.3. Bathorhodopsin (Batho) is the first true, thermally equilibrated photoproduct. There is evidence that the formation of the primary isomerisation product Photorhodopsin is finished within 200 fs, leading to a hot (T>500 K) and strongly distorted all-E retinylidene moiety that is cooling down to Batho in ~2.5 ps.[8,9] Under illumination conditions the formation of Batho is reversible, it can reverse to rhodopsin or it can go to isorhodopsin with the retinylidene ligand in the 9-Z configuration.[10] Experimental evidence was obtained that the first photoproduct Batho has a strongly distorted all-E configuration of the retinylidene chromophore in the binding pocket.[10-12] Thermal relaxation of Batho *via* several intermediates results in Metarhodopsin-II (Meta-II), the signalling state of the protein. These thermal steps are called the dark reactions.

First, Lumirhodopsin is formed followed by Metarhodopsin-I and Meta-II. In the transition of Metarhodopsin-I to Meta-II the PSB is deprotonated. Hydrolysis of the Schiff base in Meta-II results in diffusion of all-E retinal from the binding pocket. All-E retinal is enzymatically converted back to 11-Z retinal that can bind again to the apoprotein opsin.

1.3 THE STRUCTURE OF THE VERTEBRATE EYE, RODS AND CONES

At the cellular level, two compartments can be distinguished in the photoreceptor cell: the outer and inner segment separated by the cilium. All organelles essential for cell proliferation are located in the inner compartment. The outer compartment is filled with hundreds of tightly stacked membraneous discs consisting of phospholipid bilayers in which rhodopsin and other proteins are incorporated. The outer membrane of the cell contains the machinery to depolarise the membrane to generate the nerve pulse upon activation of the receptor.

The retina of humans contains two types of photoreceptor cells: rods and cones, which are functional in dim light and bright light, respectively.[13-15] The red, green or blue sensitive cones facilitate the perception of colours and are concentrated in a relatively small area around the fovea. Rods are located mainly outside the fovea and give black and white images. This thesis will focus on rhodopsin, the pigment that is found in the rod cells. Figure 1.4 is a schematic cross-section of the retina. Apart from the rods and cones a variety of nerve cells is shown.

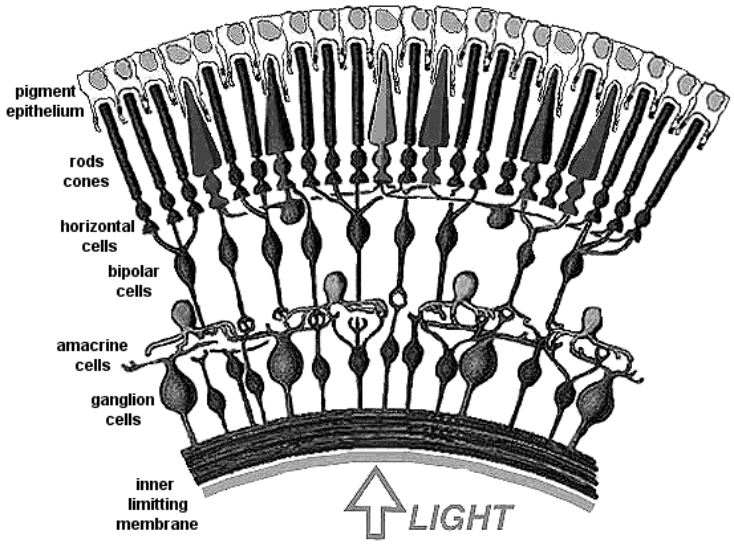

Figure 1.4 Schematic representation of a cross section of the retina

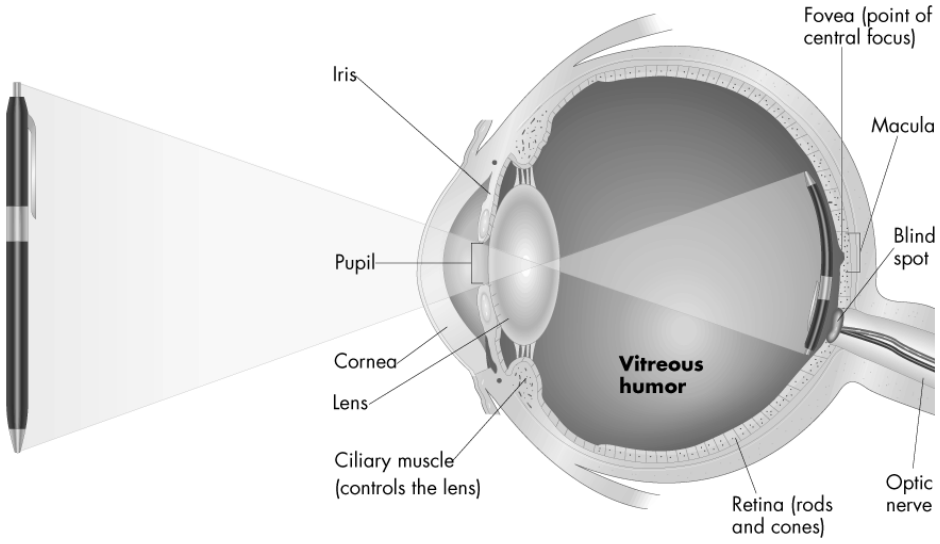

Figure 1.5 Schematic representation of a sagittal cross-section of a human eye.

An ingenious scheme of interconnections of the photoreceptor cells with nerve cells makes it possible to transmit the proper information to the brain under a wide range of light intensities. The spatial arrangement of the different cells in the retina is remarkable (Figure 1.4 and 1.5). The photoreceptor cells are located closest to the back wall of the eye. Each receptor cell is connected to nerve cells that are directed towards the inside of the eye with respect to the receptor cells. All the nerve axons and the vasculature that transports nutrients to the cells come together and leave the eye at the blind spot.

In Figure 1.5 it is shown that light entering the eye passes the cornea, the aqueous humour and the iris/pupil and is focussed on the retina by the cornea and the lens to produce an image. The retina extends over more than half the sphere of the back wall of the eye. About 3 million colour sensitive cone cells are concentrated in the small area of the fovea. The remainder of the fovea is populated with about 100 million rod cells.

1.4 G-PROTEIN COUPLED RECEPTORS

Rhodopsin is a member of the class of guanine nucleotide binding protein (G-protein) coupled receptors (GPCRs). This receptor family is a very important class of proteins in living organisms since virtually all proteins involved in processes that involve signal transduction and regulation are included in this class.[16,17] Around 40% of the current prescription drugs intervene in pathways that involve G-protein coupled receptors.[18,19] Rhodopsin is an important representative of this class of receptor molecules, since it can be harvested in a straightforward

procedure from cattle eyes that are abundantly available. In addition, its affector molecule is covalently bound, which greatly facilitates studying the protein. Rhodopsin is therefore generally considered to be a model and paradigm for the GPCR receptors class.

The signalling pathway of GPCRs involves a cascade of biochemical reactions mediated by a G-protein. The function of the G-protein cascade is to regulate and amplify the biochemical signal generated by the GPCR. For the rhodopsin the G-protein transducin forms the biochemical link between the receptor protein and the signal transduction pathway. The receptor protein rhodopsin proceeds to the active Meta-II-state upon photon absorption. The G-protein transducin has a molecule of GDP bound to its α-subunit in the quiescent state. Meta-II binds transducin, and G_α is enabled to release the bound GDP. This step initiates the biochemical cascade that leads to the nerve pulse.[20]

Provided that GTP is present in the cytoplasm, a molecule of GTP binds to the vacant nucleotide-binding site, creating the activated transducin species G•GTP (Figure 1.6). The two protein molecules then separate, with Meta-II unaltered; by analogy with other cascades, the G-protein is thought to split, with the α-subunit G_α•GTP as the active species. Upon contact G_α•GTP relieves the inhibitory influence of a phosphodiesterase (PDE) subunit. The activated PDE subsequently reduces the concentration of cGMP in the cytoplasm by catalytic hydrolyses, which causes closure of cGMP-gated channels in the plasma membrane.[21] Since Meta-II can activate ~500 transducin molecules and the hydrolysis of cGMP by PDE is catalytic the information of one single photon can be amplified to a nerve pulse.

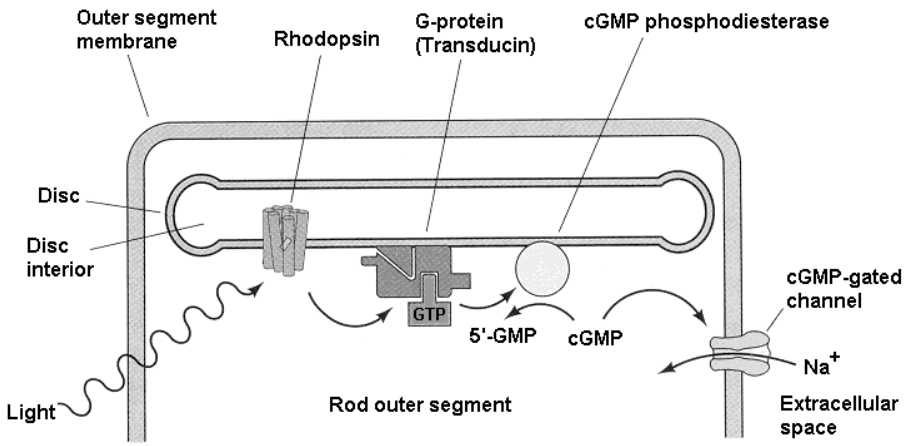

Figure 1.6 Schematic diagram of activation in the G-protein cascade of phototransduction in the vertebrate rod photoreceptor.

1.5 THE RATE AND EFFICIENCY OF THE PHOTOREACTION OF RHODOPSIN

Ultrafast transient absorption spectroscopy has shown that the primary event in the photochemical formation of Batho is finished in less than 200 fs and that the quantum yield is Φ=0.67. This makes the reaction the fastest and one of the most efficient chemical processes known in nature. An additional feature of the protein is that it stores more than 60% of the photon energy.[22-24] One of the specific aims of this thesis is to study the structural aspects underlying the rate and efficiency of this photochemical reaction.

The two elements that are considered here to describe the mechanism behind the rate and efficiency of the fast and efficient isomerisation of the retinylidene chromophore in rhodopsin are: (i) The structure of the chromophore in the ground-state, including inter- and intramolecular repulsion of functional groups and torsional angles in the central part of the polyene and (ii) The electronic configuration of the polyene in the ground state. A number of physical chemical techniques have been employed in the past to study both of these aspects.[25,26]

One of the most fascinating results obtained in recent years is the determination of the 2.8 Å X-ray structure of rhodopsin.[4] This structural model showed for the first time the precise arrangement of the helices relative to each other and to the membrane surface. This paves the way for studying the protein conformational changes during activation and resolving mechanisms that are general for all members of the GPCR class. Although recently the accuracy of the structural model was improved to 2.6Å,[27] it does not yet allow determination of essential details that describe the role of the retinylidene ligand during photoactivation at a submolecular level. For instance, intimate details like the 6-s-*cis* conformation of the β-ionone ring in the ground-state of the protein remain unresolved.[28,29] Also the dynamics involved in the photoisomerisation in rhodopsin are difficult to study with crystallographic methods.[30] One of the great merits of the structural model of rhodopsin that is obtained by crystallography is that it indicates 'hotspots' within the protein that are potentially important for the functioning of the GPCR receptors in general. Subsequently other techniques that have higher local resolution can zoom into these areas with a high selectivity to unravel functional details at the atomic level. For example, it has been demonstrated that solid-state NMR in combination with site-specific labelling with NMR sensitive nuclei (*e.g.* ^{13}C, ^{15}N) reveals structural details at a resolution of 0.15Å well beyond the capabilities of X-ray.[31]

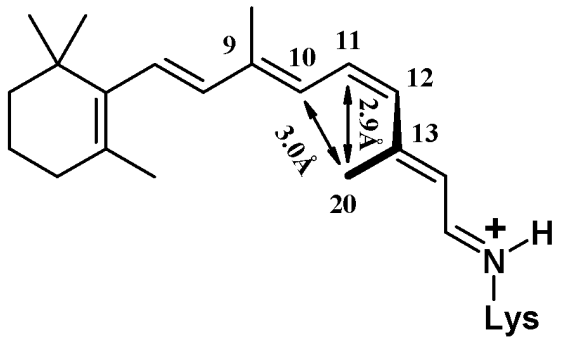

Torsional angles

C9=C10–C11=C12	+169°
C10–C11=C12–C13	–17°
C11=C12–C13=C20	–20°

Figure 1.7 Structure of the retinylidene ligand as determined by solid-state NMR 1-D Rotational Resonance. The distance constraints have been included in DFT calculations and resulted in an accurate determination of the torsional angles as indicated.

The NMR was used to determine that the torsions in the retinylidene polyene around the isomerisation region (C10••C13) add up to approximately 45º (Figure 1.7).[31-33] In addition, a HCCH torsion angle of 160°±10° was measured, corroborating the result from the distance measurement.[34]

Other examples are the NMR experiments on rhodopsin incorporated with [8,18-$^{13}C_2$]- and [8,16/17-$^{13}C_2$]-retinal with only one ^{13}C label at either of the chemically equivalent positions 16 and 17.[28,35-37] In these experiments it was shown that the ring part of the retinylidene has indeed a twisted 6-s-*cis* orientation, while the two methyl groups C16 and C17 have their own specific chemical environment in the active side of the protein. This shows that the protein locks the ionone ring with one methyl group in the equatorial position and one in the axial position without the possibility for ring flips.[28,35] In addition, evidence was presented that during the formation of the Metarhodopsin-I intermediate the ring increases its hydrophobic contacts with the binding pocket. It can be inferred that the ring part is involved in the receptor activation process by increasing the contact with helix 5 and 6, thereby triggering movement of the helices with respect to each other. This kind of specific structural detail can emerge only by the combination of techniques with high local resolution in combination with the X-ray structural model.

Other techniques with a high local resolution that are used to study the interaction of the protein-ligand interaction in the field of rhodopsin are Resonance Raman (RR) and Fourier Transform InfraRed (FTIR) difference spectroscopy. FTIR probes the vibrational ground state of the different intermediates of the chromophore, protein and lipids, whereas RR is based on

enhancing vibrations via excitation of electronic transitions. Often FTIR and RR spectroscopy spectra of photointermediates are compared with data collected from the native rhodopsin. In this way the interactions that are important for the understanding of the mechanism of isomerisation of the ligand are revealed.

RR vibrational spectroscopy has revealed that the chromophore of rhodopsin combines three striking features: an enhanced Hydrogen-Out-Of-Plane (HOOP) vibration of the C12H element, enhanced torsional vibrations of the C11=C12 motif, and a C10••C13 skeletal torsion.[10,38] The more intense the RR vibration appears in the spectrum, the larger the displacement and reorganisation energy along the corresponding degree of freedom in the excited-state. Recent DFT calculations indicate that the specific frequency and intensity of C11H and C12H HOOPs can be generated in a structural model of Batho.[12] This has been done by constraining torsions of 40° in both C11=C12 and C12–C13 bonds of an all-E PSB structure and calculating the Raman spectrum of the energy optimised structure. Also the simulation of the isomerisation of the retinylidene chromophore in its binding pocket in a hybrid quantum mechanical / molecular mechanical (QM/MM) molecular dynamics calculation suggest a formal all-E structure that is highly distorted.[39] Therefore it is suggested that the isomerisation of the initial C11=C12 *cis* double bond in rhodopsin takes place mainly by rotation of the C12H element, yielding a distorted formal *trans* bond in a binding pocket that is the same as for the *cis* structure of the ground-state. Additional evidence for this isomerisation model was obtained from a rhodopsin analogue with a 11,19-ethano retinylidene ligand with the C9=C10–C11 element in the isomerisation region locked in the ground-state conformation.[40,41] This element can not participate in the isomerisation, while the photointermediate kinetics are essentially identical to native rhodopsin. Hence, this result confirms that only a rotation of the C12H element can produce an ultrafast photoisomerisation.[26,42]

By combining the data of Resonance Raman (RR), solid-state NMR (SSNMR) and femtosecond resolved transient absorption spectroscopy it was shown that there is a relation between the rate of the isomerisation reaction and the ground-state structure.[31,43,44] For instance, time-resolved spectra of the formation of the first intermediate in 13-desmethyl rhodopsin have shown that removal of the methyl group reduces the rate and efficiency of the photoreaction compared to the native system.[44] The associated decrease of the strong C12H and C11=C12 vibrations in the RR spectra for this 13-desmethyl system suggest that the reduction of the rate and efficiency is due to the small torsional angles in the isomerisation region.[44]

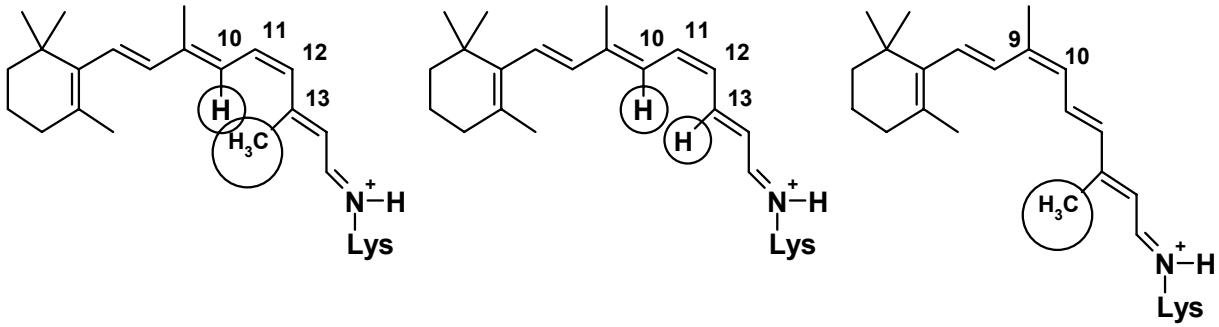

Figure 1.8 Schematic representation of the intramolecular steric interactions for native rhodopsin (left), 13-desmethyl rhodopsin (middle) and isorhodopsin (right).

Concomitantly, the reduced torsions appear to be the result of the absence of the intramolecular steric repulsion between the 13-methyl group and the hydrogen on C10 (Figure 1.8). Likewise, for isorhodopsin, with the retinylidene ligand in a 9-Z configuration, the absence of intramolecular steric interaction of the ligand is associated with a slower photochemistry of ~600 fs and a lower quantum yield of Φ=0.27 compared to rhodopsin (Figure 1.8).[44]

It is clear that the introduction or removal of methyl groups in the isomerisation region has a distinct effect on the rate and efficiency of the reaction. Introduction of a bulky methyl group at the 10-position of the rhodopsin ligand, in close spatial proximity to the 13-methyl group, results in a quantum yield of Φ=0.55, while shifting the repulsive interaction of the 13-methyl group from the 13- to the 10-position by the reconstitution of opsin with 10-methyl 13-desmethyl retinal decreases the photoefficiency of the rhodopsin analogue to Φ=0.33.[44] Hence a simple rule for the efficiency transpires: Presence of the 13-methyl group increases the quantum efficiency with 0.20, whereas presence of the 10-methyl group reduces the efficiency with 0.12. Hence an important route to understanding the mechanisms behind the fast photoreaction is studying the relation between rate, efficiency and chromophore structure of rhodopsins incorporated with retinal isomers with additional methyl substituents in the isomerisation region of the carbon frame.

NMR can also probe the electronic structure of atoms in a molecule. For instance, probing the electron density around the nuclei in the retinylidene system in rhodopsin can be done directly by determining the chemical shift of atoms using a ^{13}C labelled chromophore. This is important since the electronic structure of the polyene mediates fast switching of the retinylidene moiety from the antagonist to the agonist-form in rhodopsin. *In silico* molecular dynamics studies on a relevant retinylidene Schiff base model have shown that a conjugation defect with polaronic properties is present in the polyene of the chromophore close to the

C11=C12 double bond that isomerises after absorption of a photon.[11,33] When light excites the retinylidene chromophore an electron is promoted to the LUMO. The positive charge is repositioned at the other extreme of the polyene, towards the ionone ring, and the resonance structure of this excited-state has swapped single and double bonds. [45,46] The polyene can move away from the Frank-Condon region and adapt to this 'reversed' electron configuration by letting in the excited state the positive charge hop back to the Schiff base end of the polyene via the odd-numbered carbon atoms. As a consequence the single bonds will contract and the double bonds will extend allowing the isomerisation to take place in the transition back to the ground state. At this moment a discussion is still ongoing about the exact role of the protein pocket and specific polar amino acid residues and their interaction with the positive charge on the retinylidene chromophore.[12] It is unclear whether the protein pocket merely provides a soft counterion for the PSB that mediates fast isomerisation or that a specific switching mechanism is in place that facilitates the stabilisation of the Meta-II-state after light activation of the protein.[47,48]

1.6 Aim and scope of this thesis

The aim of this thesis is to investigate and discuss the spatial and electronic requirements for the fast and efficient photoisomerisation reaction of the retinylidene chromophore of rhodopsin. The remarkable outcome of previous work on the 10-methyl and 10-methyl-13-desmethyl rhodopsin analogues underlines the relevance of studying the behaviour of pigment analogues with additional methyl groups in the isomerisation region of the retinylidene chromophore.[32,49] Incorporation of the 11-Z and 9-Z isomers of 11-methyl, 11-methyl-13-desmehtyl and 12-methyl retinal in opsin and studying the biochemical and biophysical properties of the resulting pigment analogues are among the specific aims of this thesis. In Chapter 2 the synthesis of the required 11-methyl and 11-methyl-13-desmethyl retinal is investigated and the specific reactivity of a Wittig reagent precursor is explored leading to the implementation of a novel synthetic scheme.

In Chapter 3, the electronic properties of the ground-state conformation of the retinylidene ligand are studied by recording the solid-state NMR spectra of rhodopsin incorporated with 11-Z-[7,8,9,10,11,12,13,14,15,19,20]-$^{13}C_{10}$-retinal. Evidence is obtained that interaction between the PSB and its glutamate counterion is weak compared to a tightly bound ion pair in a model retinylidene Schiff base. This indicates that the interaction between the ligand and the protein induces a specific electron configuration that prepares the retinylidene for

fast isomerisation. The data confirm that a charge defect is present in the polyene that can help to promote extremely fast isomerisation of the ligand in the rhodopsin system.

In Chapter 4 the incorporation, photoisomerisation and activation properties of the 11-methyl, 12-methyl and 11-methyl-13-desmethyl derivatives incorporated in rhodopsin are studied and discussed. The rhodopsin analogues and photointermediates are characterised and studied by UV/Vis and FTIR spectroscopy and a G-protein activation assay. Results show that the additional methyl groups have differential effects on the primary photoreaction and the activation of rhodopsin. It appears that although 12-methyl rhodopsin has an photoisomeriation efficiency that approaches rhodopsin, all the modified ligands show delayed formation of the photointermediates.

In Chapter 5 the most important results and conclusions are evaluated and put in perspective of recent results and interpretations of data in the field of rhodopsin and finally an outlook to the future is presented

REFERENCES

(1) Wald, G. *Nature* **1934**, *134*, 65.
(2) Hubbard, R.; Wald, G. *J. Gen. Physiol.* **1952**, *36*, 269-315.
(3) Wald, G. *Nature* **1968**, *219*, 800-807.
(4) Palczewski, K.; Kumasaka, T.; Hori, T.; Behnke, C. A.; Motoshima, H.; Fox, B. A.; Le Trong, I.; Teller, D. C.; Okada, T.; Stenkamp, R. E.; Yamamoto, M.; Miyano, M. *Science* **2000**, *289*, 739-745.
(5) Bownds, D. *Nature* **1967**, *216*, 1178-1181.
(6) Hargrave, P. A.; Bownds, D.; Wang, J. K.; McDowell, J. *Methods in Enzymology* **1982**, *81*, 211-214.
(7) Shichida, Y.; Tachibanaki, S.; Mizukami, T.; Imai, H.; Terakita, A. *Methods in Enzymology* **2000**, *315*, 347-363.
(8) Kim, J. E.; Mathies, R. A. *J. Phys. Chem. A* **2002**, *106*, 8508-8515.
(9) Kim, J. E.; McCamant, D. W.; Zhu, L. Y.; Mathies, R. A. *J. Phys. Chem. B* **2001**, *105*, 1240-1249.
(10) Palings, I.; Van den Berg, E. M. M.; Lugtenburg, J.; Mathies, R. A. *Biochemistry* **1989**, *28*, 1498-1507.
(11) Buda, F.; De Groot, H. J. M.; Bifone, A. *Phys. Rev. Lett.* **1996**, *77*, 4474-4477.
(12) Yan, E. C. Y.; Ganim, Z.; Kazmi, M. A.; Chang, B. S. W.; Sakmar, T. P.; Mathies, R. A. *Biochemistry* **2004**, *43*, 10867-10876.
(13) Oprian, D. D.; Asenjo, A. B.; Lee, N.; Pelletier, S. L. *Biochemistry* **1991**, *30*, 11367-11372.
(14) Kalat, J. W. In *Biological Psychology 6th edition*; Brooks / Cole Publishing Company: California, 1998, p 147-149.
(15) Lythgoe, J. N. In *Handbook of Sensory Physiology*; Dartnall, H. J., Ed.; Spinger Verlag: New York, 1972.
(16) Spiegel, A. M.; Weinstein, L. S. *Annu. Rev. Med.* **2004**, *55*, 27-39.
(17) Lefkowitz, R. J. *Nat. Cell Biol.* **2000**, *2*, E133-E136.
(18) Marchese, A.; George, S. R.; Kolakowski, L. F.; Lynch, K. R.; O'Dowd, B. F. *Trends Pharmacol. Sci.* **1999**, *20*, 370-375.

(19) Milligan, G.; Rees, S. *Trends Pharmacol. Sci.* **1999**, *20*, 252-252.
(20) Okada, T.; Ernst, O. P.; Palczewski, K.; Hofmann, K. P. *Trends Biochem.Sci.* **2001**, *26*, 318-324.
(21) Lamb, T. D. *Proc. Natl. Acad. Sci. U. S. A.* **1996**, *93*, 566-570.
(22) Bifone, A.; De Groot, H. J. M.; Buda, F. *J. Phys. Chem. B* **1997**, *101*, 2954-2958.
(23) Cooper, A. *FEBS Lett.* **1981**, *123*, 324-326.
(24) Honig, B.; Ebrey, T.; Callender, R. H.; Dinur, U.; Ottolenghi, M. *Proc. Natl. Acad. Sci. U. S. A.* **1979**, *76*, 2503-2507.
(25) DeGrip, W. J.; Rothschild, K. J. In *Molecular Mechanisms in Visual Transduction*; Stavenga, D. G., DeGrip, W. J., Pugh Jr, E. N., Eds.; Elsevier Science: Amsterdam, 2000; Vol. 3, p 1-54.
(26) Mathies, R. A.; Lugtenburg, J. In *Handbook of Biological Physics, Volume 3*; Stavenga, D. G., DeGrip, W. J., Pugh, E. N., Eds.; Elsevier Science: Amsterdam, 2000, p 55-90.
(27) Okada, T.; Fujiyoshi, Y.; Silow, M.; Navarro, J.; Landau, E. M.; Shichida, Y. *Proc. Natl. Acad. Sci. U. S. A.* **2002**, *99*, 5982-5987.
(28) Spooner, P. J. R.; Sharples, J. M.; Verhoeven, M. A.; Lugtenburg, J.; Glaubitz, C.; Watts, A. *Biochemistry* **2002**, *41*, 7549-7555.
(29) Teller, D. C.; Okada, T.; Behnke, C. A.; Palczewski, K.; Stenkamp, R. E. *Biochemistry* **2001**, *40*, 7761-7772.
(30) Royant, A.; Edman, K.; Ursby, T.; Pebay-Peyroula, E.; Landau, E. M.; Neutze, R. *Nature* **2000**, *406*, 645-648.
(31) Verdegem, P. J. E.; Helmle, M.; Lugtenburg, J.; De Groot, H. J. M. *J. Am. Chem. Soc.* **1997**, *119*, 169-174.
(32) Verdegem, P. J. E.; Bovee-Geurts, P. H. M.; DeGrip, W. J.; Lugtenburg, J.; De Groot, H. J. M. *Biochemistry* **1999**, *38*, 11316-11324.
(33) Bifone, A.; De Groot, H. J. M.; Buda, F. *Pure Appl. Chem.* **1997**, *69*, 2105-2110.
(34) Feng, X.; Verdegem, P. J. E.; Eden, M.; Sandstrom, D.; Lee, Y. K.; Bovee-Geurts, P. H. M.; DeGrip, W. J.; Lugtenburg, J.; De Groot, H. J. M.; Levitt, M. H. *J. Biomol. NMR* **2000**, *16*, 1-8.
(35) Spooner, P. J. R.; Sharples, J. M.; Goodall, S. C.; Seedorf, H.; Verhoeven, M. A.; Lugtenburg, J.; Bovee-Geurts, P. H. M.; DeGrip, W. J.; Watts, A. *Biochemistry* **2003**, *42*, 13371-13378.
(36) Spooner, P. J. R.; Sharples, J. M.; Goodall, S. C.; Bovee-Geurts, P. H. M.; Verhoeven, M. A.; Lugtenburg, J.; Pistorius, A. M. A.; DeGrip, W. J.; Watts, A. *J. Mol. Biol.* **2004**, *343*, 719-730.
(37) Spooner, P. J. R.; Sharples, J. M.; Goodall, S. C.; Bovee-Geurts, P. H. M.; Verhoeven, M. A.; Lugtenburg, J.; Pistorius, A. M. A.; DeGrip, W. J.; Watts, A. *J. Mol. Biol.* **2005**, *345*, 1295-1295.
(38) Palings, I.; Pardoen, J. A.; Van den Berg, E. M. M.; Winkel, C.; Lugtenburg, J.; Mathies, R. A. *Biochemistry* **1987**, *26*, 2544-2556.
(39) Rohrig, U. F.; Guidoni, L.; Laio, A.; Frank, I.; Rothlisberger, U. *J. Am. Chem. Soc.* **2004**, *126*, 15328-15329.
(40) Asato, A. E.; Denny, M.; Liu, R. S. H. *J. Am. Chem. Soc.* **1986**, *108*, 5032-5033.
(41) Sheves, M.; Albeck, A.; Ottolenghi, M.; Bovee-Geurts, P. H. M.; DeGrip, W. J.; Einterz, C. M.; Lewis, J. W.; Schaechter, L. E.; Kliger, D. S. *J. Am. Chem. Soc.* **1986**, *108*, 6440-6441.
(42) Liu, R. S. H.; Hammond, G. S. *Proc. Natl. Acad. Sci. U. S. A.* **2000**, *97*, 11153-11158.
(43) Schoenlein, R. W.; Peteanu, L. A.; Mathies, R. A.; Shank, C. V. *Science* **1991**, *254*, 412-415.

(44) Kochendoerfer, G. G.; Verdegem, P. J. E.; Van der Hoef, I.; Lugtenburg, J.; Mathies, R. A. *Biochemistry* **1996**, *35*, 16230-16240.
(45) Salem, L. *Science* **1976**, *191*, 822-830.
(46) Michl, J.; Bonacic-Koutecký, V. *Electronic Aspects of Organic Photochemistry*; John Wiley: New York, 1990.
(47) Yan, E. C. Y.; Kazmi, M. A.; Ganim, Z.; Hou, J. M.; Pan, D. H.; Chang, B. S. W.; Sakmar, T. P.; Mathies, R. A. *Proc. Natl. Acad. Sci. U. S. A.* **2003**, *100*, 9262-9267.
(48) Yan, E. C. Y.; Kazmi, M. A.; De, S.; Chang, B. S. W.; Seibert, C.; Marin, E. P.; Mathies, R. A.; Sakmar, T. P. *Biochemistry* **2002**, *41*, 3620-3627.
(49) DeLange, F.; Bovee-Geurts, P. H. M.; Van Oostrum, J.; Portier, M. D.; Verdegem, P. J. E.; Lugtenburg, J.; DeGrip, W. J. *Biochemistry* **1998**, *37*, 1411-1420.

Chapter 2

Novel efficient synthesis routes to 11-methyl retinal isomers

2.1 Abstract

This chapter describes the synthesis of 11-methyl and 11-methyl-13-desmethyl retinal. Initial efforts to synthesise the compounds *via* olefination with a phosphonate reagent were hampered because a conjugate Horner-Wadsworth-Emmons reaction occurred leading to a cyclohexadiene product. Efforts to synthesise 11-methyl retinal using Wittig reagents also resulted in a cyclohexadiene product. Subsequent modifications of the reaction have led to simple and efficient routes to 11-Z and 9-Z isomers of 11-methyl retinal and its 13-desmethyl derivative. The modifications were based (i) on blocking the progress of the conjugate addition reaction by introducing a substitution at the γ-position with respect to the phosphorus atom and (ii) on temperature control by performing the reaction at kinetically controlled conditions.

2.2 Introduction

Rhodopsin is the G-protein coupled photoreceptor protein in the retina of vertebrates that initiates the visual transduction cascade in dim light vision.[1] Rhodopsin (Rho) contains a protonated 11-Z retinylidene Schiff's base in the active site of the receptor protein that functions as an inverse agonist. Upon light absorption the primary photoproduct Batho is formed in less than 200 fs with a strained protonated all-E retinylidene structure in the active site. *Via* thermal steps the signalling intermediate Meta-II is formed, which contains an all-E retinylidene structure in the active site that acts as a full agonist. Via studies on Rho analogues lacking the 9- or 13-methyl group (C19, C20) it has been established that the CH_3 groups have an important role in the various steps of the (photo)chemistry leading to the signalling state of the protein. For example, in the case of 9-desmethyl Rho, the formation of 9-desmethyl Meta-II following the photoreaction is inefficient.[2-4]

Recently, a study was started of the effect of an additional methyl group in the central part of the 11-Z retinylidene chromophore on the photochemistry and receptor action of Rho.[5-7] It has been found that 10-methyl Rho has a lower quantum yield (Φ=0.55) than the native system (Φ=0.67) and that thermal conversion of the first photoproduct Batho to the next intermediate occurs at a higher temperature than for Rho. A significant lower quantum yield of Φ=0.47 is observed when the 13-methyl group is absent and a further reduction to Φ=0.35 is observed for 10-methyl-13-desmethyl Rho. The 10- and 13-methyl groups apparently have opposite effects on the quantum yield, since the addition of a 10-methyl group decreases the quantum yield by 0.12, while removal of the 13-methyl group decreases the yield by 0.20. Also,

the 13-methyl group does not affect the decay of the Batho inthermediate. To further probe this contrasting behaviour we aimed at investigating the 11-methyl Rho analogues, which requires access to 11-Z 11-methyl retinal. In this Chapter several important steps for the synthesis of 11-Z 11-methyl retinal derivatives and the corresponding 9-Z isomers are explored and compared. Two possible routes to eliminate or reduce the formation of cyclohexadiene by-products that are formed in the reaction are implemented based on temperature control and a novel chemical procedure that specifically explores the chemical reactivity of the methyl-functionalised Wittig intermediate. Finally a novel scheme is used for synthesis of 10-methyl-13-desmethyl retinal.

2.3 RESULTS

To work out a synthetic scheme for the preparation of 11-methyl retinal, first some reactions with Horner-Wadsworth-Emmons (HWE) reagents have been re-examined. In line with previous work[8] the reaction of commercially available β-ionone (**5**) and 4-(diethyl phosphono)-3-methyl-2-butenenitrile (**6**)[9] does not lead to the 11-methyl retinal precursor 3,5-dimethyl-7-(2,6,6-trimethylcyclohexa-1-enyl)-hepta-2,4,6-trienenitrile. It gives the cyclo-hexadiene product 2-cyano-3,5,2',6'6'-pentamethyl bicyclohexyl-2,4,1'-triene (**3**). This 1,4 conjugated HWE product is formed by analogy with the 1,4 conjugated Wittig reaction described by Padwa *et al.*[10] (Scheme 2.1) This led to the exploration of alternative routes, using a more reactive aldehyde and a Wittig salt. The synthesis of 11-methyl retinal can be performed according to Scheme 2.2. Here, 2,4-dimethyl-5-cyano-penta-2,4-dienal (**7**) is prepared in two steps by olefination of 1,1-dimethoxy acetone (**8**) with 4-(diethyl phosphono)-3-methyl-2-butenenitrile and subsequent acidic deprotection of the acetal. The resulting aldehyde **7** is reacted with the ylide of β–ionyl phoshonium bromide (**9**)[11] in refluxing 1-butene oxide. After DIBAl-H reduction of the nitrile both the all-E and the 9-Z isomer of 11-methyl retinal (**1**), as well as 3-(3,5,2',6',6'-pentamethyl-bicyclohexyl-4,6,1'-triene-2-yl)but-2-enal, are obtained. The cyclohexadiene by-product is also an example of the 1,4 conjugate Wittig reaction.[10,12]

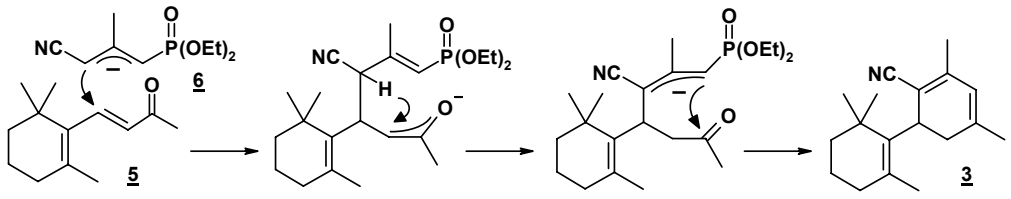

Scheme 2.1

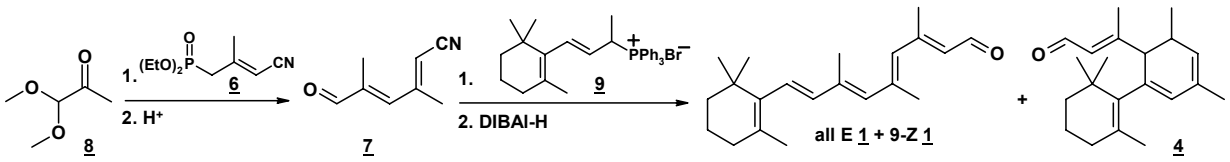

Scheme 2.2

Starting from the same reactants **7** and **9**, the reaction can be performed at –70 °C when propene oxide is used instead of 1-butene oxide, which freezes at –60 °C. In this way the reaction mixture contains <5% of the cyclohexadiene product (**4CN**), however, with only 33% yield of the nitrile (**1CN**) (Table 2.1). In a more convenient procedure the ylide is preformed with LDA in THF. After addition of the aldehyde at –70 °C the reaction mixture is warmed up gradually. With this procedure the yield of the nitrile (**1CN**) is 78% and no cyclohexadiene is formed. The procedure with LDA was also performed at high temperature, adding the aldehyde to the ylide in refluxing THF. Table 1 summarises the yield and product ratio of **1CN** and **4CN** after Wittig reaction between **7** and **9** under different temperature and salt conditions.

For the preparation of 11-Z 11-methyl retinal the reactions depicted in Scheme 2.3 were optimised. β–ionylidene acetaldehyde (**10**), which is readily accessible in high yield starting from commercially available β–ionone (**5**),[13] is treated with methyl lithium and a quantitative yield of the corresponding secondary alcohol is obtained. This unsaturated alcohol is treated with triphenyl phosphonium bromide in ethanol[11], which gives (β-ionylidene prop-2-yl) triphenylphosphonium bromide (**11**) in 60% yield. This Wittig salt (**11**) is dissolved in 1-butene oxide and 3-cyano-2-methyl-propa-2-enal (**12**) is added. Aldehyde **12** is prepared from the corresponding acetal[14] by acidic deprotection.

Table 2.1. Yields and product ratios of **1CN** to **4CN** from the reaction of **7** and **9** in presence of lithium bromide or using 'salt-free'-conditions at low and elevated temperature.

Solvent/base	–70 °C		reflux [a]	
	total yield	ratio **1CN** : **4CN**	total yield	ratio **1CN** : **4CN**
Epoxide ('salt-free') [b]	33%	95:5	82%	50:50
THF, LDA	78%	99:1	80%	50:50

[a] Boiling point 1-butene oxide 63 °C and THF 65 °C, [b] The epoxide serves as solvent as well as a reagent to abstract HBr. At –70 °C propene oxide was used instead of 1-butene oxide that freezes at –60 °C

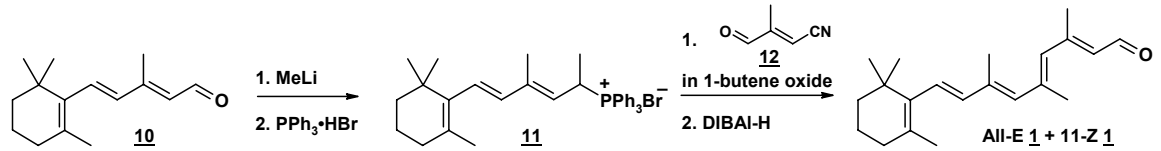

Scheme 2.3

The solution is refluxed, giving a mixture of 11-Z 11-methyl retinonitrile and its all-E isomer. After treatment with DIBAl-H a ~50:50 mixture of 11-Z retinal and the all-E isomer is obtained and the separation is straightforward using a silica column.

For the synthesis of 11-methyl-13-desmethyl retinal, 4-(diethylphosphono) buta-2-enoic ethyl ester[15] can be converted to 6,6-dimethoxy-5-methyl-2,4-hexadienoic ethyl ester (**14**) by reaction with LDA and subsequent addition of 1,1-dimethoxy aceton (**8**) at −70 °C (Scheme 2.4). After acidic deprotection of the acetal the corresponding aldehyde 5-methyl-6-oxo-hexa-2,4-dienoic ethyl ester (**15**) is obtained. Reaction of aldehyde **15** with β-ionyl triphenylphosphonium bromide (**9**)[11] (LDA,THF –70 °C) gives 11-methyl-13-desmethyl retinoic ethyl ester (**16**). The ester is reduced with DIBAl-H in petroleum ether and the resulting vinylic alcohol (**17**) is subsequently oxidised with activated MnO_2 to 11-methyl-13-desmethyl retinal (**2**).

2.4 Discussion

A central issue in the present study is the occurrence of **3** and **4** and possible routes to prevent their formation in the synthesis of 11-methyl retinal. The 1,4 conjugated Wittig or HWE reactions that lead to the formation of **3** and **4** involve the attack of the γ-carbon of an activated allylic phosphorus compound to the α,β unsaturated carbonyl compound in a 1,4 fashion (Scheme 2.5, A→D). This reaction is followed by an intramolecular acid-base reaction, which implies a proton migrating from the γ-position to the 3-position of the enolate (D→E).

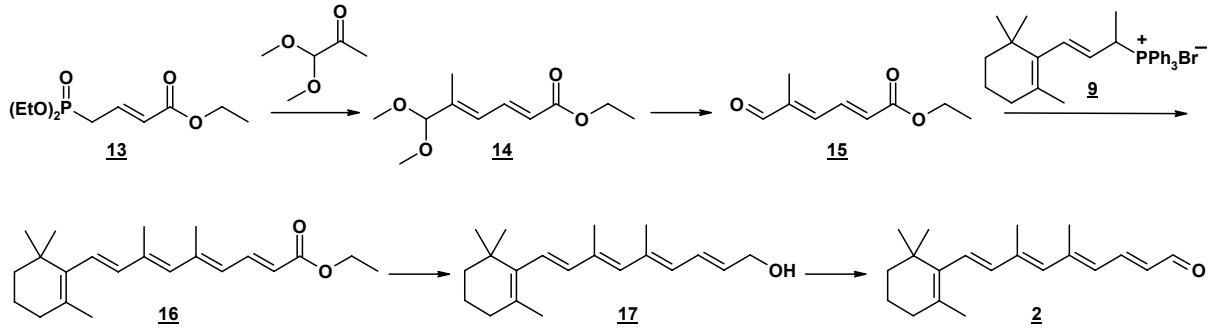

Scheme 2.4

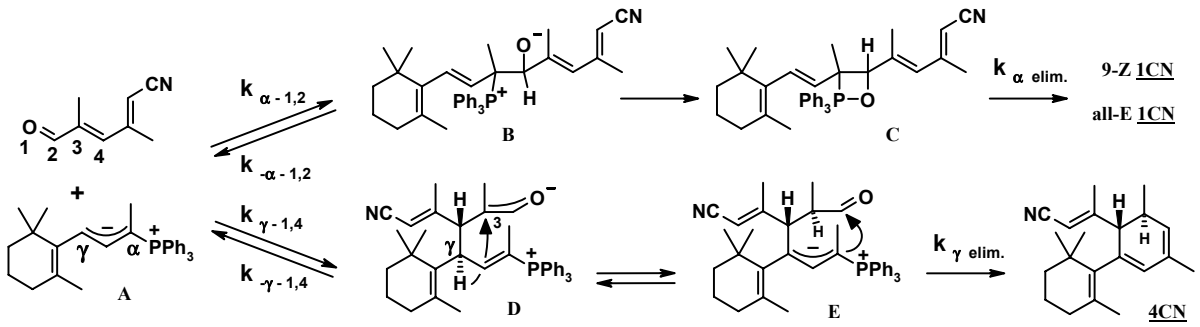

Scheme 2.5

This step produces the saturated aldehyde with a (re)activated allylic phosphorus moiety. Subsequent attack of the α-carbon of the allylic phosphorus on the carbonyl carbon and loss of phosphorus oxide compound completes the reaction (E→**4CN**).

The observation that in the case of β–ionone (**5**) and the phosphonate nitrile (**6**) a 1,4 conjugated HWE reaction takes place instead of the regular Wittig reaction is an indication that steric constraints related to the presence of the methyl functionality in **5** make it inefficient to apply a strategy involving HWE reagents to synthesise 11-methyl retinal. It can be anticipated that reaction of analogous carbon fragments with an aldehyde functionality instead of a methyl ketone could overcome this problem. The reaction of equal amounts of β-ionyl triphenyl phosphonium bromide (**9**) and 2,4-dimethyl-5-cyano-penta-2,4-dienal (**7**) was carried out successfully in refluxing 1-butene oxide, mimicking conditions that are used in the industrial scale synthesis of retinoids and carotenoids.[16,17] After DIBAl-H reduction of the retinonitrile and column separation three compounds are obtained. About 50% of the yield comprises the all-E 11-methyl retinal (all-E **1**)[8] and its 9-Z isomer (9-Z **1**)(1:1), which are the products of a regular Wittig reaction. The remaining fraction has been analysed with ^{1}H and ^{13}C NMR and is 3-(3,5,2',6',6'-pentamethyl-bicyclohexyl-4,6,1'-trien-2-yl)but-2-enal (**4**), that results from a 1,4 conjugated Wittig reaction.[10]

Since the formation of the cyclohexadiene is an unwanted reaction in the effort to synthesise 11-methyl retinal derivatives, two methods have been explored to reduce or prevent the formation of 1,4 addition products. Generally such reactions give very low yield in the sense that the normal Wittig product is present in less than 20%.[18] Although the formation of **1** and **4** in a 1:1 ratio is observed, this needs further improvement. In Scheme 2.5 there are two parallel reaction pathways. The formation of the cyclohexadiene product involves an internal proton migration step. This contrasts with the reaction of **11** with **12** in Scheme 2.3. In **11** the γ-position is blocked by a methyl group that prevents the formation of the cyclohexadiene compound.

Hence by treating (β-ionylidene prop-2-yl) triphenyl phosphonium bromide (**11**) and 2-methyl-3-cyano-propa-2-enal (**12**) only the normal Wittig product will be formed (Scheme 2.3). An additional advantage of this method is that the 11-Z isomer of 11-methyl retinal (11-Z **1**) that is essential for the present Rho studies is formed in the reaction and only the all-E isomer has to be removed before incorporation in the protein. It is interesting to note that reaction schemes for the commercial preparation of retinoids and carotenoids also have a γ-methyl group[16], although the connection with a favourable blocking effect was not yet reported.

For the 9-Z isomer the Michael addition A→D provides a handle to optimise the reaction yield. There is a strong effect of the temperature on the balance between 1,2- and 1,4-addition of enolates to enones.[19,20] A decrease of the temperature is expected to reduce the formation of the thermodynamically more favoured conjugate adduct D (Scheme 2.5) and increase the yield of kinetically favoured B and the subsequent normal olefination products. It has been found that in the reaction between ylide **9** and **7** (Scheme 2.2 and 2.5) at low temperature formation of the kinetic product (A→B) indeed prevails over the formation of thermodynamic product (A→D). Under these conditions the product is a mixture of all-E and 9-Z **1CN** with <5% of **4CN**. The threshold for formation of the final product is T>0 ºC. Since the formation of the betaine (B, Scheme 2.5) occurs at low temperatures this confirms that the elimination of triphenyl phosphorous oxide is the rate-limiting step in Scheme 2.5. In the reaction of **7** and **9** the all-E and 9-Z 11-methyl retinal and cyclohexadiene product are formed in a ~1:1:2 ratio with or without lithium bromide present. This contrasts with previous studies where an effect of salt upon the Z/E ratio in Wittig reactions at low temperature was reported. Possibly the α–methyl group in **9** interferes with the selectivity of the formation of a *syn* or *anti* betaine adduct.

2.5 Conclusion

It was shown that 9-Z and 11-Z 11-methyl retinal and also the 11-methyl-13-desmethyl derivative can be synthesised with simple and efficient schemes in good yield and without laborious generation of Z/E isomers by irradiation followed by HPLC separation. The synthesis of 11-Z 11-methyl retinal proceeds well when a Wittig reagent with functionalised γ-carbon is used to block progress of the 1,4 conjugate Wittig reaction with the substrate. Finally, it is demonstrated that the 1,4 conjugate Wittig or HWE reactions can be prevented by performing the reaction under kinetically controlled conditions.

2.6 EXPERIMENTAL DETAILS

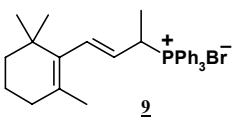

9

β-ionyl triphenyl phosphonium bromide (**9**): previously described by J. L. Olive *et al.*[11]

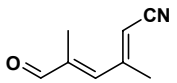

7

2,4-dimethyl-5-cyano-penta-2,4-dienal (**7**): 25 mmol (5.43 g) of 4-(diethyl phosphono)-3-methyl-2-butenenitrile (**6**)[9] was dissolved in 125 mL THF. At 0 °C 25 mmol (15.6 mL of a 1.6 M solution) butyl lithium solution was added via a syringe to the stirring solution. After 15 minutes 20 mmol (2.36 g) of commercially available 1,1-dimethoxy acetone (**8**) in some THF was added slowly. The reaction was followed with TLC (ethyl acetate-PE 5:2) with 2,4-dinitrophenylhydrazine as staining reagent. When the reaction was finished 50 mL of a saturated ammonium chloride solution was added and the layers were separated. The aqueous layer was extracted with ether (3x). The ethereal layers were combined and washed with brine, dried over $MgSO_4$ and filtered. After evaporation of the solvent under vacuum the raw 6,6-dimethoxy-3,5-dimethylhexa-2,4-dienenitrile was purified on silica gel. The pure material (3.1 g, 17 mmol, 86%) was dissolved in 50 mL acetone and a solution of 1M HCl was added until the pH of the solution was approx. 2. The reaction was followed with TLC (ether-PE 1:1) and again 2,4-dinitrophenylhydrazine was used to stain. When the reaction was finished solid K_2CO_3 and $MgSO_4$ was added and the solution was filtered and evaporated under vacuum. Purification on silica gel gave a quantitative yield of 2.2 g (17 mmol).

6,6-dimethoxy-3,5-dimethylhexa-2,4-dienenitrile: ^{1}H 200 MHz ($CDCl_3$) δ 6.13 (1H, s, H-4), 5.22 (1H, s, H-2), 4.55 (1H, s, H-6), 3.34 (6H, s, OCH_3), 2,20 (3H, s, 5-CH_3), 1.84 (3H, s, 3-CH_3)

2,4-dimethyl-5-cyano-penta-2,4-dienal (**7**): ^{1}H 300 MHz ($CDCl_3$) δ 9.50 (1H, s, H-6), 6.76 (1H, s, H-4), 5.53 (1H, s, H-2), 2.36 (3H, s, 3-CH_3), 2.00 (3H, s, 5-CH_3)
^{13}C 75 MHz ($CDCl_3$) δ 194.4 (C6), 155,3 (C5), 146.4 (C4), 141.9 (C3), 116.2 (C1), 103.3 (C2), 20.0 (5-CH_3), 11.1 (3-CH_3).

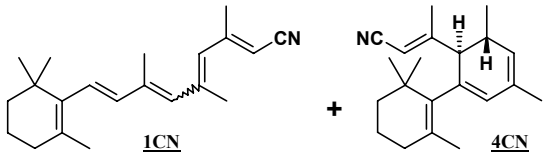

All-E and 9-Z 3,5,7-trimethyl-9-(2,6,6-trimethylcyclohexa-1-enyl)-nona-2,4,6,8-tetranitrile (all-E and 9-Z **1CN**) and 3-(3,5,2',6',6'-pentamethyl-bicyclohexa-4,6,1'-triene-2-yl)-but-2-enenitrile (**4CN**):

7+9 at 65 °C: 5.2 g (10 mmol) of (**9**) and 8.1 mmol (1.0 g) of (**7**) in 50 mL of 1-butenoxide were heated under reflux. When the reaction was completed according to TLC analysis, the reaction mixture was allowed to cool and the 1-butenoxide was removed under vacuum. The residue was purified using silica gel chromatography (ether-PE 1:4), this gave 2.0 g (82%) of a mixture of **1CN** and **4CN**.

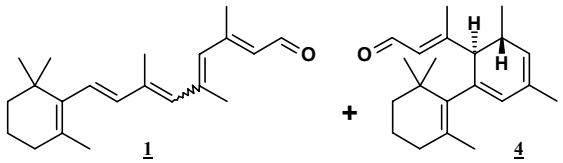

All-E and 9-Z-11-methyl retinal (all-E and 9-Z **1**) and 3-(3,5,2',6',6'-pentamethyl-bicyclohexa-4,6,1'-triene-2-yl)-but-2-enenal (**4**): Mixture of 2,2 g of **1CN** and **4CN** was dissolved in 50 mL dry PE. At –60 °C 11 mmol (11 mL of a 1.0 M solution) DIBAl-H was added via a syringe. The mixture was stirred at –60 °C for 30 minutes and then allowed to warm to room temperature. When the reaction was completed according to TLC analysis 20 g of a mixture of 0.4 mL water/g silica was added at 0 °C to work-up the reaction. $MgSO_4$ was added to absorb the water content and slurry was filtered over a glass-fritted filter, the residue was washed with diethyl ether. The solvent was evaporated under vacuum and the residue was purified with silica gel chromatography. This gave 0.83 g (2.8 mmol, 41%) of **1** (all-E and 9-Z) and 0.78 g (2.6 mmol, 39%) of **4**.

all-E 11-methyl retinal (all-E **1**) spectroscopic data are identical to Tsujimoto *et al.*[8]

9-Z-11-methyl-retinal (9-Z **1**): ^{1}H 600 MHz ($CDCl_3$): δ 10,07 (1H,d, H-15, ^{3}J=8.2 Hz), 6.48 (1H, d, H-8, ^{3}J=16.2 Hz), 6.29 (1H, d, H-7, ^{3}J=16.2 Hz), 5.99 (1H, d, H-14, ^{3}J=8.2 Hz), 5.92 (1H, s, H-12), 5.86 (1H, s, H-10), 2.29 (3H, s, 13-CH_3), 2.02 (3H, s, 11-CH_3), 2.01 (2H, t, H-4), 1.98 (3H, s, 9-CH_3), 1.69 (3H, s, 5-CH_3), 1.61 (2H, m, H-3), 1.47 (2H, m, 2-H), 1.02 (6H, s, H16/17).

^{13}C 100 MHz ($CDCl_3$): δ 191.3 (C20), 155.9 (C13), 141.9 (C11), 137.9 (C6), 136.5 (C9), 132.3, 132.1, 131.5, 129.9, 129,7 (C5), 39.6 (C2), 34.2 (C1), 33.0 (C4), 29.0 (C16/C17), 21.8, 21.4, 20.6, 19.2 (C3), 18.4.

3-(3,5,2',6',6'-pentamethyl-bicyclohexyl-4,6,1'-trien-2-yl)but-2-enal (**4**): ^{1}H 400 MHz ($CDCl_3$): (bc=bicyclohexyl) δ 9.96 (1H, d, CHO, ^{3}J=8 Hz), 5.85 (1H s, bcCH-6), 5.81 (1H, d, H-2, ^{3}J=8 Hz), 5.24 (1H, s, bcCH-4), 3.61 (1H, m, bcCH-3), 2.74 (1H, d, bcCH-2, ^{3}J=8 Hz), 2.12 (3H, s, 4-CH_3), 1.90 (2H, m, bc3'-CH_2) 1.74 (3H, s, bc3-CH_3), 1.71 (3H, s, bc5-CH_3), 1.60 (2H, m, bc4'-CH_2), 1.50 (3H, s, bc2'-CH_3), 1.48 (2H, m, bc5'-CH_2), 1.14 (3H, s, bc6'-CH_3), 1.00 (3H, s, bc6'-CH_3).
^{13}C 400MHz ($CDCl_3$): (bc=bicyclohexyl) δ191.2(C1), 162.5 (C3), 136.5 (bc1'), 135.7 (bc1), 132.3 (bc5), 130.0 (bc4), 129.0 (bc2'), 125.6/125.5(2C, 2/bc6), 52.9(bc2), 41.9(bc3), 39.8(bc5')), 35.9(bc6'), 33.4(bc3'), 28.7/28.0(2C, bc6'-CH_3), 23.8(bc5-CH_3), 22.3(bc2'-CH_3), 20.6(C4), 19.1(bc4')

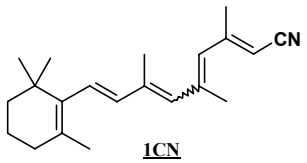

1CN

all-E and 9-Z 3,5,7-trimethyl-9-(2,6,6-trimethylcyclohexa-1-enyl)-nona-2,4,6,8-tetranitrile (all-E and 9-Z **1CN**)
9+7 at –70 °C: 0.19 g (1.92 mmol) of diisopropyamine was reacted with 1.2 mL of a 1.6 M solution of butyl lithium (1.92 mmol) in 50 mL of THF. 1.0 g (1.92 mmol) of 3 was added and the mixture was cooled to –70 °C. 0.19 g (1.54 mmol) of 7 in a small volume of THF was added dropwise. The mixture was allowed to warm to room temperature slowly. At –20 °C TLC analysis showed reaction progress and the mixture was kept at this temperature until the starting material had disappeared. The reaction was quenched by addition of saturated ammonium chloride solution. The layers were separated and the water layer was extracted with diethyl ether (3x). The ethereal layers were combined and washed with brine, dried over $MgSO_4$ and filtered. After evaporation of the solvent under vacuum the material purified on silica gel. Yield 0.35 g (1.2 mmol) **1CN**, which is 78% with respect to the amount of **7** used.

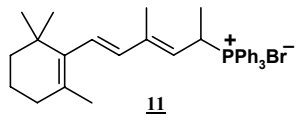

11

(β-ionylidene prop-2-yl) triphenyl phosphonium bromide (**11**): 4.9 g (22 mmol) of all-E β-ionylidene acetaldehyde (**10**)[13] was dissolved in 100 mL of THF. At –70 °C 18 mL of a 1 M solution of methyl lithium was added slowly *via* a syringe. After completion of the

reaction according to TLC analysis a saturated solution of ammonium chloride was added and the layers were separated. The aqueous layer was extracted with ether (3x). The ethereal layers were combined and washed with brine, dried over $MgSO_4$ and filtered. After evaporation of the solvent under vacuum the raw 1,3-dimethyl-5-(2,6,6-trimethylcyclohexa-1-enyl)-penta-2,4-dienol was purified on silica gel. The pure material (22 mmol, 99%) was dissolved in 20 mL of dry ethanol and 7.8 g (23 mmol) of triphenyl phosphonium bromide was added. The reaction was stirred in the dark to prevent isomerization. After 72 hours solvent was evaporated and the material was crystallised from a mixture of ethyl acetate and diethyl ether. Yield 7.3 g (13 mmol) of **11** containing a small residue of PPh_3•HBr.

^{1}H 400 MHz ($CDCl_3$) δ 7.87 (m, Ph), 7.32 (m, Ph), 6.15 (1H, d, H-5, ^{3}J=16.1 Hz), 5.89 (1H, d, H-4, ^{3}J=16.1 Hz), 5.50 (1H, m, H-1), 5.00 (1H, dd, H-2, ^{3}J~8.5 Hz/^{3}J~9.7 Hz), 1.98(2H, d, H-3', ^{3}J=6.1 Hz), 1.91 (3H, d, 3-CH_3, ^{5}J(P)=3 Hz), 1.66 (3H, d, 1-CH_3, ^{3}J(P)=7 Hz), 1.63 (3H, s, 2'-CH_3), 1.59 (2H, m, H-4'), 1.44 (2H, m, H-5'), 0.98 (3H, s, 6'-CH_3), 0.97 (3H, s, 6'-CH_3).
^{13}C 100 MHz ($CDCl_3$): δ 142.6 (d, C-3, ^{3}J(P)=14Hz), 137.0 (C1'), 135.3 (d, C-4, ^{4}J(P)=4Hz), 134.8 (p-Ph), 134.1 (d, o-Ph, ^{2}J(P)=9Hz), 130.2 (d, m-Ph, ^{3}J(P)=12Hz), 129.6 (C-2'), 129.3 (d, C-5, ^{5}J(P)=4Hz), 120.0 (d, C-2, ^{2}J(P)=7Hz), 117.4 (d, Ph, ^{1}J(P)=82Hz), 39.2 (C-5'), 33.9 (C-6'), 32.6 (C-3'), 30.8 (d, C-1, ^{1}J(P)=47Hz), 28.7/28.6 (2x6'CH_3), 21.4 (2'-CH_3), 18.9 (C-4'), 16.9 (3-CH_3), 14.2 (1-CH_3).
^{31}P 162 MHz ($CDCl_3$): δ 27.2

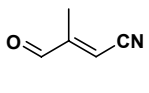

12

2-methyl-3-cyano-propa-2-enal (**12**) is prepared from 1,1-dimethoxy acetone and (diethyl phosphono)acetonitrile according to: Jansen, F.-J. H. M *et al.*[14], followed by deprotection in 2% aqueous phosphoric acid at 60 °C, spectroscopic characteristics are identical to Chen.[21]

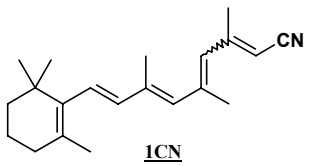

1CN

All-E and 11-Z 3,5,7-trimethyl-9-(2,6,6-trimethylcyclo hexa-1-enyl)-nona-2,4,6,8-tetranitrile (all-E and 11-Z **1CN**): **11+12 at 65 °C**: like **7**+**9** at 65°C (above) with 2.2 g (4.0 mmol) **11** and 0.29 g (3.0 mmol) **12** gave 0.78 g (2.6 mmol, 87%) of pure **1CN** isomers.

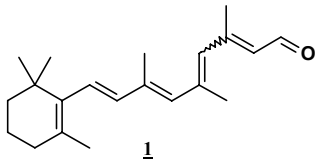

1

All-E and 11-Z-11-methyl retinal (all-E and 11-Z **1**): like all-E and 9-Z **1** (above) with 2.6 mmol of **1CN** and 3.9 mmol (3.9 mL of a 1M solution) DIBAl-H gave 0.45 g (1.5 mmol, 58%) of a mixture of all-E and 11-Z **1**, spectroscopic data are identical to Tsujimoto *et al*.[8]

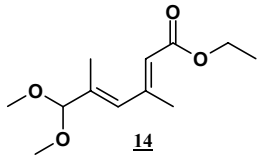

14

6,6-dimethoxy-5-methyl-2,4-hexadienoic ethyl ester (**14**): 25 mmol of diisopropyl amine was dissolved in 100 mL THF. At –20 °C 25 mmol (1.56 mL of a 1.6 M solution) of butyl lithium was added via a syringe. After stirring for 15 minutes, 25 mmol (6.23 g) of 4-(diethyl phosphono)-2-butenoic ethyl ester dissolved in 25 mL THF was added. After 15 minutes 20 mmol (2.36 g) of 1,1-dimethoxy aceton (**8**) was added slowly. The reaction progress was monitored with TLC (ethylacetate-PE 5:2) with 2,4-dinitrophenylhydrazine as colour reagent. Both the starting material and the product react with the colour reagent, however the spot of the ketone appears much faster and is more intense. When the reaction was finished according to TLC 50 mL of a saturated ammonium sulfate solution was added and the layers were separated. The aqueous layer was extracted 3 times with ether. The ethereal layers were combined and washed with brine, dried over $MgSO_4$ and filtered. After evaporation of the solvent under vacuum the raw material was purified on silica gel. The yield of 17 mmol (3.7 g) is 86% with respect to the amount of ketone used.

^{1}H 200 MHz ($CDCl_3$) δ 7.58 (1H, dd, H-3, ^{3}J=12 Hz, ^{3}J=16 Hz), 6.34 (1H, d, H-4, ^{3}J=12 Hz), 5.94 (1H, d, H-2, ^{3}J=16 Hz), 4.63 (1H, s, H-6), 4.22 (2H, q, ethyl CH_2, ^{3}J=6 Hz), 3.30 (6H, s, OCH_3), 1.87 (3H, s, 5-CH_3), 1.30 (3H, t, ethyl CH_3, ^{3}J=6 Hz).

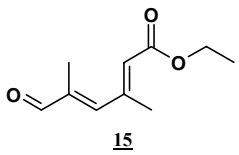

15

5-methyl-6-oxo-hexa-2,4-dienoic ethyl ester (**15**): 17 mmol of **14** was dissolved in 50 mL acetone and a solution of 1 M HCl was added until the pH of the solution was approx. 2. The reaction progress was monitored with TLC (ether-PE 1:1) and 2,4-dinitrophenylhydrazine as colour reagent. When the reaction was finished solid K_2CO_3 and $MgSO_4$ were added and the solution was filtered and evaporated under vacuum. Purification on silica gel gave a quantitative yield of 2.8 g (17 mmol).

^{1}H 300 MHz ($CDCl_3$) δ 9.56 (1H, s, H-6), 7.70 (1H, dd, H-3, ^{3}J=11.6 Hz, ^{3}J=15.3 Hz), 6.92 (1H, d, H-4, ^{3}J=11.6 Hz), 6.28 (1H, d, H-2, ^{3}J=15.3 Hz), 4.26 (2H, q, ethyl CH_2, ^{3}J=7.1 Hz), 1.97 (3H, s, 5-CH_3), 1.34 (3H, q, ethyl CH_3, ^{3}J=7.1 Hz).
^{13}C 75 MHz ($CDCl_3$) δ 194.3 (C6), 165.8 (C1), 143.8 (C5), 143.7 (C4), 137.5 (C3), 128.6 (C2), 60.9 (ethyl CH_2), 14.2 (ethyl CH_3), 10.0 (5-CH_3).

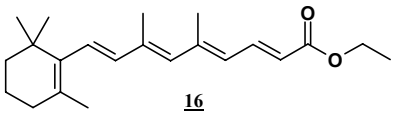

16

5,7-dimethyl-9-(2,6,6-trimethylcyclohexa-1-enyl)-nona-2,4,6,8-tetraenoic ethyl ester (**16**): 1.19 g (12 mmol) of diisopropyamine was reacted with 7.5 mL of a 1.6 M solution of butyl lithium (12 mmol) in 250 mL of THF. A 12 mmol (6.4 g) amount of **9** was added through a funnel and stirred for 1 hour at room temperature. A 9.5 mmol (1.6 g) amount of **15** in THF was added drop wise at −70 °C and the reaction mixture was allowed to room temperature. When the reaction was finished according to TLC analysis a saturated ammonium sulphate was added. The layers were separated and the water layer was extracted with diethyl ether (3x). The ethereal layers were combined and washed with brine, dried over $MgSO_4$ and filtered. After evaporation of the solvent under vacuum the oil was purified using silica gel chromatography (ether-PE 1:4), this gave 2.33 g (7.1 mmol, 75%) of **16**.

Two isomers ^{1}H 300 MHz ($CDCl_3$): 7.66 (1H, dd, H-13, ^{3}J=11.9 Hz ^{3}J=15.0 Hz), 7.63 (1H, dd, H-13', ^{3}J=11.9 Hz ^{3}J=15.1 Hz), 6.54 (1H, d, H-8', ^{3}J=16.2 Hz), 6.28 (1H, d, H-7', ^{3}J=16.2 Hz), 6.17 (3x1H, 3xd, H-7/H12/H-12'), 6.13 (1H, d, H-8, 16.0), 5.97 (1H, s, H-10), 5.87 (1H, s, H-10'), 5.86/5.82 (2x1H, 2xd, H-14/H-14'), 4.21 (2x2H, 2xq, ethyl CH_2), 2.09 (3H, s, 11-CH_3), 2.04 (3H, s, 9-CH_3), 2.02 (3H, s, 11'-CH_3), 1.99 (3H, 9'-CH_3), 1.72 (3H, s, 5'-CH_3), 1.71 (3H, s, 5-CH_3), 1.62 (2x2H, 2xm, H3/H-3'), 1.46 (2x2H, 2xm, H-2/H-2'). 1.30 (2x3H, 2xt, ethyl CH_3), 1.03 (2x6H, 2xs, 1-CH_3/1'-CH_3)

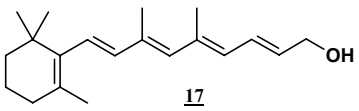

17

5,7-dimethyl-9-(2,6,6-trimethylcyclohexa-1-enyl)-nona-2,4,6,8-tetraenol (**17**): 2.33 g (7.1 mmol) of **16** was dissolved in 50 mL of dry PE and cooled to –60 °C. 18 mmol (18 mL of a 1.0 M solution) of DIBAl-H was added via a syringe. The mixture was stirred at –60 °C for 30 minutes and then allowed to warm to room temperature. When the reaction was completed according to TLC analysis at 0 °C 20 g of a mixture of 0.4 mL water/g silica was added to work-up the reaction.

$MgSO_4$ was added to absorb the water content and the slurry was filtered over a glass-fritted filter. The solvent was evaporated under vacuum and the residue was purified with silica gel chromatography. This gave 1.8 g (6.3 mmol, 89%) of **17**

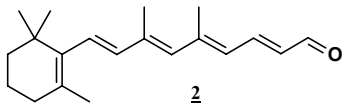

2

11-methyl-13-desmethyl-retinal (**2**) 6.3 mmol (1.8 g) of **17** and 15 equivalents (8.2 g) of MnO_2 were stirred in 75 mL DCM. After 20 hours the MnO_2 was filtered of over Celite and rinsed with ether. The solvents were evaporated under vacuum. Silica gel chromatography (ether-PE, 1:4) of the residue gave 0.90 g (3.2 mmol, 50%) of **2**.

9-Z isomer: ^{1}H 400 MHz ($CDCl_3$): 9.60 (1H, d, H15, ^{3}J=8.0 Hz), 7.46 (1H, dd, H-13, ^{3}J=14.9 Hz ^{3}J=11.7 Hz), 6.54 (1H, d, H-8, ^{3}J=16.2 Hz), 6.34 (1H, d, H-7, ^{3}J=16.2 Hz), 6.33 (1H, d, H-12, ^{3}J=11.7 Hz), 6.12 (1H, dd, H-14, ^{3}J=8.0 Hz ^{3}J=14.9 Hz), 5.91 (1H, s, H-10), 2.07 (3H, s, 11-CH_3), 2.01 (3H, s, 9-CH_3), 1.72 (3H, s, 5-CH_3), 1.60 (2H, m, H-3), 1.46 (2H, m, H-2), 1.02 (6H, s, 1-CH_3).

11-Z isomer: ^{1}H 400 MHz ($CDCl_3$): 9.52 (1H, d, H-15, ^{3}J=8.1 Hz), 7.14 (1H, dd, H-13, ^{3}J=11.4 Hz ^{3}J=15.2 Hz), 6.27 (1H, d, H-7, ^{3}J=16.3 Hz), 6.24 (1H, d, H-12, ^{3}J=11.4 Hz), 6.16 (1H, d, H-8, ^{3}J=16.3 Hz), 6.10 (1H, dd, H-14, ^{3}J=8.1 Hz ^{3}J=15.2 Hz), 6.02 (1H, s, H-10), 2.03 (3H, s, 11-CH_3), 1.82 (3H, s, 9-CH_3), 1.74 (3H, s, 5-CH_3), 1.6 (2H, m, H-3), 1.50 (2H, m, H-2), 1.05 (6H, s, 1-CH_3).

All-E isomer: ^{1}H 400 MHz ($CDCl_3$): 9.61 (1H, d, H-15, ^{3}J=8.0 Hz), 7.48 (1H, dd, H-13, ^{3}J=11.8 Hz ^{3}J=14.8 Hz), 6.34 (1H, d, H-12, ^{3}J=11,8 Hz), 6.28 (1H, d, H-7, ^{3}J=16,0 Hz), 6.16 (1H, dd, H-14, ^{3}J=8.0 Hz, ^{3}J=14.8 Hz), 6.10 (1H, d, H-8, ^{3}J=16.0 Hz), 6.01 (1H, s, H-10), 2.15 (3H, s, 11-CH_3), 2.07 (3H, s, 9-CH_3), 2.02 (2H, t, H-4), 1.71 (3H, s, 5-CH_3), 1.61 (2H, m, H-3), 1.45 (2H, m, H-2), 1.03 (6H, s, 1-CH_3)

REFERENCES

(1) Mathies, R. A.; Lugtenburg, J. *Molecular Mechanisms in Visual Transduction*; Elsevier Science: Amsterdam, 2000.

(2) Vogel, R.; Fan, G. B.; Sheves, M.; Siebert, F. *Biochemistry* **2000**, *39*, 8895-8908.

(3) Han, M.; Groesbeek, M.; Sakmar, T. P.; Smith, S. O. *Proc. Natl. Acad. Sci. U. S. A.* **1997**, *94*, 13442-13447.

(4) Ganter, U. M.; Schmid, E. D.; Perezsala, D.; Rando, R. R.; Siebert, F. *Biochemistry* **1989**, *28*, 5954-5962.

(5) Verdegem, P. J. E.; Monnee, M. C. F.; Lugtenburg, J. *J. Org. Chem.* **2001**, *66*, 1269-1282.

(6) Verdegem, P. J. E.; Bovee-Geurts, P. H. M.; DeGrip, W. J.; Lugtenburg, J.; De Groot, H. J. M. *Biochemistry* **1999**, *38*, 11316-11324.
(7) DeLange, F.; Bovee-Geurts, P. H. M.; Van Oostrum, J.; Portier, M. D.; Verdegem, P. J. E.; Lugtenburg, J.; DeGrip, W. J. *Biochemistry* **1998**, *37*, 1411-1420.
(8) Tsujimoto, K.; Shirasaka, Y.; Mizukami, T.; Ohashi, M. *Chem. Lett.* **1997**, 813-814.
(9) Creemers, A. F. L.; Lugtenburg, J. *J. Am. Chem. Soc.* **2002**, *124*, 6324-6334.
(10) Padwa, A.; Brodsky, L. *J. Org. Chem.* **1974**, *39*, 1318-1320.
(11) Olive, J. L.; Mousserom, M.; Dornand, J. *Bull. Soc. Chim. Fr.* **1969**, 3247.
(12) Dauben, W. G.; Ipaktsch.J *J. Am. Chem. Soc.* **1973**, *95*, 5088-5089.
(13) Groesbeek, M.; Rood, G. A.; Lugtenburg, J. *Recl. Trav. Chim. Pay B.* **1992**, *111*, 149-154.
(14) Jansen, F.-J. H. M.; Kwestro, M.; Schmitt, D.; Lugtenburg, J. *Recl. Trav. Chim. Pays B.* **1994**, *113*, 552-562.
(15) Sato, K.; Mizuno, S.; Hirayama, M. *J. Org. Chem.* **1967**, *32*, 177.
(16) Paust, J. *Pure & Appl. Chem.* **1991**, *63*, 45-58.
(17) Paust, J. In *Carotenoids Volume 2: Synthesis*; Britton, G., Ed.; Birkhäuser Verlag: Basel, 1996.
(18) Bohlmann, F.; Zdero, C. *Chem. Ber.-Recl.* **1973**, *106*, 3779-3787.
(19) Heathcock, C. H.; Oare, D. A. *J. Org. Chem.* **1985**, *50*, 3022-3024.
(20) Heathcock, C. H.; Henderson, M. A.; Oare, D. A.; Sanner, M. A. *J. Org. Chem.* **1985**, *50*, 3019-3022.
(21) Chen, S. *Experentia* **1981**, 543.

Chapter 3

The electronic structure of the retinylidene chromophore in rhodopsin*

* This chapter has been published in *Biochemistry* **2001,** 40, 3282-3288

3.1 ABSTRACT

11-Z-[8,9,10,11,12,13,14,15,19,20-$^{13}C_{10}$]-retinal prepared by total synthesis is reconstituted with opsin to form rhodopsin in the natural lipid membrane environment. The ^{13}C shifts are assigned with Magic Angle Spinning NMR dipolar correlation spectroscopy in a single experiment and compared with data of singly labeled retinylidene ligands in detergent-solubilized rhodopsin. The use of multispin labeling in combination with 2-D correlation spectroscopy improves the relative accuracy of the shift measurements. We have used the chemical shift data to analyze the electronic structure of the retinylidene ligand at three levels of understanding, (i) by specifying interactions between the ^{13}C labeled ligand and the G-protein coupled receptor target; (ii) by making a charge assessment of the protonation of the Schiff base in rhodopsin, and (iii) by evaluating the total charge on the carbons of the retinylidene chromophore. In this way it is shown that a conjugation defect is the predominant ground-state property governing the molecular electronics of retinylidene chromophore in rhodopsin. The cumulative chemical shifts at the odd-numbered carbons ($\Delta\sigma_{odd}$) of 11-Z protonated Schiff base models relative to the unprotonated Schiff base can be used to measure the extent of delocalization of positive charge into the polyene. For a series of 11-Z protonated Schiff base models and rhodopsin $\Delta\sigma_{odd}$ appears to correlate linearly with the frequency of maximum visible absorption. Since rhodopsin has the largest value of $\Delta\sigma_{odd}$, the data contribute to existing and converging spectroscopic evidence for a complex counterion stabilizing the protonated Schiff base in the binding pocket.

3.2 INTRODUCTION

Rhodopsin is the G-protein coupled photoreceptor protein in the retina of vertebrates that initiates the visual signal transduction cascade in dim light vision. It is considered a paradigm for the superfamily of 7 transmembrane helix G-protein coupled receptors (GPCRs) which comprises a physiologically widespread and pharmacologically very significant class of signal mediators[1-4] GPCRs trigger a wide variety of physiological processes that involve signaling by neurotransmitters, hormones and neuropeptides. They are the major pharmaceutical targets for pharmacological intervention in human pathology. Characterization of the electronic structure of the ground-state of ligands bound to their receptor targets will help to reveal the molecular mechanisms of receptor activation, thus facilitating identification of pharmacophores and improving drug design. The ligand in rhodopsin is 11-Z-retinal that is covalently bound to the protein *via* a protonated Schiff base (PSB) linkage with lysine residue 296 to form the

retinylidene chromophore. Upon absorption of a photon, the C11=C12 bond of the retinylidene ligand isomerizes from the 11-Z to the all-E configuration.[5,6]

In recent years, rhodopsin has been studied in detail with MAS NMR techniques.[7-12] The chemical shifts of the carbons in the polyene of the retinylidene ligand have been probed in a series of experiments using mono ^{13}C labeled preparations.[7] In such an approach, each experiment involves labeling of retinal with a ^{13}C isotope at a single predetermined position by chemical total synthesis, followed by isolation of the synthetic 11-Z isomer from the mixture of retinal isomers. After reconstitution of the singly labeled retinal into opsin to form rhodopsin, the MAS NMR response of the ^{13}C isotope can be measured. The rate-limiting step in this approach is the need for development of efficient total synthesis schemes for site specific labeling. The few examples where this tedious scheme has been applied have taken more than a decade, which is an unrealistic time scale for routine studies of ligand-protein interactions. Recent developments in the field of MAS NMR have provided broadband dipolar recoupling techniques that can be applied in a 2-D correlation experiments.[13,14] These new techniques were recently used to detect, and partially assign, correlation signals from a multispin labeled pheophytin cofactor that was prepared *via* biosynthetic methods and incorporated into a 125 kDa photosynthetic reaction center membrane protein complex.[15] One purpose of this study is to demonstrate that MAS NMR dipolar correlation spectroscopy on a synthetically prepared multispin labeled retinal incorporated in opsin in its natural membrane environment can be used for a complete assignment of a predetermined multispin cluster, providing a MAS NMR shift image for characterization of the electronic structure in a single 2-D experiment. This sets the stage for creating chemical shift assays of the interaction of a ligand with its G-protein coupled receptor target in the natural membrane environment. The utility of such images is illustrated with an assay of the electronic structure of the retinylidene group. We interpret the shift pattern in terms of a positive polaronlike conjugation defect stabilized by a negative complex counterion for the Schiff base (SB) environment in the active site of this GPCR.

3.3 MATERIALS AND METHODS

To incorporate a multispin cluster in the chromophore in rhodopsin, an efficient and cost-effective synthetic scheme was developed. The specific aim of this investigation is to incorporate the ^{13}C labels in the polyene part of the retinal towards the SB end. In that part the photo-isomerization takes place and the positive charge of the chromophore in the ground state is established by protonation of the SB nitrogen. To probe this region [8,9,10,11,12,13,14,15,19,20-$^{13}C_{10}$]-retinal was synthesized from natural abundance

β-cyclocitral and the $^{13}C_5$ labeled building block [1,2,3,4,(3-methyl)-$^{13}C_5$]-3-methyl-4-(diethyl phosphono)-2-butenitrile that contains the recurring segment in the polyene.[16] In Figure 3.1A the ^{13}C label positions are indicated with their respective number. The purified mixture of configurational retinal isomers obtained by synthesis was irradiated in acetonitrile to generate the 11-Z-isomer in a maximum amount. The 11-Z-isomer was separated from this mixture by straight phase HPLC (silicagel, 1.2 × 25 cm, Dupont).[17]

Retinas were dissected from approximately 50 fresh cow eyes, within 4 hours after slaughter. Bleached membrane fragments containing opsin, the apoprotein of rhodopsin, were isolated and regenerated with a ~3-fold excess of the 11-Z-$^{13}C_{10}$-retinal following published procedures.[18] Excess of retinal was removed by extraction with β-cyclodextrin.[19] Incorporation was checked by optical spectroscopy, the observed (A_{280}/A_{500}) ratio was 2.0, corresponding with an incorporation level of the labeled retinal of more than 90 %. The rhodopsin sample containing the multiply labeled chromophore was concentrated by centrifugation and loaded into a 4 mm zirconium oxide rotor and sealed with a Kel-F cap. CP/MAS spectra were recorded with a Bruker DSX-750 spectrometer operating at a ^{13}C frequency of 188 MHz and equipped with a 4 mm MAS probe. Ramped cross polarization[20] with a contact time of 2.0 ms and the TPPM decoupling scheme[21] were used. The sample was cooled with nitrogen gas at a temperature of 223K. The 1-D spectrum was recorded using a MAS frequency of 12.000 Hz ± 3 Hz, and the cycle time between scans was 2 s. Prior to Fourier transformation the FID arrays were zero-filled to 2 K points and an exponential line-broadening function of 50 Hz was applied. 2-D RFDR spectra were also recorded using a MAS frequency of 12.000 ± 3 Hz and a mixing time τ_m= 2.67 ms, while during mixing CW-decoupling was used with a nutation frequency of 83 kHz. In the t_1 domain 200 slices with 10 μs increments were collected and for each slice 480 transients were recorded in the t_2 domain. TPPM-decoupling was used during acquisition and the cycle time between scans was 2 s. Prior to double Fourier transformation the t_2 dimension was zero-filled to 2 K points and an exponential line-broadening function of 75 Hz was applied. Zero-filling in t_1 was to 512 points and a quadratic sine apodization window shifted by 2.7/π was applied. Chemical shifts are reported relative to TMS, using the shift that was determined previously for C-11 as internal references.[11] To calculate the chemical shift differences ^{13}C NMR data for the PSB model N-(11-Z-retinylidene) propyliminium chloride

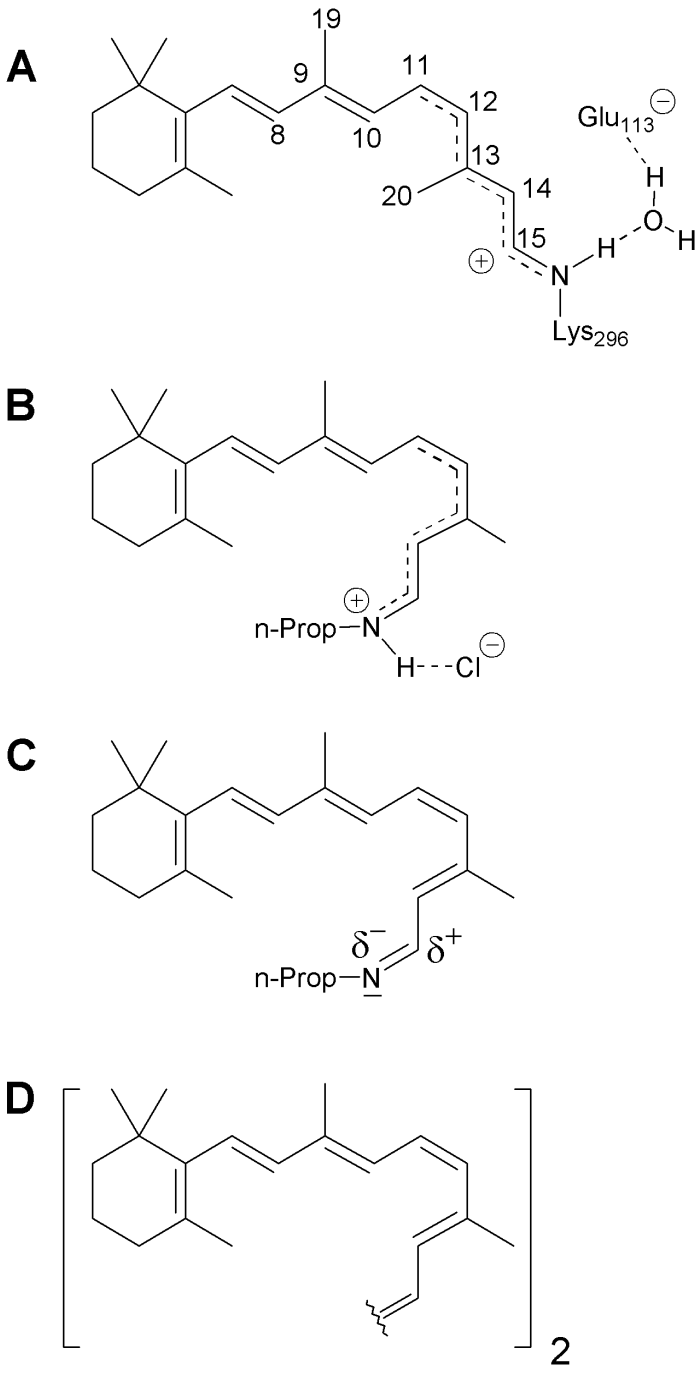

Figure 3.1: Chemical structures of the four retinylidene species discussed in this study. (A) The chromophore in rhodopsin, the numbers indicate the position of the ^{13}C labels. (B) The 11-Z-PSB N-(11-Z-retinylidene) propyliminium chloride as in solution, (C) the corresponding 11-Z-SB, as in solution and (D) 11-Z-β-carotene as in solution.

(Figure 3.1B),[22] the SB model N-(11-Z-retinylidene) propylimine (Figure 3.1C),[22] and 11-Z-β-carotene (Figure 3.1D),[23] in solution, were taken from the literature. Data for two 11-Z PSB salts, N-(11-Z-retinylidene) propyliminium trifluoroacetate and bromide, in Figure 3.5, were taken from reference[22] and[24] respectively. The crystal structure data of two all-E PSB salts, N-(all-E-retinylidene) *tert*-butyliminium perchlorate and triflate, used in the discussion are from reference.[25]

3.4 RESULTS

The 1-D spectrum of rhodopsin reconstituted with the 10-fold ^{13}C labeled retinal (Figure 3.1A) is shown in Figure 3.2A, while Figure 3.2B gives the natural abundance ^{13}C spectrum of native rhodopsin. In the spectrum of native rhodopsin the natural abundance ^{13}C nuclei of the saturated carbons including the aliphatic carbons of the amino acid side chains of the protein and membrane phospholipids resonate between 0 and 70 ppm. At ~127 ppm the natural abundance response from the unsaturated carbons in the phospholipids and aromatic carbons in the protein residues is observed. Finally, the broad signal around 175 ppm is a superposition of the peptide carbonyl and lipid ester response.

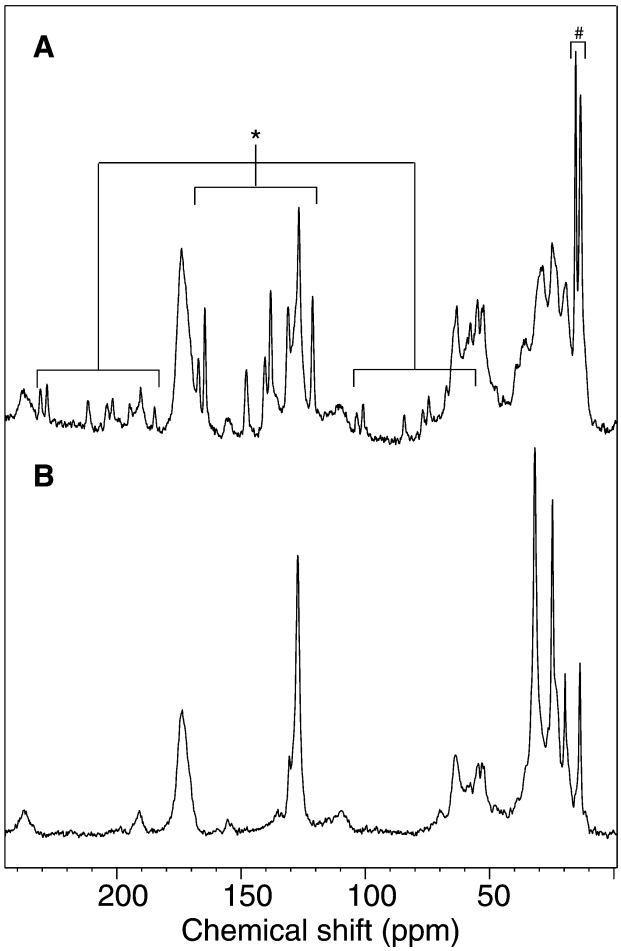

Figure 3.2: (A) Proton-decoupled ^{13}C CP/MAS spectra of rhodopsin containing a 10-fold ^{13}C labeled retinylidene chromophore. The centerband region of the vinylic carbons (*) and the spinning side band regions on both sides are indicated. The resonances of the methyl groups 19 and 20 are also indicated (#). (B) The spectrum of native rhodopsin shows the natural abundance ^{13}C signals of the protein and natural phospholipid membrane. The carbonyl signals of protein and phospholipids are found at ~175 ppm, saturated carbons of phospholipids and aromatic amino acid residues resonate with ~127 ppm and aliphatic signals are observed upfield at 0-70 ppm. The spectra were recorded with the same instrument settings with a temperature of 223 K and with a spinning frequency of 12.000 Hz ± 3 Hz.

The spectrum of rhodopsin with the 10-fold labeled retinylidene ligand shows additional sharp resonances of the centerbands and sidebands of the enriched carbon nuclei in the retinylidene chromophore. For instance, the two strong signals in the aliphatic region at 13.8 and 15.8 ppm are the resonances from the C-19 and C-20 methyl groups (Table 3.1). These signals do not show spinning side bands, due a small shift anisotropy ($|\sigma_{11}|$ and $|\sigma_{33}| << \omega_r$) of these sp^3 hybrid atoms. In the vinylic region the 8 remaining centerband signals are detected. Seven signals are well resolved with isotropic shifts between 120 and 170 ppm. A response around 128 ppm is superimposed on the natural abundance response of the phospholipids. This label signal can be assigned unambiguously by its spinning side band at 191 ppm, since the anisotropy of the phospholipid signals is relatively small and the side band signal in this region is weak (cf. Figure 3.2B). The chemical shifts for the resolved resonances of the labeled positions in the retinylidene suggest an NMR response analogous to signals previously reported by Smith *et al*. (Table 3.1).[7] However, a correlation experiment is needed to arrive at an unambiguous assignment of all resonances of the multispin labeled ligand.

Table 3.1: Isotropic ^{13}C MAS NMR shifts for the labeled positions in the 10-fold ^{13}C labeled retinylidene chromophore of rhodopsin in the native membrane obtained in a direct approach using homonuclear correlation spectroscopy (Figure 3.3). The shifts are compared with ^{13}C shift collected in a step-wise approach using rhodopsins solubilized in detergent (Ammonyx-LO).

Carbon	rhodopsin in native membrane	rhodopsin in Ammonyx-LO[a]	Δσ
8	138.5	139.2	–0.7
9	148.2	148.5	–0.3
10	127.2	127.8	–0.6
11	140.8	141.6	–0.8
12	131.5	132.1	–0.6
13	167.6	168.9	–1.3
14	121.6	121.2	+0.4
15	165.0	165.4	–0.4
19	13.8	12.0	+1.8
20	15.8	16.8	–1.0

[a] Data from ref. 7

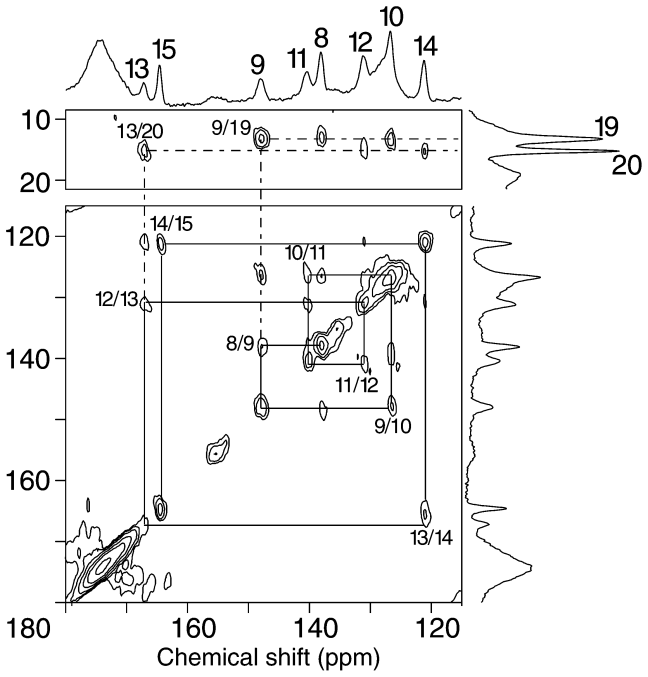

Figure 3.3: Detail of the contour plot of the ^{13}C MAS 2-D dipolar correlation spectrum collected from rhodopsin reconstituted with a 10-fold ^{13}C labeled retinal. The data are recorded at 223K and with a spinning frequency of 12.000 Hz ± 3 Hz. The solid lines indicate the correlation network of the ^{13}C labeled carbons in the polyene and the dashed lines indicate the connectivities with the methyl groups. The complete assignment of the carbons is indicated in the projection.

The incorporation of a multispin ^{13}C cluster gives the possibility to assign the NMR response with broadband dipolar correlation spectroscopy. To assign all ^{13}C labeled carbons in a single experiment, we have performed 2-D RFDR dipolar correlation spectroscopy with simulated phase sensitive detection in t_1.[26] This approach is easy to implement and it has been shown in experimental and theoretical studies that it is much more broadband than originally thought.[26,27] In particular, in practical cases it provides strong correlation signals when the chemical shift differences are small, *i.e.* cross peaks close to the diagonal in the 2-D experiment.

The connectivities between adjacent ^{13}C isotopes that are obtained with the 2-D spectrum shown in Figure 3.3 confirm the utility of the phase sensitive RFDR experiment for the assignment of olefinic carbons with small chemical shift dispersion in the solid state and lead to a complete assignment of the signals from the labels (Table 3.1). Additional weak correlations reveal some relayed magnetization transfer in the multispin ^{13}C network and they support the assignments listed in the Table 3.1. The chemical shift measurements obtained with a multispin labeled cluster in the retinylidene have a relative precision of ~0.1 ppm, considerably better than the ~1 ppm reported for the data collected from the specifically labeled retinals that were used in a stepwise serial approach.[8]

3.5 DISCUSSION

The multispin labeling and the assignment of the ^{13}C signals from dipolar correlation spectroscopy on the multispin cluster can be used to resolve essential details of the electronic structure of the ligand in the G-protein coupled receptor target in a single experiment. In Figure 3.4 three different schemes are presented for translating the chemical shift information into a MAS NMR shift image using color-encoded spheres around the labeled carbon atoms. The size of the spheres corresponds with 0.85 Å, which is equal to half the Van der Waals radius of carbon.[28] In rhodopsin the chromophore carries a full positive charge, due to the protonation of the SB nitrogen (Figure 3.1A).

The difference between rhodopsin (Figure 3.1A) and the PSB model N-(11-Z-retinylidene) propyliminium chloride (Figure 3.1B) is represented by plotting the chemical shift differences $\Delta\sigma_{PSB}=\sigma_{Rho}-\sigma_{PSB}$ at each atom (Table 3.2). The corresponding effect on the ν_{max} is commonly referred to as the 'opsin shift'.[29] In Figure 3.4A the effect of the protein environment on the charge distribution is visualized.

Table 3.2: Chemical shift differences for the 11-Z-PSB in rhodopsin relative to the model compounds 11-Z-PSB ($\Delta\sigma_{PSB}$), 11-SB ($\Delta\sigma_{SB}$) and 11-Z-β-carotene ($\Delta\sigma_{Car}$).

carbon	$\Delta\sigma_{PSB}$ [a]	$\Delta\sigma_{SB}$ [a]	$\Delta\sigma_{Car}$ [b]
8	1.3	0.5	0.7
9	1.6	8.9	11.2
10	0.8	0.9	0.1
11	3.3	13.1	15.7
12	2.5	–0.2	–2.1
13	4.9	22.6	31.2
14	0.3	–8.4	–11.4
15	1.1	5.4	35.0
19	1.4	1.6	1.0
20	–3.0	–1.9	–1.5

[a] Data on the PSB and SB from ref.22 [b] Data on carotene from ref. 23

When the new assignment is compared with the earlier results, it transpires that the effect of the medium containing the protein on details of its electronic structure is small (Table 3.1). The chemical shifts of the polyene carbons agree with those reported for the series of single label experiments, essentially within its error margin of 1 ppm. The difference of 1.5 ppm for C-13 and the systematic deviation of the other carbons may however indicate slightly less positive charge polarization in the natural lipid environment compared to the rhodopsins in detergent (Table 3.1). The structure of the isomerization region of the retinylidene chromophore in rhodopsin has been determined at high resolution with MAS NMR distance measurements and Car-Parrinello *ab initio* density functional methods.[11,30]

The ligand is forced into a nonplanar 12-s-*trans* conformation by nonbonding steric constraints of the protein binding pocket. This structure is different from the more relaxed 12-s-*cis* conformation commonly observed for 11-Z-PSB models in solution.[31,32] The upfield shift of C-20 relative to the PSB model is not yet explained in detail. The stabilization of additional positive charge at C-13 and the adjacent polyene carbons has been attributed before to mutual polarization effects between the polyene and the Glu113.[7,8] A recent X-ray model for rhodopsin confirms that Glu113 stabilizes the PSB in rhodopsin. However in the X-ray model Glu113 is positioned somewhat closer to the PSB nitrogen than for a seminal 3-D structural model inferred from chemical shift constraints.[24,33]

The shift differences $\Delta\sigma_{SB}=\sigma_{Rho}-\sigma_{SB}$ between rhodopsin and the unprotonated 11-Z-SB (Figure 3.1C) are visualized in Figure 3.4B. The more extended the delocalization of positive charge into the polyene, the more excess positive charge is stabilized on the odd-numbered atoms and the more downfield their chemical shift values. Hence, the Figure 3.4B clearly shows that the chemistry of protonation of the SB involves delocalization of the positive charge into the polyene. In addition, there is an increase of charge density alternation between the odd and even numbered atoms at the SB end of the chromophore, which is reflected in downfield and upfield $\Delta\sigma_{SB}$. The positive charges on the odd-numbered lattice positions induce correlated negative charge polarization on the even-numbered positions *via* the Coulomb interaction. As a general rule, the upfield shifts for the even-numbered carbons increase when the delocalization of the positive charge at the odd-numbered carbons is more pronounced.[34]

Finally, we show in Figure 3.4C the difference $\Delta\sigma_{Car}=\sigma_{Rho}-\sigma_{Car}$ between corresponding carbons in rhodopsin and 11-Z-β-carotene (Figure 3.1D). This carotenoid represents an unpolarized reference compound with the characteristic structural properties of an 11-Z retinoid (Figure 3.1D).

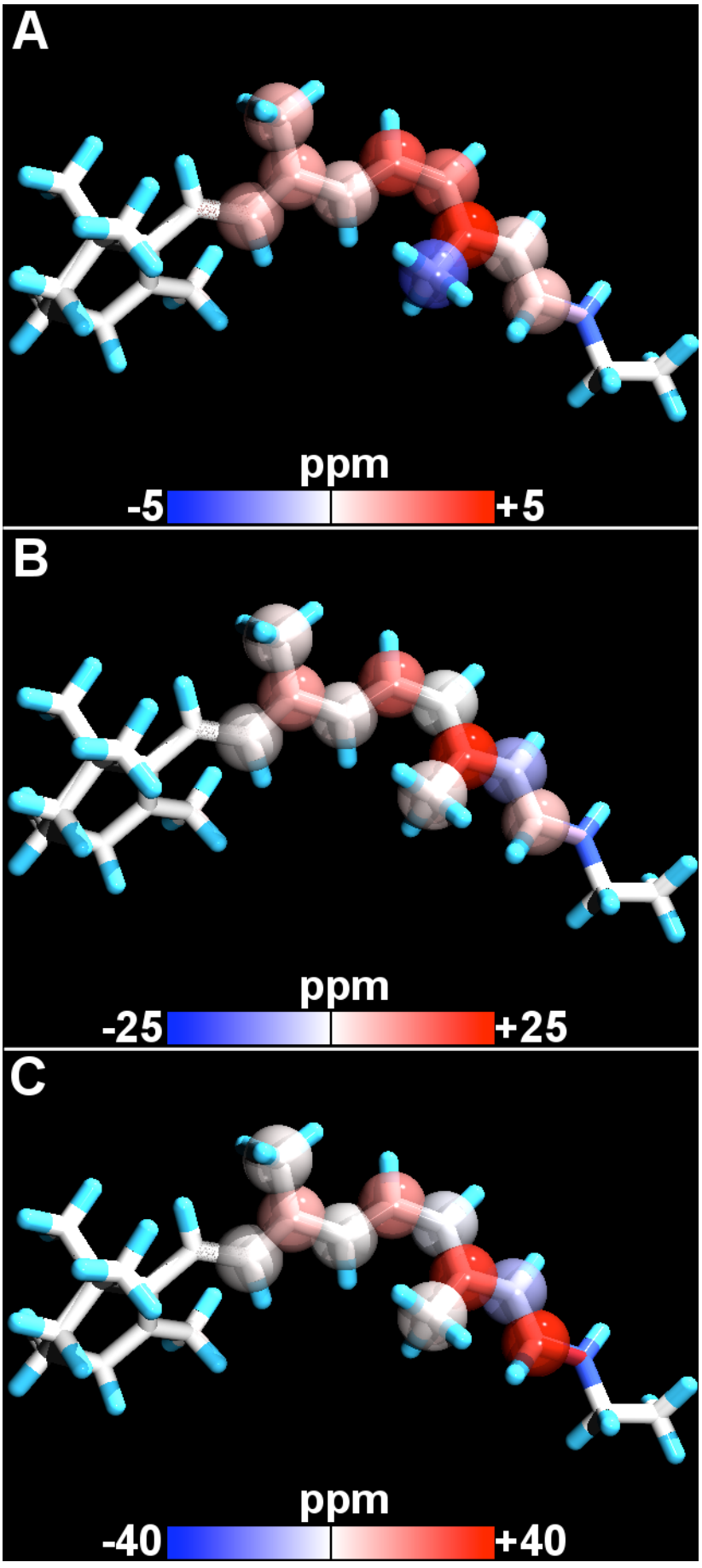

Figure 3.4: MAS NMR shift images of the retinylidene chromophore in rhodopsin. The structural model is taken from reference[30]. The Δσ are indicated with translucent spheres around the atom. Blue and red indicate upfield and downfield shifts, respectively, and the larger the shift the darker the color. (A) Difference $\Delta\sigma_{PSB}$ between rhodopsin and PSB model N-(11-Z-retinylidene) propyl iminium chloride. (B) Difference $\Delta\sigma_{SB}$ between rhodopsin and the analogue SB. (C) Difference $\Delta\sigma_{Car}$ between rhodopsin and the 11-Z-carotene. The shift differences correspond with Table 3.2.

Presented in this way, the $\Delta\sigma_{Car}$ reveal the positively charged conjugation defect that was extensively discussed in recent literature.[30,35-39] The conjugation defect is an emerging property with a half-width of about 3 bond lengths. It is autolocalized due to a balance between the energy gain associated with delocalization of the electrons involved on the one hand, and the energy cost due to the deformation of the underlying molecular frame. The defect is thermodynamically stable in the ground state and corresponds chemically with a region of enhanced nonbonding character and a nodal plane in the molecular electronic structure. The conjugation defect in the polyene of rhodopsin is thought to mediate the primary step in vision in a classically coherent dynamic process by increasing the effective mass of the electronic charge by two orders of magnitude. Its autolocalized nodal plane can be confined to the isomerization region and transferred over a carbon-carbon bond. In this scheme the Z to E isomerization process is driven by the necessity to preserve the overall bonding character in the retinylidene moiety and involves only very minor atomic displacements, mainly the transfer of a single H-12 to the opposite side of the C11=C12 bond.[30,36,40]

This mechanism is essentially different from a scheme that involves a significant motion of the C-13 methyl group or the H-10 driving the isomerization process by releasing nonbonding steric interaction, as has been inferred from linear extrapolation of excited state surface motion upon photoexcitation.[41] It is however in line with FTOA measurement that provide strong evidence that a motion of hydrogens attached to the C11=C12 double bond becomes predominant during photoisomerization at a time scale of more than 70 fs after photoexcitation.[42]

The total amount of positive charge that is induced on the carbons in the retinylidene of rhodopsin can now be divided into three synergistic contributions: 1. polarization by the electronegative SB nitrogen, 2. protonation of the SB nitrogen and 3. mutual polarization effects between the counterion and the protonated SB nitrogen. An approximately linear relation between ^{13}C shift difference and relative atomic charge density has been reported for conjugated systems.[43-45] The cumulative changes $\Delta\sigma^{tot}$ for the observed polyene carbons listed in Table 3.2 can be translated into electronic charge density differences by using a conversion factor of +155 ppm/unit charge. In this way the total polarization associated with each of the three terms can be estimated. Comparing rhodopsin with the 11-Z-β-carotene, the $\Delta\sigma^{tot}_{Car}$ listed in the last column in Table 3.2 add-up to 80.5 ppm. Hence the total amount of positive charge accumulated by the polyene carbons is approximately ~0.5 electronic equivalent, which is mainly located on C-15 and C-13. This is an important observation, since it indicates that the center of the conjugation

defect may be inside the polyene, in qualitative agreement with the theoretical predictions.[30,36] Such a delocalized charge is expected to affect the C–C/C=C bond length alternation pattern, in the same way a polaronic exitation perturbs the polyene bond alternation pattern in an infinite conjugated chain.[46,47] The coupling between electronic configuration and the underlying molecular framework in a polyene is particularly strong. A charge in a polyene perturbs the backbone locally and corresponds with a HOMO with nonbonding character that is self-localized and confined to a region in which the bond length alternation is reduced.[46,48] In the case of rhodopsin such a perturbation causes that the double bond character of the C-15/N and C-13/C-14 will be reduced, while the C-14/C-15 bond will have increased double bond character. The delocalization of positive charge and the region in which the bond length alternation pattern is affected are schematically indicated in Figure 3.1A. Crystal structure data for PSB model compounds provide strong support for the concept of a decrease of bond length alternation due to charging. To detect the center of the conjugation defect in the polyene the dimerization amplitudes[49]

$$D_{i,j,k} = d_{i,j} - d_{j,k} \qquad (1)$$

can be calculated following reference [30]. Here $d_{i,j}$ and $d_{j,k}$ denote the bondlengths between atoms i,j and j,k of adjacent bonds. A conjugation defect is present in the polyene when a $D_{i,j,k}$ has the same sign as $D_{i+1,j+1,k+1}$. For instance, for (all-E)-β-carotene, without charge or polarization, the sign of the dimerization amplitude alternates over the entire polyene with $|D_{i,j,k}| \sim 0.15$ Å.[50] This contrasts with high resolution X-ray structural data obtained for PSB models N-(all-E-retinylidene) *tert*-butyliminium perchlorate and triflate[25] which clearly show reduced bond length alternation with the smallest value of $D_{13,14,15} = -0.05$ Å at the SB end of the polyene chain.[25] Since the electron-lattice interaction is generally the pre-dominant interaction in polyenes, the results for the PSB models imply that a similar defect and associated decreased bond length alternation can be expected for the Schiff base in rhodopsin upon charging.

According to the values of $\Delta\sigma_{Car}$ in Table 3.2, the C-15 of the retinylidene in rhodopsin accumulates ~0.23 electronic equivalents of positive charge, slightly more than the ~0.20 equivalents on C13. In addition, the total cumulative charge difference between the carbon atoms of rhodopsin and carotene appears not larger than ~0.5 electronic equivalent. This suggests that the conjugation defect has not entirely moved into the carbon part of the polyene. It

contrasts with theoretical calculations of the system in vacuum, which put a conjugation defect between C13 and C15, as calculated from the sign pattern of the dimerization amplitude.[30]

Protonation of the SB nitrogen also increases the amount of delocalized charge on the carbons. The shift pattern provides additional support for a conjugation defect located in the polyene close to the SB nitrogen, fully established by the protonation event. The excess charge injected into the polyene of rhodopsin by the protonation yields a total cumulative shift of 43.0 ppm, calculated from the $\Delta\sigma_{SB}$ in Table 3.2. This leads to the conclusion that an estimated ~0.3 electronic equivalent out of the total of ~0.5 calculated for the $\Delta\sigma^{tot}_{Car}$ is associated with the process of protonation in the binding site, measured by $\Delta\sigma^{tot}_{SB}$. It is a crucial observation that this ~0.3 charge is mainly transferred to the C11 and the C13, and not to the C15, fully in line with the concept of an autolocalized defect! (Figure 3.4B). It also illustrates that the polarization due to the electronegative nitrogen in the SB provides a considerable contribution of ~0.2 electronic equivalent to the total amount of positive charge in the polyene (Figure 3.1C).

Recently, it was concluded from ^{15}N MAS NMR studies that the PSB in rhodopsin is stabilized by a complex counterion.[12] This was based on a set of correlations between ^{15}N shift and the ν_{max} and between ν_{max} and the effective center-center distance between counterion and the PSB nitrogen. The weaker the interaction between PSB and counterion, the more extended the delocalization of the positive charge from the protonated nitrogen into the polyene. The charge $\Delta\sigma^{tot}_{PSB}$ between the PSB in rhodopsin (Figure 3.1A) and the PSB model (Figure 3.1B) yield a moderate total shift of 15.9 ppm, corresponding with ~0.1 electronic equivalent. This is attributed to a complex counterion environment in the protein. The delocalization of positive charge over the polyene establishes a HOMO and LUMO, both with pronounced nonbonding character, well inside the gap between the π and $\pi*$ molecular orbital manifolds.

Protonation of the SB nitrogen and decreasing the counterion strength will give rise to an increase of the energy of the HOMO, accompanied by a decrease of the energy of the LUMO.[30,51] It is thus interesting to search for a correlation between the HOMO-LUMO gap measured by the ν_{max} and the extent of the polarization into the polyene that is measured in our NMR experiment. This is most conveniently done by taking the 11-Z unprotonated SB as the reference compound (cf. Figure 3.4C). The extent of positive charge delocalization on the odd-numbered carbons due to protonation can be estimated for several 11-Z-6-s-*cis*-PSB models with different counterions by taking the cumulative shift difference of the odd-numbered carbons, $\Delta\sigma_{odd} = \Sigma(\sigma_{PSB,odd} - \sigma_{SB,odd})$.

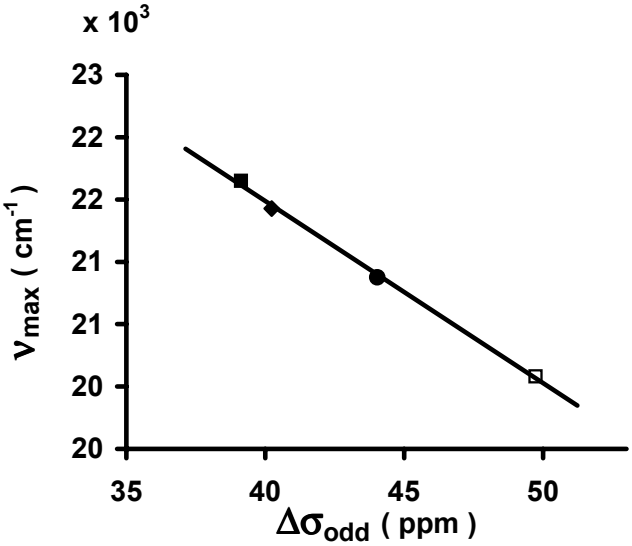

Figure 3.5: Relation between ν_{max} and $\Delta\sigma_{odd}$ for 11-Z-PSB salts with different counterions and rhodopsin. The line represents the linear least-squares fit to the points with $R^2 = 0.998$. The 11-Z-PSB salts are indicated with solid markers: N-(11-Z-retinylidene) propylimine chloride ref. 22 (■), the trifluoroacetaat ref. 22 (♦) and the bromide ref. 24 and 12 (●). Rhodopsin is indicated with an open marker, values are from this work (□).

Figure 3.5 shows that $\Delta\sigma_{odd}$ is well correlated with ν_{max}. The shift difference at C-15 going from the SB to the 11-Z-PSB model or rhodopsin is small and hence the C-15 has a small contribution to $\Delta\sigma_{odd}$. By consequence, $\Delta\sigma_{odd}$ mainly reflects differences at the C-13 and C-11. Thus, the correlation between ν_{max} and $\Delta\sigma_{odd}$ measures the extent of positive charge delocalization into the polyene. An approximate linear relation transpires after performing a linear least-square fit according to:

$$\nu_{max} = -1.46 \times 10^2 \, (\Delta\sigma_{odd}) + 27.3 \times 10^3 \qquad (2).$$

Eq. 2 fulfills the requirement of self-consistency that the offset 27.3×10^3 is nearly the same as the ν_{max} of 27.4×10^3 cm^{-1} of the SB, the uncharged point of reference. This confirms that the correlation is almost linear. Eq. 2 encompasses rhodopsin and, compared to the PSB models, for rhodopsin a small HOMO-LUMO gap correlates with a large extent of positive charge delocalization. Since the data point for rhodopsin in Figure 3.5 is well outside the region spanned by the model compounds, our data provide strong evidence that the anion provided by the protein is very weak. This is an essential characteristic of some form of a complex counterion, fully in line with the analysis of recent ^{15}N MAS NMR measurements on rhodopsin.[12] It is remarkable that both the decrease of charge measured by the nitrogen shift and

the resulting increase of positive charge measured with the carbons shifts correlate with ν_{max}, which validates the use of both ^{15}N and ^{13}C shifts to probe the counterion strength. A relation between the ν_{max} and the effective center-center distance

$$d_{eff} = 24.17\ [\nu_{max} - (1.70 \times 10^4)]^{-1/2} \qquad (3)$$

between the centers of the counterion and the SB nitrogen was deduced for 11-Z and all-E-PSBs in solution.[12] Since $\Delta\sigma_{odd}$ also correlates with the ν_{max}, Eq. 3 yields an effective center-center distance of 0.43 nm of the ion-pair in the active site of rhodopsin. In this way the ^{13}C MAS NMR contributes to converging spectroscopic evidence for a complex counterion stabilizing the PSB in rhodopsin. The effective distance of 0.43 nm is considerably larger than the ~0.34 nm proposed in the recently derived crystal structure model of rhodopsin.[32] This suggests the presence of a hydrogen bonded water molecule between the PSB and the carboxylate of Glu113 (N^+–H···OH_2···O^-).[12] In parallel, the Eqs. 2 and 3 indicate that spectral tuning of rhodopsins and the cone pigments responsible for color vision, in the regime λ<500 nm, can be accomplished also by varying the anionic interactions exerted by the protein pocket in the vicinity of the PSB.

3.6 Conclusions

2-D solid-state NMR correlation data collected from rhodopsin reconstituted with synthetically prepared multispin labeled retinal can be used to assign the chemical shifts of the chromophore and to provide a MAS NMR shift image of the ligand-protein interactions and the electronic structure of the ligand. This direct method is much faster and considerably improves the relative precision of the shift measurements compared to the established method of using specifically labeled retinals in a serial approach. The ^{13}C chemical shifts observed for the carbons in the polyene of the chromophore in rhodopsin in its native lipid environment are marginally different from the shifts determined for the detergent-solubilized system. It is illustrated how multispin labeling in combination with solid-state 2-D correlation spectroscopy can be a versatile method for assessment of ligand-protein interactions for GPCR targets and other membrane proteins. An analysis of the SB environment supports the model of stabilization of the protonation by a complex counterion. In addition, it is shown that the excess positive charge in the polyene is due to the three synergistic contributions:

the electronegative nitrogen, the protonation and the counterion strength. Finally, NMR analysis of the molecular electronics of the retinylidene chromophore reveals essential characteristics of a conjugation defect in the polyene of rhodopsin that is stable in the ground state.

REFERENCES

(1) Watson, S.; Arkinstall, S. *The G-protein Linked Receptor Fact Book*; Academic Press: San Diego, 1994.
(2) Tang, L.; Ebrey, T. G.; Subramaniam, S. *Isr. J. Chem.* **1995**, *35*, 193-209.
(3) Pogozheva, I. D.; Lomize, A. L.; Mosberg, H. I. *Biophys. J.* **1997**, *72*, 1963-1985.
(4) Verdegem, P. J. E.; Lugtenburg, J.; De Groot, H. J. M. In *Pharmacochemistry Library Vol. 26 Stable Isotopes in Pharmaceutical Research*; Browne, T. R., Ed.; Elsevier: Amsterdam, 1997, Chapter 10.
(5) Wald, G. *Science* **1962**, *162*, 230-239.
(6) Hubbard, R.; Kropf, A. *Proc. Natl. Acad. Sci. U. S. A.* **1958**, *44*, 130-139.
(7) Smith, S. O.; Palings, I.; Miley, M. E.; Courtin, J.; De Groot, H. J. M.; Lugtenburg, J.; Mathies, R. A.; Griffin, R. G. *Biochemistry* **1990**, *29*, 8158-8164.
(8) Smith, S. O.; Courtin, J.; De Groot, H. J. M.; Gebhard, R.; Lugtenburg, J. *Biochemistry* **1991**, *30*, 7409-7415.
(9) Smith, S. O.; De Groot, H. J. M.; Gebhard, R.; Lugtenburg, J. *Photochem. Photobiol.* **1992**, *56*, 1035-1039.
(10) Feng, X.; Verdegem, P. J. E.; Lee, Y. K.; Sandstrom, D.; Eden, M.; Bovee-Geurts, P. H. M.; DeGrip, W. J.; Lugtenburg, J.; De Groot, H. J. M.; Levitt, M. H. *J. Am. Chem. Soc.* **1997**, *119*, 6853-6857.
(11) Verdegem, P. J. E.; Bovee-Geurts, P. H. M.; DeGrip, W. J.; Lugtenburg, J.; De Groot, H. J. M. *Biochemistry* **1999**, *38*, 11316-11324.
(12) Creemers, A. F. L.; Klaassen, C. H. W.; Bovee-Geurts, P. H. M.; Kelle, R.; Kragl, U.; Raap, J.; DeGrip, W. J.; Lugtenburg, J.; De Groot, H. J. M. *Biochemistry* **1999**, *38*, 7195-7199.
(13) Bennett, A. E.; Ok, J. H.; Griffin, R. G.; Vega, S. *J. Chem. Phys.* **1992**, *96*, 8624-8627.
(14) Griffin, R. G. *Nat. Struct. Biol.* **1998**, *5*, 508-512.
(15) EgorovaZachernyuk, T. A.; vanRossum, B.; Boender, G. J.; Franken, E.; Ashurst, J.; Raap, J.; Gast, P.; Hoff, A. J.; Oschkinat, H.; De Groot, H. J. M. *Biochemistry* **1997**, *36*, 7513-7519.
(16) Lugtenburg, J.; Creemers, A. F. L.; Verhoeven, M. A.; van Wijk, A. A. C.; Verdegem, P. J. E.; Monnee, M. C. F.; Jansen, F. J. H. M. *Pure Appl. Chem.* **1999**, *71*, 2245-2251.
(17) Lugtenburg, J. *Pure Appl. Chem.* **1985**, *57*, 753-762.
(18) DeGrip, W. J.; Deamen, F. J. M.; Bonting, S. L. *Meth. Enzym.* **1980**, *67*, 301-320.
(19) DeLange, F.; Bovee-Geurts, P. H. M.; VanOostrum, J.; Portier, M. D.; Verdegem, P. J. E.; Lugtenburg, J.; DeGrip, W. J. *Biochemistry* **1998**, *37*, 1411-1420.
(20) Metz, G.; Wu, X. L.; Smith, S. O. *J. Magn. Reson. Ser. A* **1994**, *110*, 219-227.
(21) Bennett, A. E.; Rienstra, C. M.; Auger, M.; Lakshmi, K. V.; Griffin, R. G. *J. Chem. Phys.* **1995**, *103*, 6951-6958.
(22) Shriver, J. W.; Mateescu, G. D.; Abrahamson, E. W. *Biochemistry* **1979**, *18*, 4785-4792.
(23) Englert, G. In *Carotenoids Volume 1B: Spectroscopy*; Britton, G., Liaaen-Jensen, S., Pfander, H., Eds.; Birkhauser Verlag: Basel, 1995, p 212 and 214.
(24) Han, M.; Dedecker, B. S.; Smith, S. O. *Biophys. J.* **1993**, *65*, 899-906.
(25) Elia, G. R.; Childs, R. F.; Britten, J. F.; Yang, D. S. C.; Santarsiero, B. D. *Can. J. Chem.* **1996**, *74*, 591-601.

(26) Boender, G. J.; Raap, J.; Prytulla, S.; Oschkinat, H.; De Groot, H. J. M. *Chem. Phys. Lett.* **1995**, *237*, 502-508.
(27) Boender, G. J.; Vega, S.; De Groot, H. J. M. *J. Chem. Phys.* **2000**, *112*, 1096-1106.
(28) Bondi, A. *J. Phys. Chem.* **1964**, *68*, 441-451.
(29) Nakanishi, K.; Baloghnair, V.; Arnaboldi, M.; Tsujimoto, K.; Honig, B. *J. Am. Chem. Soc.* **1980**, *102*, 7945-7947.
(30) Buda, F.; De Groot, H. J. M.; Bifone, A. *Phys. Rev. Lett.* **1996**, *77*, 4474-4477.
(31) Albeck, A.; Livnah, N.; Gottlieb, H.; Sheves, M. *J. Am. Chem. Soc.* **1992**, *114*, 2400-2411.
(32) Palczewski, K.; Kumasaka, T.; Hori, T.; Behnke, C. A.; Motoshima, H.; Fox, B. A.; Le Trong, I.; Teller, D. C.; Okada, T.; Stenkamp, R. E.; Yamamoto, M.; Miyano, M. *Science* **2000**, *289*, 739-745.
(33) Han, M.; Smith, S. O. *Biochemistry* **1995**, *34*, 1425-1432.
(34) Boudreaux, D. S.; Chance, R. R.; Bredas, J. L.; Silbey, R. *Phys. Rev. B* **1983**, *28*, 6927-6936.
(35) Bifone, A.; De Groot, H. J. M.; Buda, F. *Pure Appl. Chem.* **1997**, *69*, 2105-2110.
(36) Bifone, A.; De Groot, H. J. M.; Buda, F. *J. Phys. Chem. B* **1997**, *101*, 2954-2958.
(37) Aalberts, D. P.; Vos, F. L. J.; vanSaarloos, W. *Pure Appl. Chem.* **1997**, *69*, 2099-2104.
(38) La Penna, G.; Buda, F.; Bifone, A.; De Groot, H. J. M. *Chem. Phys. Lett.* **1998**, *294*, 447-453.
(39) De Groot, H. J. M. *Curr. Opin. Struct. Biol.* **2000**, *10*, 593-600.
(40) Buss, V.; Weingart, O.; Sugihara, M. *Angew. Chem.-Int. Edit.* **2000**, *39*, 2784-2786.
(41) Kochendoerfer, G. G.; Verdegem, P. J. E.; Van der Hoef, I.; Lugtenburg, J.; Mathies, R. A. *Biochemistry* **1996**, *35*, 16230-16240.
(42) Kakitani, T.; Akiyama, R.; Hatano, Y.; Imamoto, Y.; Shichida, Y.; Verdegem, P.; Lugtenburg, J. *J. Phys. Chem. B* **1998**, *102*, 1334-1339.
(43) Spiesecke, H.; Schneider, W. G. *Tetrahedron Lett.* **1961**, 468-472.
(44) Lauterbur, P. *J. Am. Chem. Soc.* **1961**, *83*, 1838-1846.
(45) Tokuhiro, T.; Fraenkel, G. *J. Am. Chem. Soc.* **1969**, *91*, 5005-5013.
(46) Pople, J. A.; Walmsley, S. H. *Mol. Phys.* **1962**, *5*, 15-20.
(47) Su, W. P.; Schrieffer, J. R.; Heeger, A. J. *Phys. Rev. B* **1980**, *22*, 2099-2111.
(48) Salaneck, W. R.; Friend, R. H.; Bredas, J. L. *Phys. Rep.-Rev. Sec. Phys. Lett.* **1999**, *319*, 232-251.
(49) Peierls, R. E. *Quantum theory of solids*; Oxford University Press: London, 1955.
(50) Sterling, C. *Acta Crystallographica* **1964**, *17*, 1224-1228.
(51) Lu Yu *Solitons & polarons in conducting polymers*; World Scientific Press: Singapore, 1988.

Chapter 4

Methyl substituents at the 11- or 12-position of retinal profoundly affect photochemistry and function of rhodopsin

4.1 Abstract

In this chapter the protein-ligand interactions, photoisomerisation and receptor activation of the rhodopsin analogues resulting from incorporation of 11-Z 11-methyl, 11-Z 12-methyl and 11-Z and 9-Z 11-methyl-13-desmethyl retinal into opsin are investigated. UV-Vis and FTIR spectroscopy and a G-protein activation assay are used to resolve details of the ligand-receptor communication and photoactivation for the native pigment of the receptor and for its photointermediates. The results indicate that the formation of the first photointermediate is slowed down by the presence of an 11-methyl substituent, while for the 12-methyl substituent a Batho-like intermediate is formed reversibly and with Φ=0.54±0.08, nearly as efficient as in the native pigment (Φ=0.67). These results suggest that counter rotation of the C11H and C12H elements of the polyene lead to the required *trans* position in bathorodopsin, in contrast with a rotation of C12H only.

In addition, the data in this study show that, compared to the native system 11- or 12-methyl modification of the retinylidene chromophore leads to a lower incorporation efficiency, delays the formation of the late photointermediates and finally yields a low activity state of the receptor (<30%). The removal of the 13-methyl group in 11-methyl-13-desmethyl rhodopsin partly compensates for these effects. The receptor activation data suggest that pronounced spatial perturbations of the protein in the vicinity of the extracellular loop 2 triggered by the relaxation of the distorted retinylidene ligand produce a more disordered protein that crosses the energy barrier towards the active receptor conformation more easily.

4.2 Introduction

Rhodopsin is the G-protein coupled photoreceptor protein in the retina of vertebrates that initiates the visual transduction cascade in dim light vision.[1,2] Rhodopsin (Rho) contains a protonated 11-Z retinylidene Schiff base in the active site of the receptor protein that functions as an inverse agonist. The protein binds this ligand in the 12-s-*trans* conformation and the nonbonding interactions between the C13 methyl group and the C10 hydrogen give rise to a nonplanar structure.[3] The resulting torsions in the chromophore configure the polyene tail for fast photoisomerisation around the C11=C12 double bond.[3-5] Within 200 fs following light absorption a primary photoproduct bathorhodopsin (Batho) is formed that contains a highly strained protonated all-E retinylidene Schiff base in the active site.[4,6] Subsequent thermal steps lead within milliseconds to the signalling intermediate metarhodopsin-II (Meta-II), which contains a relaxed unprotonated all-E retinylidene Schiff base in the active site that acts as a full

agonist.[7] Studies on Rho analogues without the 9- or 13-methyl group (C19, C20) have established that these methyl groups contribute significantly to the propagation of the photochemical cascade leading to the signalling state of the protein.[2,8,9] For example, the absence of the 13-methyl group leads to a significant lower quantum yield of Φ=0.47 compared to Φ=0.67 for native Rho, while upon light absorption by 9-desmethyl Rho, the active state 9-desmethyl Meta-II is generated with much lower efficiency.

Chemical modification of the isomerisation region of the 11-Z retinylidene moiety (C10••C13) can help to provide insight into the structural basis of the high rate and efficiency of the photochemical reaction.[2,9] For instance, it was observed that 10-methyl Rho has a lower quantum yield Φ=0.55 compared to the native system and that thermal conversion of the first photoproduct (Batho) to the next intermediate is shifted to a higher temperature.[2,10,11] An additive effect is observed upon removal of the 13-methyl group, further reducing the quantum yield of 10-methyl-13-desmethyl Rho to Φ=0.35.[8]

Here, the effect of methyl substitution in three novel rhodopsin analogues prepared from 11-methyl, 12-methyl and 11-methyl-13-desmethyl retinal (Scheme 4.1) is investigated. The photochemical and biochemical properties of the 11-Z and the 9-Z analogues are studied with the aid of UV-Vis and FTIR spectroscopy techniques and a G-protein activation assay. The aim of this study is to resolve and understand details of ligand-receptor communication and photoactivation in the native pigment. The results indicate mixed effects of methyl group insertion at these positions on (i) protein-ligand interaction and at two stages in the photosequence, (ii) the photoisomerisation and (iii) receptor activation at the final stage.

4.3 Materials and Methods

4.3.1 Synthesis

All syntheses have been performed via Wittig and Horner-Wadsworth-Emmons strategies that are generally used for retinoids and carotenoids.[12,13] Synthesis of 9-Z 11-methyl retinal is performed in the dark and is accomplished by the condensation of β-ionylidene phosphonium bromide[14] and aldehyde 2,4-dimethyl-5-cyano-penta-2,4-dienal in THF at –20° with LDA as a base. The aldehyde can be prepared from 1,1-dimethoxy acetone and 4-(diethyl phosphono)-3-methyl-2-butenenitrile followed by acidic deprotection of the acetal. Reduction of the retinonitrile with DIBAl-H gives a mixture of all-E and 9-Z retinal isomers that can be separated by column chromatography (silica with diethylether/PE-20/80 v/v as eluent).

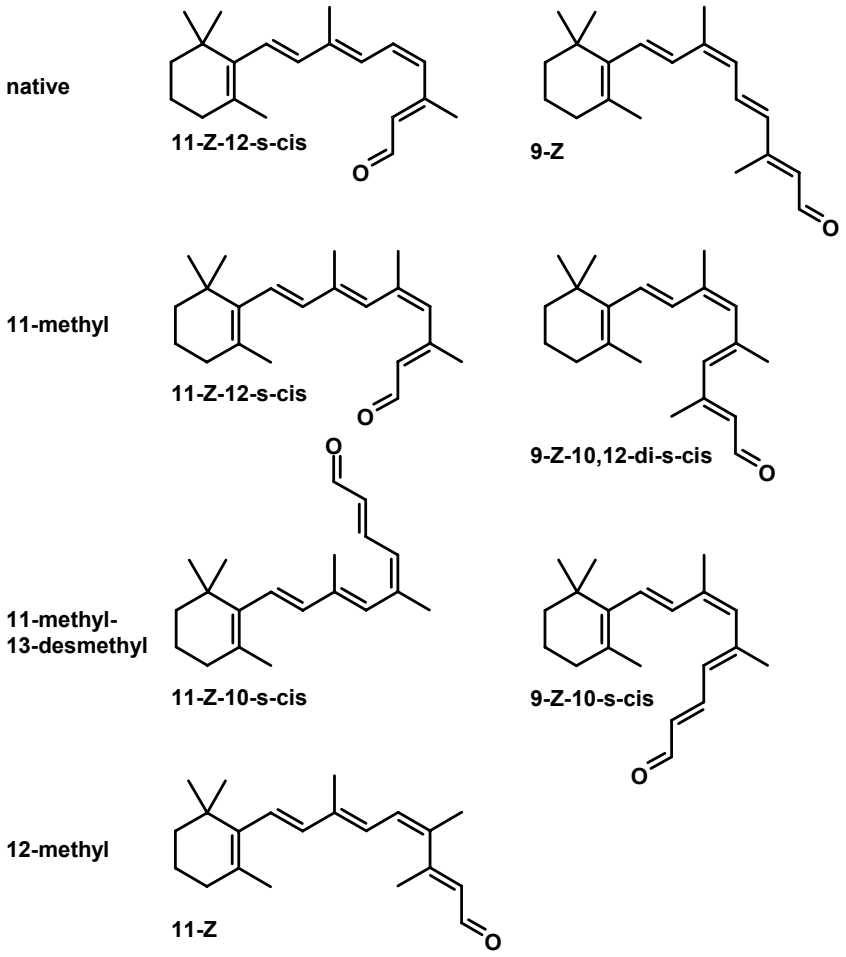

Scheme 4.1. Principal solution conformations of the retinal derivatives used in this study determined by NOE NMR spectroscopy. On the left the structures of the 11-Z configurations are shown, on the right the 9-Z structures.

Synthesis of 11-Z 11-methyl retinal is done in the dark by condensation of (β-ionylidene prop-2-yl) triphenylphosphonium bromide and 3-cyano-2-methyl-propa-2-enal in refluxing 1-butene oxide. The Wittig salt is prepared from β-ionylidene acetaldehyde,[15] by reduction of the aldehyde function with methyl lithium and coversion of the resulting secondary alcohol to the phosphonium salt according to Olive *et al.*[14] The aldehyde is made from the previously described acetal[16] by acidic deprotection of the acetal in 2% phosphoric acid at 60°C. Reduction of the retinonitrile with DIBAl-H gives all-E and 11-Z isomers that can be separated by column chromatography (silica with diethylether/PE-20/80 v/v as eluent). Synthesis of 11-methyl-13-desmethyl retinal is accomplished by condensation of β-ionylidene phosphonium bromide[14] and aldehyde 5-methyl-6-oxo-hexa-2,4-dienoic ethyl ester in refluxing 1-butene oxide. The latter aldehyde is prepared from 4-(diethylphosphono) buta-2-enoic ethyl ester[17] and 1,1-dimethoxy acetone with subsequent deprotection of the acetal. Reduction of the retinoic ester to the alcohol by titration with at least 2 equiv. DIBAl-H in dry PE and oxidation of the alcohol with MnO_2 in

dichloromethane gives a mixture of retinal isomers. This mixture is enriched in the 9-Z and 11-Z isomers by irradiation and the isomers are subsequently isolated by HPLC.[13] Synthesis of 12-methyl retinal is accomplished by reaction of β-ionylidene acetaldehyde with 2-(diethyl phosphono) propanoic ethyl ester[18] and subsequent conversion of the ester to the methyl ketone by reaction with methyllithium in the presence of trimethylsilylchloride at −100 °C.[19] Aqueous work-up yields the methyl ketone that is converted to 12-methyl retinal by reaction with diethylphosphono acetonitrile and subsequent reduction with DIBAl-H. After irradiation the 11-Z isomer is isolated by HPLC separation.[13] The 9-Z 12-methyl retinal isomer was present as a minor component of presumably the 13-Z fraction and is not used in this study. Scheme 4.1 illustrates the principal solution structures of the compounds used in this study determined by 2-D NOE NMR spectroscopy.

4.3.2 Generation of rhodopsin analogues

Bovine rod outer segment membranes in the opsin form (opsin membranes) were prepared from fresh, light-adapted eyes.[20] The regeneration capacity of these preparations was estimated from the A280/A500 ratio that is obtained after incubation with a 3-fold excess of 11-Z retinal. A ratio of 2.0 represents membranes in which the Rho binding site is saturated with ligand. The opsin membranes that were used showed a regeneration capacity in the range of 90-100% for native 11-Z retinal. All manipulations were performed under dim red light (λ>610 nm, Schott RG610 long-pass filter) and the incubation was performed in an inert argon atmosphere. Opsin membranes were suspended in buffer A (20mM Pipes, 130mM NaCl, 4mM KCl, 2 mM $CaCl_2$, 0.1 mM EDTA and 1mM dithioerythreitol, pH 6.5), to a final opsin concentration of 50 μM. Aliquots of 2-3-fold molar excess of retinal or retinal derivative were added in a small volume of dimethylformamide (≤ 4% final volume) with 12 hour intervals until pigment formation had levelled. The pigment analogues were incubated for at least 12 and up to 48 hour with up to 10 equivalents of retinal derivative. The extent of pigment formation was assessed after every 12 hours of incubation by measuring an UV-Vis difference spectrum from a small aliquot (*cf.* 4.3.3). When pigment formation had levelled, the amount of opsin remaining was assessed in a small test sample from the incubation vessel, from the additional amount of Rho formed upon addition of 1 equivalent of 11-Z retinal. The total absorbance of pigment that was finally obtained in this sample $(A_{\lambda_{max}}^{\text{analogue}} + A_{498}^{\text{Rho}})$ was always within 10% of the control value (A_{498}^{Rho}). Hence, the molar extinction coefficients of the analogue pigments match the ε_{Rho} and were taken as ε_{An}=40,000. ± 4,000 $M^{-1}cm^{-1}$. To remove the excess of retinal analogue it was first converted into the corresponding oxime by addition of hydroxylamine to a concentration of 10

mM. Subsequently two extractions were performed with 50mM solutions of heptakis-(2,6-di-O-methyl)-β-cyclodextrin (Aldrich),[2,21] followed by washing twice with doubly distilled water. For 12-methyl Rho no hydroxylamine was used and only a single extraction step with cyclodextrin was performed. When a native lipid/protein ratio was required, the pigments were solubilised in 20 mM nonyl-1-β-glucoside in buffer A and mixed with a 50-fold molar excess of Asolectin (Sigma), a crude soybean lipid extract containing a mixture of natural phospholipids. Reconstitution in proteoliposomes was accomplished by centrifugation through a discontinuous sucrose gradient.[21] The resulting pigment membranes were washed with doubly distilled water and stored at –80 °C until further use.

4.3.3 Spectral analysis of the rhodopsin derivatives and photointermediate formation

The wavelengths of maximum absorbance (λ_{max}) for the various pigments were determined from the peak position in a difference spectrum obtained by subtracting the spectrum after 300 s illumination through a Schott GG430 long-pass filter from the dark-state spectrum. The data were collected in a mixed micellar solution with 10 mM hydroxylamine and 20 mM dodecyl-1-β-maltoside (DDM) in buffer A.

To assess the formation of photointermediates data were recorded from pigment membranes suspended in buffer A to a final concentration of 1 μM in pigment using a Perkin-Elmer Lambda 18 double beam spectrometer equipped with an end-on photomultiplier detector. A circulating bath was used to control the sample temperature. The sample was bleached for 10 s using a Schott OG530 long-pass filter and spectra were taken after selected time-intervals. After 40 minutes a spectrum was recorded in the presence of 10 mM hydroxylamine, followed by a spectrum after full bleaching.

4.3.4 Photosensitivity of pigments

The quantum yields of the analogue pigments were determined relative to $\Phi_{Rho} = 0.67$ or Isorhodopsin $\Phi_{Iso} = 0.27$ that are well characterised experimentally.[8,22,23] Pigments were solubilised in buffer A with 10 mM DDM and 10 mM hydroxylamine to give an absorbance at 500 nm of about 0.16. Solutions were kept at 10 °C and illuminated through a 504±5 nm or 497±10 nm interference filter (Schott). The illumination conditions were such that the halftime of pigment bleaching was between 30 and 60 minutes. Spectra were taken during 2 hours with intervals of 5-10 minutes. The halftime of the pigment absorbance decay in the dark provides a measure of pigment stability and was >20 hours. The slope S of a straight line through $A_f - \log(10^{A_t} - 10^{A_f})$ is a measure of the photosensitivity $\varepsilon\Phi$.[2,22] In this expression A_t denotes the absorbance at a selected wavelength after time t, and A_f is the absorbance after complete

bleaching. Comparison of the slopes gives the quantum yield of the pigment analogue (Φ_{An}) according to

$$\Phi_{An} = \frac{S_{An}}{S_{Rho}} \frac{\varepsilon_{Rho}}{\varepsilon_{An}} \Phi_{Rho} \qquad (1)$$

A similar analysis was performed for isorhodopsin (Iso) and 13-desmethyl Rho. According to our regeneration experiments the molar extinction coefficients of the pigment analogues are within 10% of the Rho value (see above) and Eq. 1 was used in a simplified form

$$\Phi_{An} = \frac{S_{An}}{S_{Rho}} \Phi_{Rho} \qquad (2)$$

The molar absorbance coefficient of Rho is ε_{Rho} = 40.600±500 M^{-1} cm^{-1} at 498 nm (λ_{max}). The molar absorbance coefficient of Iso ε_{Iso} = 43.000 M^{-1} cm^{-1} at λ_{max} (485 nm). At the excitation wavelength it matches the Rho absorption.[24]

4.3.5 FTIR spectroscopy

FTIR analyses were performed with a Bruker IFS 66/S spectrometer equipped with a liquid nitrogen-cooled, narrow band HgCdTe (MCT) detector. Spectra were taken with 2 cm^{-1} resolution. The sample temperature was computer controlled using a variable temperature helium-cooled cryostat (Heliostat, APD cryogenics Inc.) covered with a set of NaCl windows in the infrared light path. Membrane films of the samples were prepared by isopotential spin drying of 1-2 nmol of pigment on AgCl windows (Crystran Limited, UK) [25], which were subsequently rehydrated with buffer A and sealed using a second AgCl window and a rubber O-ring spacer.[26] Samples were illuminated in the spectrometer using a modified (150W halogen) fiberoptics ring illuminator (Schott) equipped with a 488 ± 10 nm interference filter (Schott) and a set of long-pass filters. Generally six spectra of the dark-state receptor of 1280 scans each with 120 s acquisition time per spectrum were taken and added. Subsequently, following 300 s illumination through the 488 nm filter, spectra of the photointermediate were taken. Difference spectra were calculated by subtracting the spectrum of Rho from the spectrum of the photointermediate. For analysis of the first photoproduct (Batho in rhodopsin) the sample temperature was kept at 80.0±0.2 K. Photoreversal of this intermediate to the ground state was attempted by illuminating the sample for 300 s with light λ>610 nm (Schott RG610 long-pass filter). Later intermediates were examined at 253 K and 283 K, since at these temperatures respectively the Meta-I

intermediate and the active Meta-II intermediate of rhodopsin are sufficiently stable to allow such analyses.

4.3.6 Signal transduction

Activation of the rhodopsin-associated G-protein transducin was monitored using a fluorescence assay.[27,28] The intrinsic fluorescence of activated bovine transducin is enhanced upon binding of GTP which was recorded on a Shimadzu RF-5301PC spectrofluorometer (excitation: 295 nm, bandwidth 1.5 nm; emission 337 nm, bandwidth 15 nm). Measurements were performed at pH 7.4 and 20 °C with about 100 nM transducin and 5 nM of pigment in a buffer containing 20 mM HEPPS, 100 mM NaCl, 2 mM $MgCl_2$, 1 mM DTE, and 0.01% (w/v) DDM at a final volume of 2 mL. A hypotonic extract of isotonically washed rod outer segments served as the source for transducin.[29] Immediately before data acquisition, the reaction mixture was bleached for 300 s in bright white light. After reaching a steady fluorescence level, GTP-γ-S (Boehringer Mannheim) was added to a final concentration of 2.5 μM and the subsequent increase in tryptophan fluorescence of the α-subunit of transducin ($G_t\alpha$) was monitored. In one set of measurements, rhodopsin was always included as a 100% control. Opsin membranes served as a negative control. Initial rates were calculated and converted to a percentage of the rhodopsin activity.

4.4 Results and Discussion

Using the modified retinal derivatives ligand-protein interactions, the photoisomerisation and finally the effect of the substituents on protein mechanisms leading to protein activation can be studied. First, the efficiency and rate of binding and spatial properties of the analogue in the binding site provide information about ligand-protein interaction. In particular, steric effects that hinder binding and lead to distortions of the chromophore can be probed. Second, photoisomerisation transforms the 11-Z retinylidene ligand into a strained all-E conformation. In this ultrafast step (< 200 fs) the shape of the protein-binding pocket, fitted to accommodate the 11-Z configuration of the chromophore, is essentially preserved. This restrains the relaxation of the chromophore leading to pronounced torsions in the primary photoproduct.[1,3,6,30,31] The protein subsequently transforms from the inactive to the active form triggered by the relaxation of conformational energy (~35 kcal/mol) that is stored in the strained chromophore during the isomerisation step.[32-34] In contrast with the primary event, receptor activation involves changes in the protein structure and requires much longer time-scale (up to ~1 ms).[2,7,35,36] There is abundant evidence that all three processes are differentially sensitive to the presence of a methyl

substituent at C9, C10 and/or C13.[1,2,37] Here this picture is complemented by analysing effects of methyl substituents at C11 or C12. Conformational transitions representing the formation of the primary photoproduct and the putative active state, respectively, are probed by vibrational spectroscopy. A functional parameter of the photoisomerisation process is presented in the quantum yield, while photochemical transitions and G-protein activation are used in a functional characterisation of active state formation.

4.4.1 11-methyl rhodopsin

Ligand-protein interaction: Figure 4.1 shows the UV-Vis spectra for 11-Z 11-methyl retinal (Scheme 4.1), the corresponding pigment, and the spectra for native 11-Z retinal and Rho. Prior to incorporation the spectra of the retinal analogues were recorded in hexane. The λ_{max} of the α band and the overall absorption profile of the ligand, including the intensities of the β and γ band reveal information about torsions in the polyene tail.[38]

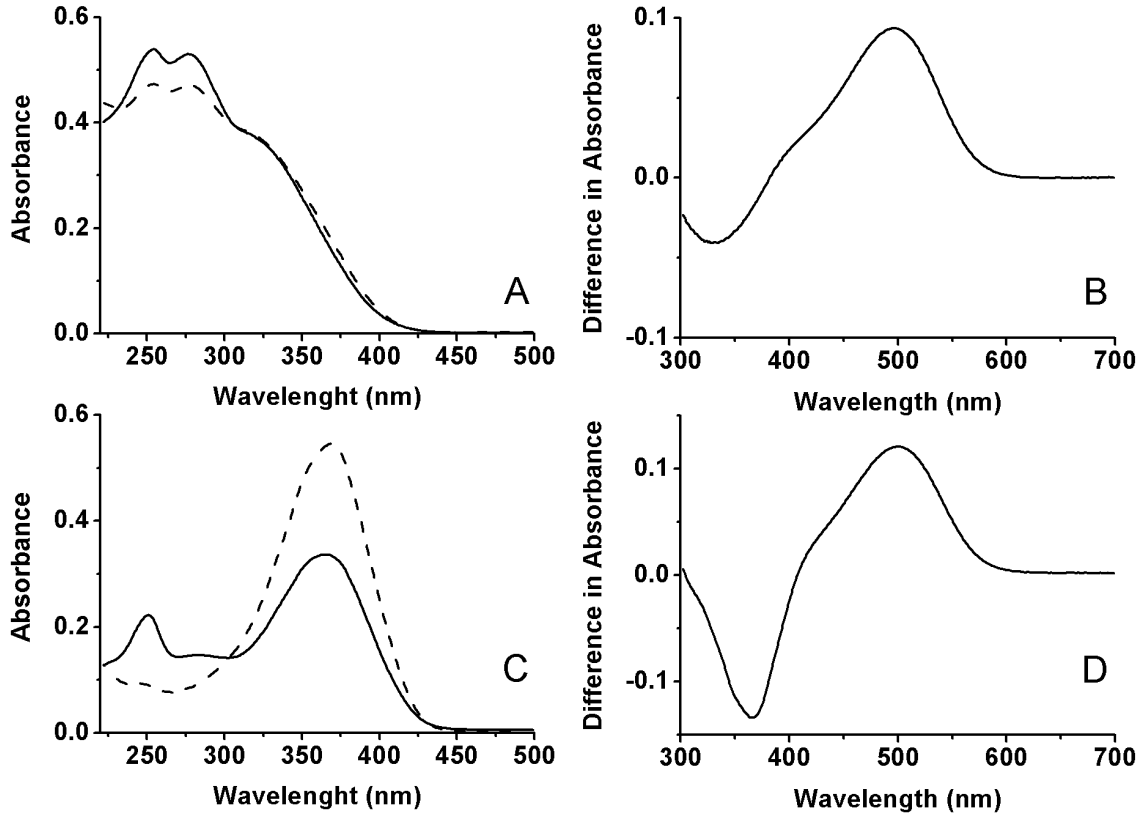

Figure 4.1. (A/C) UV-Vis spectra of the 11-Z 11-methyl and native 11-Z retinal respectively, in hexane in the dark (solid line) and after illumination in presence of iodine (dashed line). (B/D) UV-Vis difference spectra of 11-methyl and native Rho in micelles, respectively. In the difference spectra the data after illumination are subtracted from the dark spectrum.

Addition of a dilute iodine solution to the retinal in solution and subsequent illumination for 60 s establishes a photoequilibrium containing the thermodynamically most favourable conformations. Figure 4.1A shows the spectral properties of 11-Z 11-methyl retinal in hexane in the dark and after illumination in the presence of iodine. The α-band that is observed at 380 nm in native 11-Z retinal (Figure 4.1C) is shifted to a lower wavelength (~320 nm) in the 11-methyl analogue suggesting strong torsions in the 11-Z isomer of this analogue.[38,39] In Figure 4.1C an increase of the absorption at 380 nm upon reaching photoequilibrium indicates a stabilisation of predominantly the relaxed native all-E retinal isomer. In contrast, the spectrum of 11-Z 11-methyl retinal does not show an increase of the absorption around 380 nm upon illumination in the presence of dilute iodine solution (Figure 4.1A). This suggests that the thermodynamically most favourable conformation of 11-methyl retinal has a distorted polyene backbone as well. NMR experiments on all-E 11-methyl retinal in $CDCl_3$ confirm that the molecule is in a 10,12-di-s-*cis* conformation, to avoid intramolecular hindrance of adjacent methyl groups.[40]

In Figure 4.1B the difference spectrum of 11-methyl Rho is shown, calculated from spectra in the dark and after illumination at pH 6.5 in a micellar solution and indicating an absorbance maximum at 496±2 nm (Table 4.1), close to the native Rho (λ_{max}=498 nm). It is generally accepted that the Rho binding pocket requires a ligand that has the 10,12-di-s-*trans* conformation.[41] For the 11-methyl retinal, a steric clash with protein residues of the extracellular loop 2 (E2) is expected when the X-ray structure of Rho is considered. The rate of incorporation of this ligand is at least 100-fold slower than for the native 11-Z retinal and the incorporation efficiency is only 54±5 % (Table 4.1), which supports the idea of steric hindrance for this homologue. The absorbance maximum of 496±2 nm is in line with preliminary data obtained by Liu *et al.* (λ_{max}=498 nm). However, these authors report a lower regeneration efficiency (<30%).[41]

Table 4.1 Regeneration efficiencies and λ_{max} of the pigments used in this study.

retinal	native		11-methyl	12-methyl	11-methyl-13-desmethyl	
	11-Z	9-Z	11-Z	11-Z	11-Z	9-Z
regeneration efficiency (% of Rho)	100	100	54	37	13	35
λ_{max} (±2 nm)	498	486	496	500	496	486

Although it can be concluded that the 11-methyl analogue does not fit well into the binding site, it generates a pigment that is stable against detergent solubilisation and 10 mM hydroxylamine at ambient temperature. Based on the X-ray structure of Rho it is suggested that the 11-methyl substitution interacts with protein residues of the E2 loop, in particular Thr118, Gly114 and Cys187. Finally, the 9-Z isomer of 11-methyl retinal (Scheme 4.1) shows only very low efficiency of pigment formation upon incubation with opsin (≤6%). This pigment was not studied in detail.

Photoisomerisation: Figure 4.2 shows the FTIR difference spectrum for photoproduct formation for the native and modified pigments at 80 K. The Rho vibrations correspond with the negative signals in these spectra. The peaks in the region 1800-1550cm^{-1} represent changes in the protein, while below 1550cm^{-1} mainly changes related to the chromophore are observed.[2,7] For Rho most of the bands in the difference spectrum can be attributed to specific vibrations in the retinylidene backbone, C=C and C–C at ~1550 and ~1200 cm^{-1} respectively, and wag vibrations below 1000 cm^{-1}.[7,42] One striking difference between the Rho and the 11-methyl pigment is the absence of any distinct hydrogen-out-of-plane (HOOP) wags[2,42] in the 11-methyl photoproduct in the 800-1100 cm^{-1} region. The presence of the 11-methyl group affects the HOOP vibrations related to the C11 and the C10–C11=C12 segment. For instance the weak Rho vibration at 969cm^{-1} assigned to the coupled C11H and C12H wags and the strong band at 921cm^{-1} that is assigned to the C11H wag in Batho are suppressed in the 11-methyl analogue.[43,44]

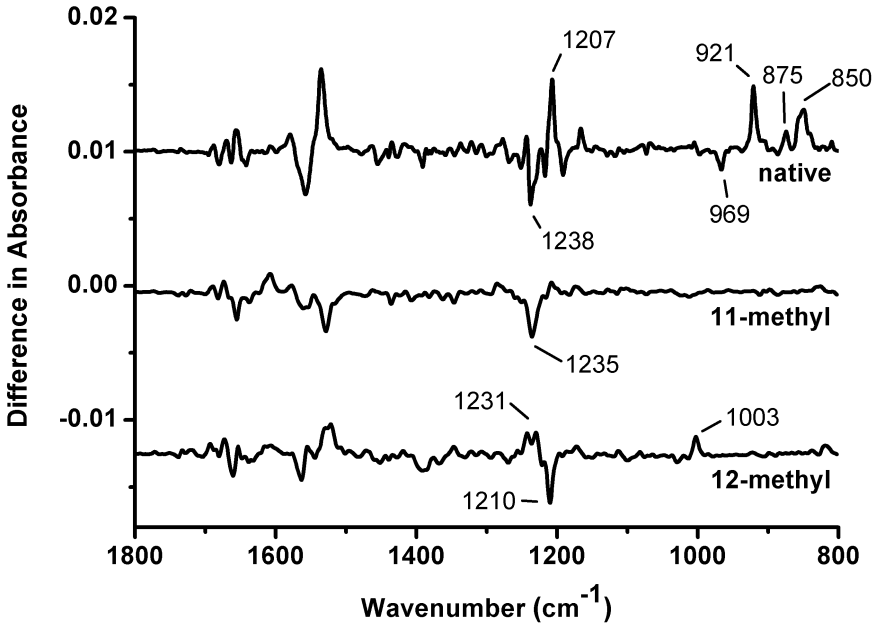

Figure 4.2 FTIR difference spectra of the native, 11-methyl and 12-methyl pigments after irradiation at 80 K.

In addition, the 875, 850, 858 and 838cm^{-1} Batho bands assigned to the wags of the C10H, C14H, C12H and C7H=C8H respectively,[42] are also either strongly attenuated or entirely absent in the analogue. In the single bond region the strong Batho vibration at 1207cm^{-1} is absent while the vibration at 1238 cm^{-1} in Rho that is related to reorientation of the C12–C13 bond after isomerisation is shifted to 1235 cm^{-1} in the difference spectrum of 11-methyl Rho.

Photoreversal of Batho to Rho can be achieved by illumination of the photoproduct through a λ>610 nm filter while eventually no reversal is observed for the 11-methyl photoproduct. This indicates that the torsional strain is distributed over the polyene of the 11-methyl photoproduct, apparently resulting in a retinylidene geometry that is different from the initial dark structure. The quantum yield of the 11-methyl Rho pigment relative to native Rho was determined by fitting the time-dependent decrease in the main band absorbance recorded under continuous low-bleaching conditions. The quantum yield for the 11-Z 11-methyl pigment analogue was determined as Φ=0.28±0.04 (Table 4.2), which is considerably less than the Φ=0.67 for the conversion of Rho to its first photointermediate. Apparently the additional methyl group and associated conformational constraints in the ground state of the chromophore decrease the transition rate of the excited state to the Batho analogue.

Table 4.2 Summary of the experimental results of quantum conversion and transducin activation efficiency.

Retinal derivative		Quantum conversion			Transducin activation (% of native Rho) [g]
		Slope (S) [a] $\times10^{-2}$	R^2	Φ_{An} [b]	
native	11-Z	3.15 [c]/1.66 [d]	0.992/0.996	0.67 [e]	100±16
	9-Z	–	–	0.27 [f]	100±8
11-methyl	11-Z	1.08 [c]	0.999	0.28	29±1
12-methyl	11-Z	1.37 [d]	0.987	0.54	6±4
11-methyl-13-desmethyl	11-Z	0.70 [c]	0.992	0.18	70±3
	9-Z	–	–	–	110±19
10-methyl	11-Z	–	–	0.55 [f]	35±5
13-desmethyl	11-Z	1.71 [c]	0.999	0.44	53±29
	9-Z	–	–	–	37±8

[a] error ±10%, [b] error ±14%, [c] obtained with a filter of 497±10 nm, [d] obtained with a filter of 504±5 nm, [e] reference 22, [f] reference 2, [g] average of 4 experiments

This is in line with the spectrum of the 11-methyl photoproduct below 1000cm^{-1} in Figure 4.2. For native Batho the vibrations between 800-1000 cm^{-1} indicate structural reorganisation in the HC11=C12H element (Figure 4.2, top). The absence of any significant vibration in this area for 11-methyl Batho indicates a more rigid CH_3C11=C12H moiety. This effect is comparable to the quenching of vibrations below 1000 cm^{-1} in the Raman spectrum of 13-desmethyl Batho, which is formed with a quantum yield of Φ=0.47.[8]

Receptor activation: Figure 4.3 shows the UV-Vis spectra of 11-methyl Rho and native Rho before and after illumination at pH 6.5 in membranes. For native Rho membranes the spectrum indicates after 10 s illumination illustrates nearly full conversion to Meta-II (Figure 4.3C). The spectra between 10 s and 40 minutes show only changes caused by decay of Meta-II with the release of retinal from the binding pocket on the minute timescale and the subsequent formation of the Meta-III intermediate (Figure 4.3C). The formation of Meta-III is also illustrated by the decrease of absorbance at ~380 nm and the associated increase of absorbance at ~450 nm in the difference between the spectra taken directly after illumination and 40 minutes later (Figure 4.3D dotted line).

The 11-methyl Rho absorbance is superimposed on a large background of a scattering signal. This is evident from the fully bleached spectrum in Figure 4.3A. This background is due to the high concentration and particle size distribution of the proteoliposome population. Figure 4.3A shows that a Meta-II-like photointermediate of 11-methyl Rho forms inefficiently at pH 6.5, which is illustrated by the modest decrease of the absorption around 500 nm. Hydroxylamine converts the ligand of all photointermediates from Batho through Meta-III to the corresponding oxime that absorbs at ~360 nm. The difference spectrum after addition of hydroxylamine gives an indication of the amount of bleached pigment. Illumination in the presence of hydroxylamine bleaches any remaining pigment and gives an indication of the total amount of pigment in the sample. For 11-methyl Rho less than 20 % of the total amount of material has proceeded to a deprotonated Meta-II-like state after 40 minutes, whereas ~50 % of the pigment present is bleached upon addition of hydroxylamine (Figure 4.3B). This is an additional indication of the inefficient formation of late photointermediates for 11-methyl Rho.

Since illumination of Rho yields an equilibrium of Meta-I and Meta-II that is pH-dependent,[38] it was also investigated whether photointermediate formation of the 11-methyl pigment depends on the pH of the buffer solution.

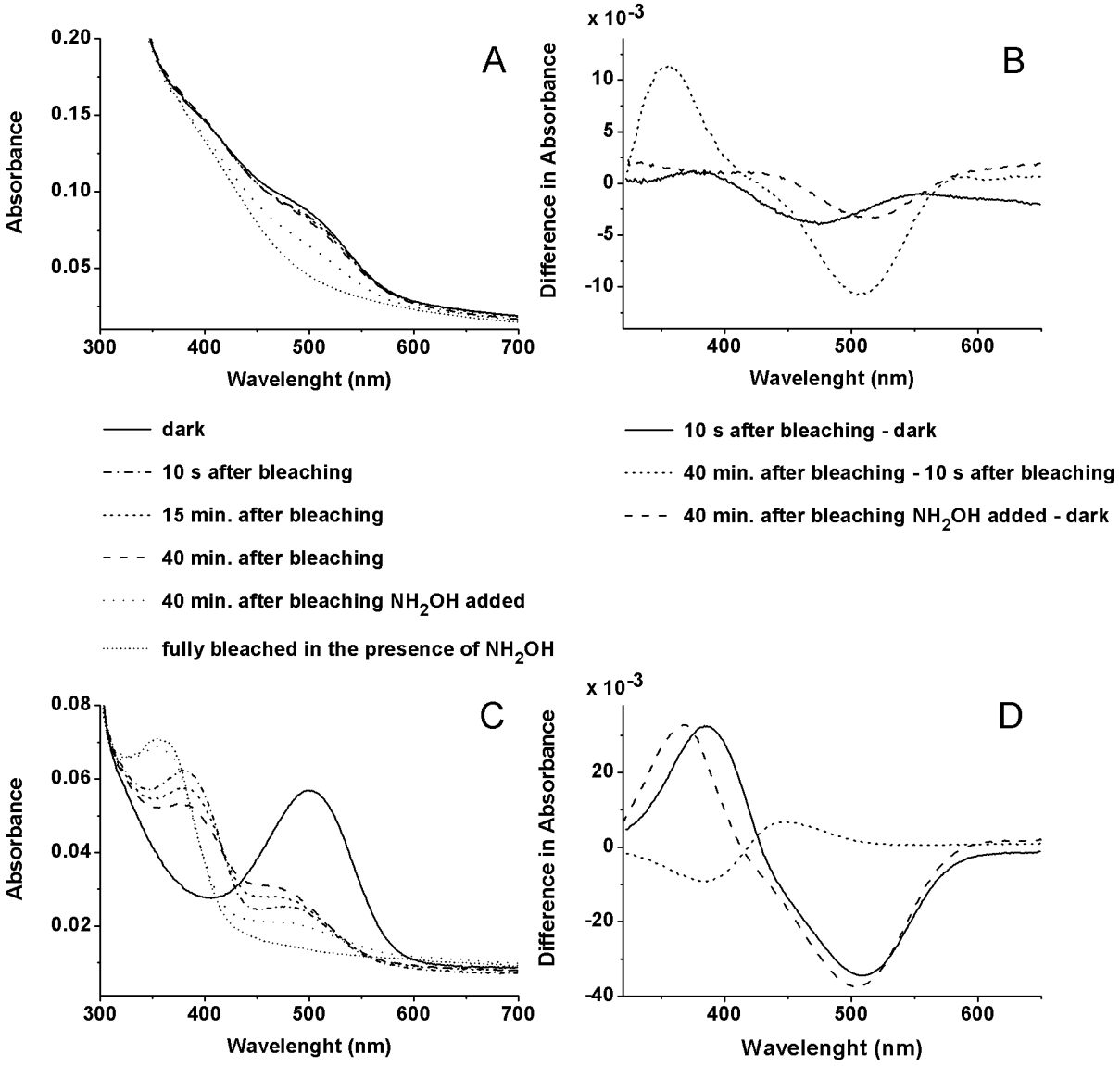

Figure 4.3 (A,C) UV-Vis spectra of membrane suspensions of 11-methyl Rho and native Rho, respectively, in the dark and at different intervals after illumination, with and without hydroxylamine at 10°C and pH 6.5. (B,D) A set of difference spectra is shown on the right.

Figure 4.4 shows difference spectra at 10 °C for the 11-methyl Rho illuminated at pH 7.5 (A), 6.5 (B) and 5.5 (C) and for native Rho at pH 6.5 (D) as a reference. The spectra of Rho show the transitions of Rho→Meta-II (solid line) and Meta-II→Meta-III (dashed line, Figure 4.4D). Illumination of 11-methyl Rho clearly shows pH dependence with a slowly decaying intermediate around 520 nm at higher pH shifting to a product at 380 nm at lower pH (Figure 4.4A→C). The latter appears to decay slowly to a product at 440 nm and probably reflects the transition of the 11-methyl Meta-II analogue to the Meta-III analogue (Figure 4.4C).

The intermediate at 520 nm might represent a 11-methyl Meta-I analogue is strongly red-shifted from the native Meta-I at 480 nm. Alternatively it might represent the Lumi analogue that is found at 504 nm for the native system. However, in that case a complex Lumi↔Meta-I/II equilibrium is invoked by the presence of the 11-methyl group.

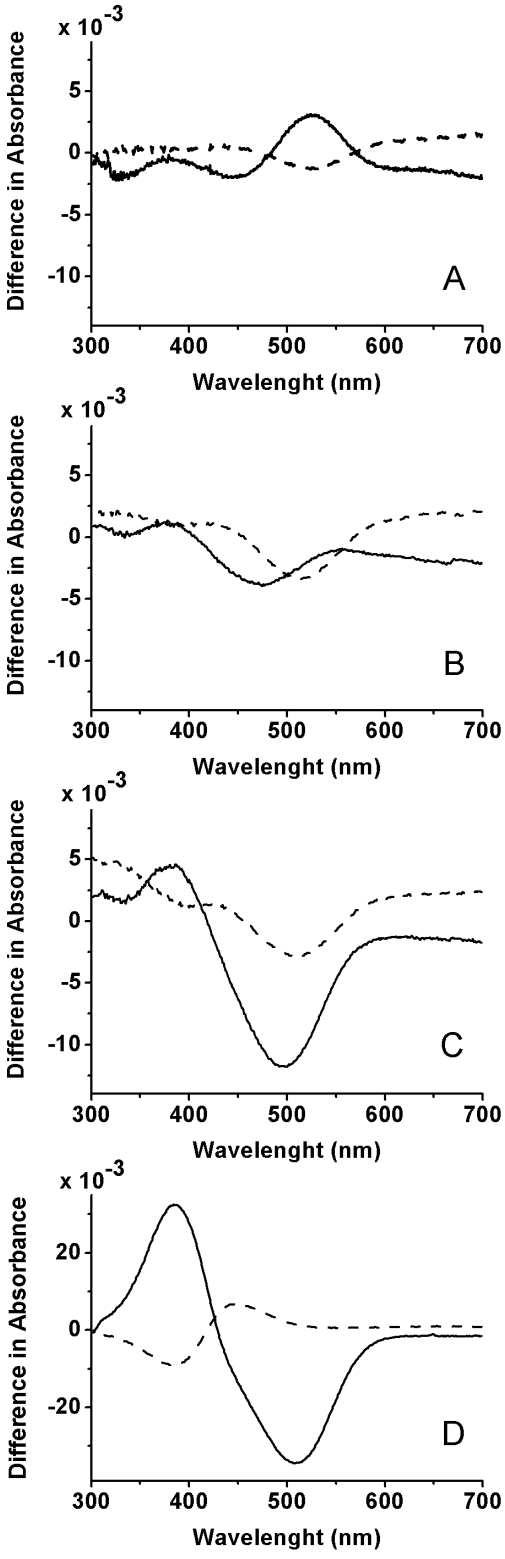

Figure 4.4 UV-Vis difference spectra for 11-methyl Rho at pH 7.5 (A), 6.5 (B) and 5.5 (C) and for the reference native Rho at pH 6.5 (D), recorded at 10 °C in membrane suspensions. The solid lines represent the difference between the spectra 10 s after bleaching and the dark spectra. The dashed lines represent the difference between the spectra 40 minutes after bleaching and the spectra 10 s after bleaching.

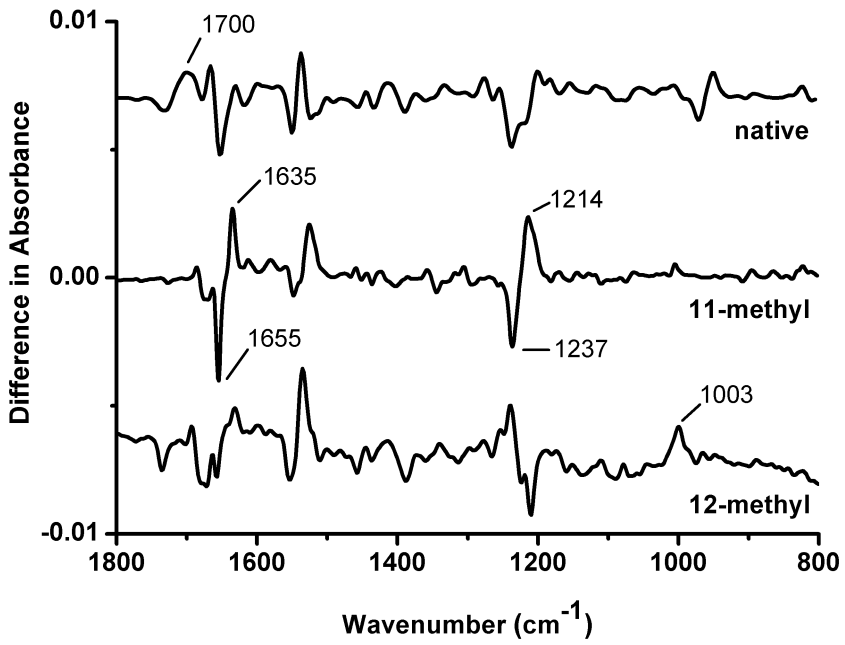

Figure 4.5 FTIR difference spectra of the pigments of 11-methyl and 12-methyl retinal after irradiation at –20 °C.

Figure 4.5 and 4.6 show the FTIR difference spectra recorded at the transition temperatures for Rho→Meta-I at –20 °C and Rho→Meta-II at 10 °C in the native system. The sharp peaks at 1655 and 1635 cm^{-1} and the absence of a broad peak at 1700 cm^{-1} in the difference spectrum of 11-methyl Rho at –20 °C (Figure 4.5) strongly resemble the the data for the Lumi transition of native Rho.[7,35] This corroborates the evidence from UV-Vis data that the formation of the late intermediates is less efficient in the modified pigment. The relatively strong vibrations at 1237 cm^{-1} and 1214 cm^{-1} in the difference spectrum are attributed to the repositioning of the single bonds with respect to polar residues of the protein that are located in the vicinity of the isomerisation region.[45] The positive peak at 1214 cm^{-1} probably originates from the C10–C11 single bond after repositioning as a consequence of the release of steric interaction of the 11-methyl group with the methyl on C9 or with residues in the protein following isomerisation.

From Figure 4.6 it is clear that at 10 °C and pH 5.5-6.0 the difference spectrum for 11-methyl Rho in the range from 1767 to 1680 cm^{-1} has clear features of Meta-II, although the signals at 1767, 1750, 1710, 1437 and 1391 cm^{-1} are clearly attenuated. This confirms a less efficient formation of the Meta-II intermediate for 11-methyl Rho observed with UV-Vis spectroscopy (Figure 4.3). A vibration at 1214cm^{-1} (+) in the 11-methyl analogue suggests that some interaction with the protein remains present even in the 'relaxed' Meta-II state.

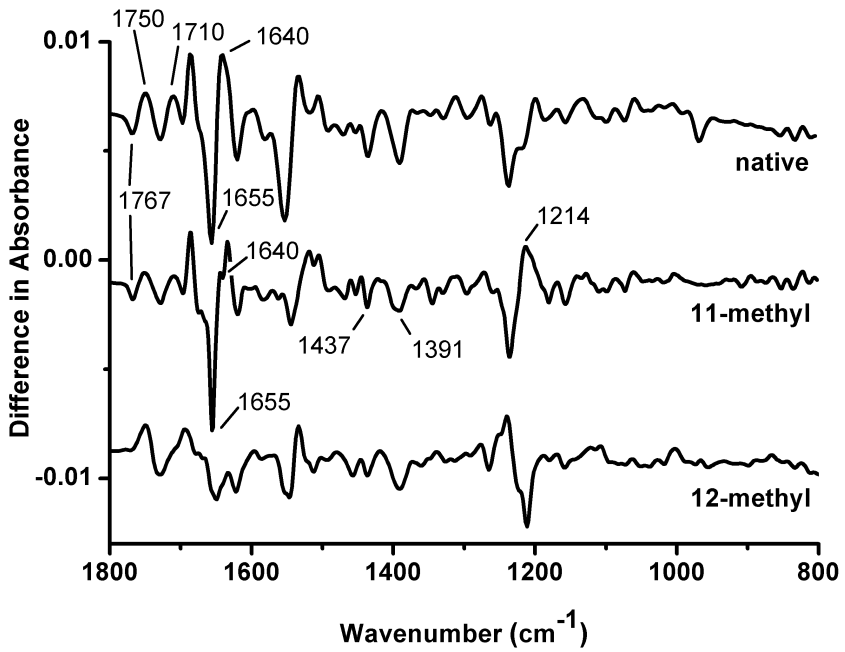

Figure 4.6 FTIR difference spectra of native 11-methyl and 12-methyl Rho after irradiation at 10 °C and at an approximate pH of 5.5-6.0.

The last column of Table 4.2 presents data concerning transducin activation of the modified pigments. The 11-methyl pigment is able to activate transducin at a moderate 29% of the rate of Rho, indicating that the photochemically relaxed 11-methyl retinylidene is only a moderate agonist for receptor activation comparable to 10-methyl Rho. The picture that emerges from these results is that the inefficient formation of late intermediates including Meta-II leads also to inefficient activation of the G-protein.

4.4.2 12-methyl rhodopsin

Ligand-protein interaction: The UV/Vis spectrum of 11-Z 12-methyl retinal (Scheme 4.1) in hexane shows a strong absorption at 285 nm that shifts to 385 nm upon illumination in the presence of iodine. This reflects a transition of the 11-Z to the all-E form (Figure 4.7A). The incorporation efficiency of 11-Z 12-methyl retinal into opsin is only 37±10 % and the incorporation rate is at least 100-fold slower than the rate of native 11-Z retinal. Assuming that the 10,12-di-s-*trans* conformation is adopted severe steric hindrance with the protein pocket is expected. This would explain the low rate and efficiency of incorporation. In addition, the 12-methyl pigment is only moderately stable towards hydroxylamine at low temperatures (≤10 °C), which is another indication of considerable strain in the binding pocket. Incorporation of 11-Z 12-methyl retinal into opsin yields an analogue pigment with λ_{max} = 500±2 nm (Figure 4.7B and Table 4.1). Liu *et al.* only achieved a very low regeneration efficiency (<5%) and estimated a λ_{max} of 495 nm.[46]

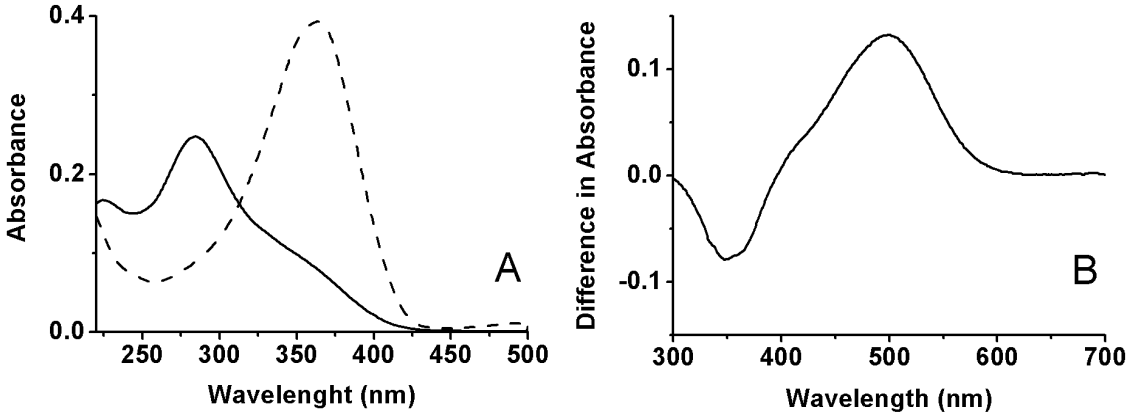

Figure 4.7 (A) UV-Vis spectrum of the retinal derivative 11-Z 12-methyl retinal, in hexane in the dark (solid line) and after illumination in presence of iodine (dashed line). (B) UV-Vis difference spectrum of 12-methyl Rho in micelles, the data obtained after illumination are subtracted from the dark spectrum.

Photoisomerisation: In the FTIR difference spectrum representing the first photoproduct of 12-methyl Rho (Figure 4.2, bottom) the C12-C13 vibration of the pigment at 1238cm^{-1} (–) is shifted to 1210 cm^{-1} which is probably a direct effect of the additional C12 methyl group. Similar to 11-methyl Rho the 12-methyl Rho photoproduct does not show any peak in the HOOP region, including those that have been assigned to C10H, C11H, C14H and C7=C8. The photoproduct does show a peak at 1003 cm^{-1} that is not yet explained and could result from a wag of a highly distorted C=C bond or a methyl wag that has become active due to steric interaction. In contrast to 11-methyl Rho, the 12-methyl photoproduct can be photoreversed by illumination with light λ>610 nm, indicating that it behaves like a normal Batho. From the fit of the time-dependent decrease of the main absorbance band under low-bleaching conditions a quantum yield for 12-methyl Rho of Φ=0.54±0.08 is estimated, somewhat lower than the Φ=0.67 of the native Rho. Previously, it was suggested that the mechanism underlying the efficient isomerisation of the retinylidene ligand in the excited-state of Rho involves the expansion of the C=C double bonds accompanied by a displacement of the hydrogens in the C11H=C12H motif from a *cis* to a *trans* position.[1,5,30] For native Rho the main displacement would be a rotation at the site of the C12H element in the chromophore,[4] which would agree with the observation that the locked 11,19-ethano Rho analogue shows normal photointermediate kinetics.[47] It has been suggested that a prerequisite for an efficient isomerisation is a steep and coherent path over the excited state surface and that the speed and efficiency are closely correlated.[1,8] Since the efficiency of the primary step of the photoreaction for 12-methyl Rho is comparable with native Rho and the inertia of the C12CH_3 element is much

too large for considerable rotation at sub-picosecond timescale, rotation of a C12H element may not be the exclusive path with a steep gradient on the excited-state surface that leads to efficient isomerisation. The quantum yield of 11-methyl Rho is considerably reduced and that for 12-methyl Rho C11H rotation may be the only rapid isomerisation pathway. Since the Raman spectrum of native Batho indicates that the reorganisation energies are high for both the C11H and C12H element, it is possible to consider an isomerisation mechanism for Rho in which counter rotation of C11H and C12H leads to their relative *trans* position in Batho. Steric restraints in the protein pocket may be present to direct such motion, like the Thr118βOH↔H11 distance of ~2.6 Å and the Cys187O↔H12 distance of ~2.0 Å.[45]

Receptor activation: Photoactivation of 12-methyl Rho in a membrane environment at pH 6.5 produces a slowly decaying intermediate at 477 nm, most likely representing a 12-methyl Meta-I-like intermediate (Figure 4.8A). The difference spectrum directly after illumination (Figure 4.9B solid line) is virtually identical to the data obtained for Rho at pH 8.0, corresponding with the transition to Meta-I. Similar results are observed for 12-methyl Rho at pH 7.5 and 5.5. This suggests that the dark reactions of 12-methyl Rho proceed to a Meta-I-like stage that probably decays by release of the ligand (Figure 4.9B).

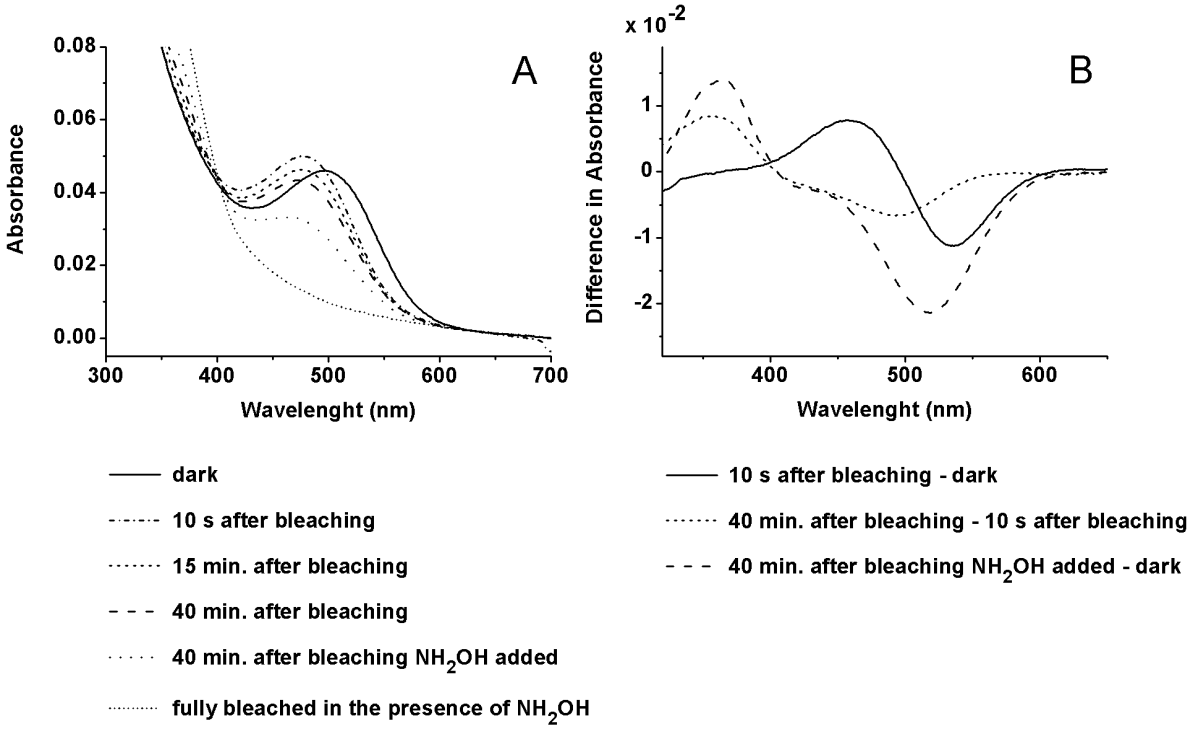

Figure 4.8 (A) UV-Vis spectra of 12-methyl Rho in the dark and at different intervals after illumination, with and without hydroxylamine added at 10 °C and pH 6.5. (B) On the right a set of difference spectra is shown.

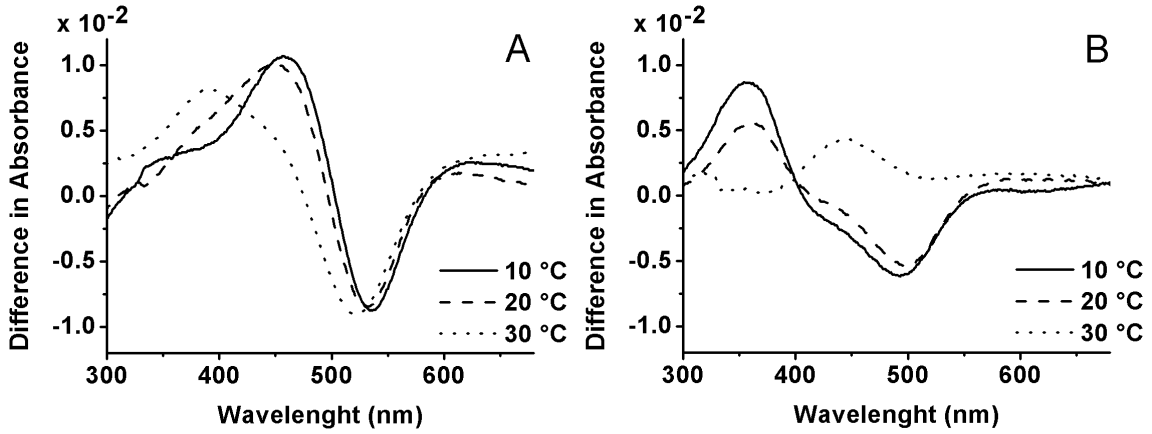

Figure 4.9 UV/Vis difference spectra for 12-methyl Rho recorded at 10, 20 and 30 °C. (A) shows the difference between 10 s after bleaching and dark (B) shows the difference between the spectrum 20 minutes after bleaching and the spectrum 10 s after bleaching is shown.

To investigate the stability of the 12-methyl Meta-I-like intermediate at different temperatures the photolysis was also performed at 20 and 30 °C and pH 6.5 (Figure 4.9). The difference spectra at 10 and 20 °C are very similar and indicate exclusive formation of a slowly decaying Meta-I-like intermediate. At 30 °C this intermediate appears less stable and there is the suggestion of formation of Meta-II and Meta-III-like intermediates. These conclusions are supported by the vibrational analysis shown in Figure 4.5 and 4.6. The 12-methyl Rho difference spectrum at –20 °C shows many features of the native Rho→Meta-I transition, except for the protein region between 1600-1800 cm^{-1}. The similarity of the FTIR difference spectra of 12-methyl Rho recorded at the –20 °C and 10 °C below 1550cm^{-1} is evident and indicates that only minor structural changes in the chromophore are taking place after raising the temperature beyond the threshold for native Meta-II formation (Figure 4.5 and 4.6). The protein region at 10 °C strongly differs from the corresponding region in the native Meta-II data set (Figure 4.6). Bands at 1767(–) and 1750(+) cm^{-1} that are indicative for H-bonding changes in protein residue Asp83 in native Meta-II, are absent. Also the feature at 1710cm^{-1} indicative for protonation of Glu113 is not observed. These observations suggest that the 12-methyl chromophore can proceed to a Meta-I-like conformation while blocking rearrangements in the binding site required to proceed to Meta-II. In line with these results the G-protein activation rate of the 12-methyl pigment is insignificantly low at 6% of native Rho (Table 4.2). Possibly, the ligand cannot reposition efficiently and remains protonated. Since the protein is efficiently 'locked' in a Meta-I-form the rate of transducin activation is also low. Hydrolysis of the Schiff base linkage on the minute time scale eventually results in an inactivated receptor (Figure 4.8).

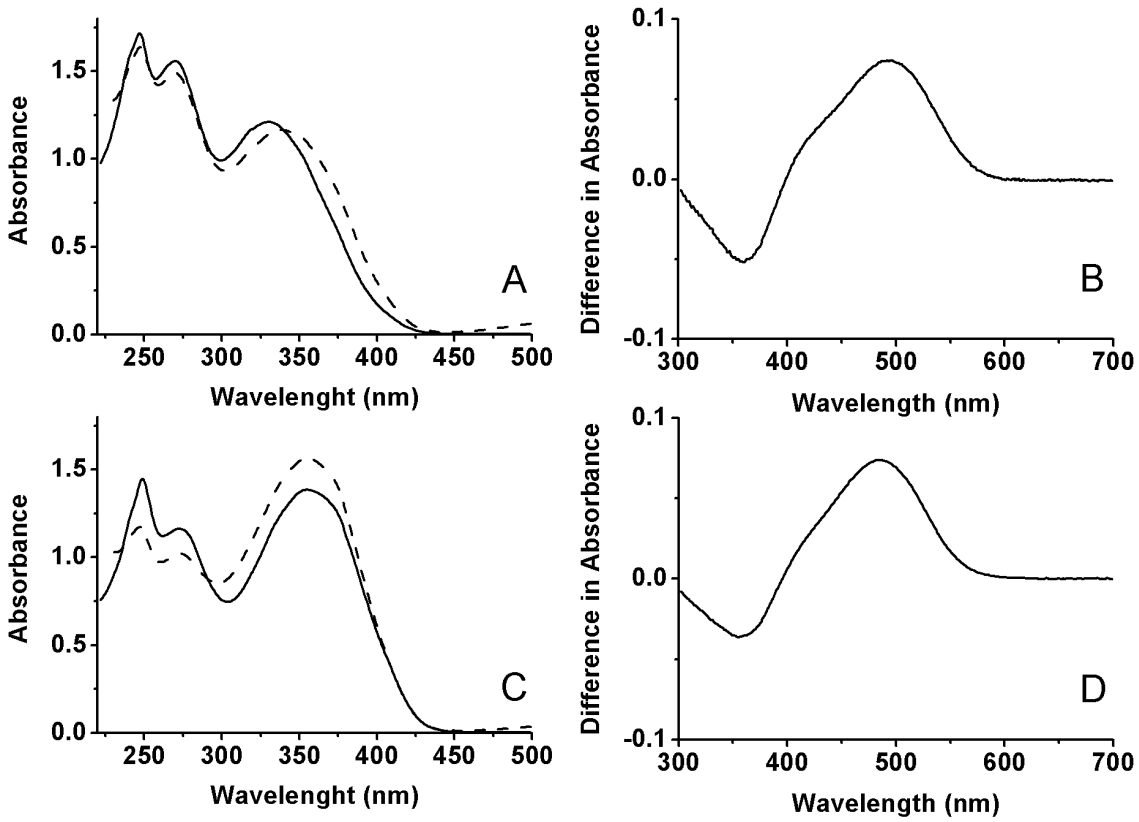

Figure 4.10 (A,C) UV-Vis spectra of the retinal derivatives 11-Z and 9-Z 11-methyl-13desmethyl retinal, respectively, in hexane in the dark (solid line) and after illumination in the presence of iodine (dashed line). (B,D) UV-Vis difference spectra the Rho and Iso pigments of 11-methyl-13-desmethyl, respectively, in micelles. The spectrum after illumination is subtracted from the dark spectrum.

4.4.3 11-methyl-13-desmethyl rhodopsin and isorhodopsin

Ligand-protein interactions: The spectra of 11-Z and 9-Z 11-methyl-13-desmethyl retinal (Scheme 4.1) before and after illumination are depicted in Figure 4.10A and C respectively. For the 11-Z 11-methyl-13-desmethyl analogue a shift of the absorbance from 330 nm to 340 nm signifies the transformation from the 11-Z to the all-E isomer upon illumination. The α-band of the 9-Z 11-methyl-13-desmethyl retinal isomer appears at 356 nm, significantly higher than the 11-Z isomer reflecting a less sterically congested solution structure (Scheme 4.1). Both isomers have strong β- and γ-bands in their spectra before as well as after illumination, indicating strong torsions even in the thermodynamically most favourable conformation.

The moderate incorporation of 13% for the 11-Z 11-methyl-13-desmethyl ligand suggests that the ligand does not fit well in the protein binding pocket (Table 4.1). Apparently, the ligand is forced into a distorted and thermodynamically unfavourable conformation, which can be a consequence of the irregular shape of the solution structure of the retinal (Scheme 4.1).

Incorporation of the 11-Z 11-methyl-13-desmethyl derivative into opsin yields an analogue pigment with λ_{max} = 496±2 nm, slightly less than for native Rho. For 9-Z 11-methyl-13-desmethyl retinal a pigment analogue with λ_{max} = 486±2 nm is obtained, nearly identical to Iso. The incorporation efficiency for 9-Z 11-methyl-13-desmethyl retinal is significantly better at 35% (Table 4.1). The major solution structure of the 9-Z ligand resembles the native 11-Z retinal structure, which might explain that the incorporation efficiency is higher than the 11-methyl-13-desmethyl 11-Z isomer.

Photoisomerisation: Similar to 11-methyl Rho the negative peak in the FTIR spectrum that is associated with the reorientation of the C12–C13 bond upon illumination is shifted from 1238 cm^{-1} in Rho to 1231 cm^{-1} for 11-methyl-13-desmethyl Rho (Figure 4.11). This indicates release of steric constraints upon illumination. In line with the data for 11-methyl and 13-desmethyl Rho the HOOP vibrations are strongly attenuated.[8,48] However, in contrast to 11-methyl Rho, the 11-methyl-13-desmethyl Rho shows a HOOP feature at 970 cm^{-1}. This vibration probably appears due the absence of the 13-methyl group and originates from the ethylenic wag of the HC13=C14H motif, similar to 13-desmethyl Rho.[8] The quantum yield of 11-methyl-13-desmethyl Rho is Φ=0.18±0.03, the lowest value reported thus far for any Rho analogue (Table 4.2). This is probably due to the cumulative effects of the 13-desmethyl and the 11-methyl derivatisation of the chromophore.

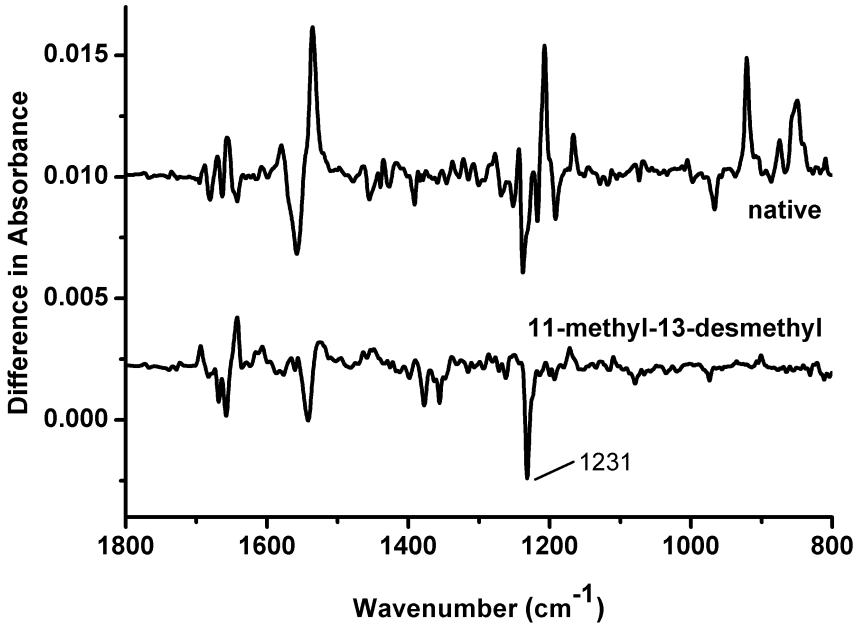

Figure 4.11 FTIR difference spectra of the pigments of native and 11-methyl-13-desmethyl retinal after irradiation at 80 K.

Here, the absence of the intramolecular steric interaction between the C13 methyl group and the C10 hydrogen further reduces the quantum yield of the 11-methyl pigment from Φ=0.28 to Φ=0.18.

Receptor activation: Figure 4.12 shows the UV-Vis spectra following illumination of the 11-methyl-13-desmethyl pigment. The slow decrease of the absorbance in time and the significant amount of oxime that is released upon addition of hydroxylamine indicate an inefficient formation of the photointermediates (Figure 4.12B). However, the absence of the 13-methyl group attenuates the effect of the 11-methyl group in the sense that at pH 6.5 and 10 °C already a significant amount of a Meta-II-like intermediate at ~380 nm is generated, that slowly decays to a Meta-III like form (Figure 4.12B). This agrees with an improved efficiency of transducin activation of 70% relative to 29% for 11-methyl Rho (Table 4.2). Compared to the transducin activation rate of about 53% for the 13-desmethyl Rho, the 70% of 11-methyl 13-desmethyl Rho is high. This may indicate that the decrease in activation rate upon removal of the methyl group on C13 is partially reversed by introduction of a methyl on C11. This suggests that the presence of a methyl group near the β4 strand of the E2 loop influences the Meta-I/II equilibrium.

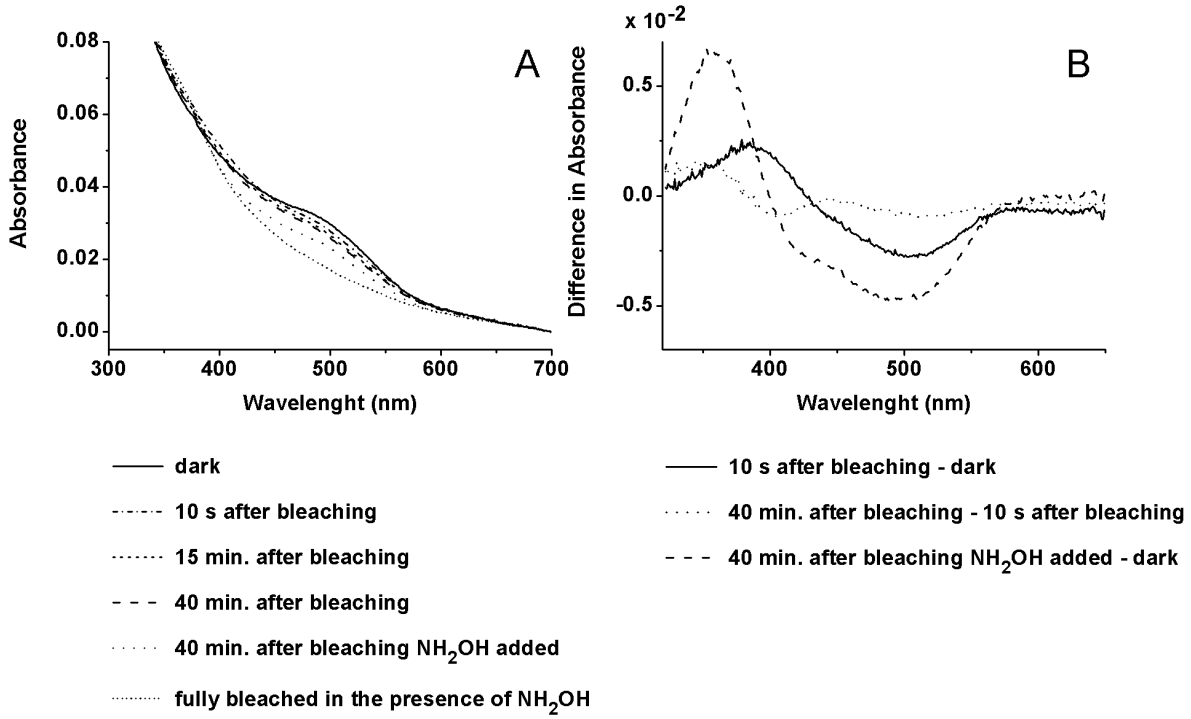

Figure 4.12 (A) shows UV-Vis spectra of 11-methyl-13-desmethyl Rho in the dark and at different intervals after illumination, with and without hydroxylamine at 10 °C and pH 6.5. (B) On the right a set of difference spectra is shown.

This phenomenon is probably governed by nonspecific ligand-protein interactions of the relaxing ligand that perturb the local protein structure[49,50] and agrees with changes in H-bonded network upon activation of the receptor.[51-53]

The transducin activation data for the 11-methyl-13-desmethyl Iso analogue are remarkable. Its ability to activate the receptor of 110±19% is significantly higher than for the 11-methyl-13-desmethyl Rho analogue and comparable to native Rho. It is generally accepted that, at the millisecond time scale of the formation of Meta-II, both Rho and Iso yield identical relaxed all-E retinylidene structures. However the 11-methyl group is differently oriented in the binding pocket for the 9-Z and the 11-Z pigment. It is possible that in this case the photointermediate cascade proceeds differently for Rho and Iso. In particular, the methyl group on C11 of 11-Z 11-methyl-13-desmethyl Rho may become trapped in an unfavourable conformation that hinders formation of Meta-II or that produces a less active Meta-II state. This may be related to a structural rearrangement of the binding pocket during the photosequence, which may be more pronounced for 11-methyl-13-desmethyl Iso and native Rho than for 11-methyl-13-desmethyl Rho (Scheme 4.2). The data suggest that propagation of the photocascade proceeds from the distorted all-E retinylidene conformation in Batho to Meta-II through a protein state with increased entropy that is essential for crossing the energy barrier to the activated receptor.[49,50] The free energy profile of the photointermediates indeed indicates that the Meta-I↔Meta-II transition must be entropy-driven.[54,55] The lower abilities of 13-desmethyl Rho (53%) and Iso (37%) to generate an activated receptor are also in line with this concept. In addition, recent observations of Palczewski *et al*. indicate that when the changes in the spatial structure of the bound ligand upon photoisomerisation are marginal, the G-protein activation rates remains below 30 % of Rho.[56]

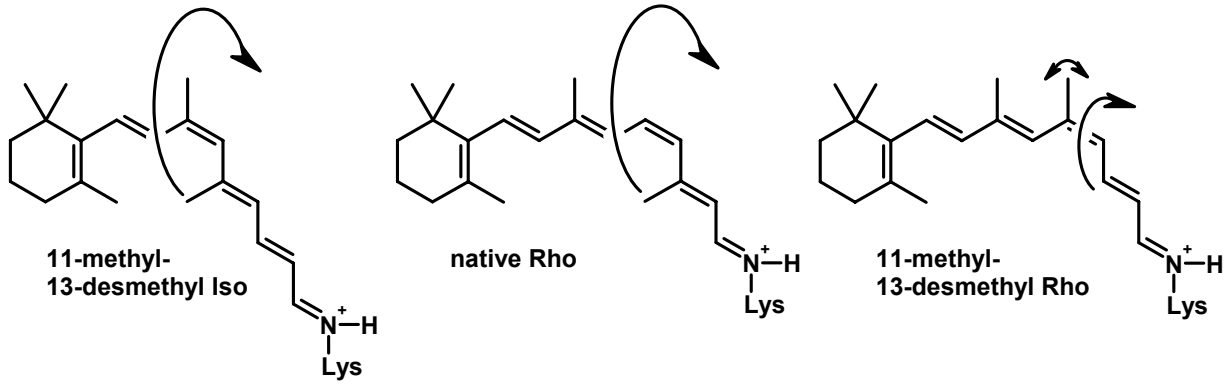

Scheme 4.2 During isomerisation of 11-methyl-13-desmethyl Iso and native Rho the rotation of the methyl group triggers more spatial perturbations as the β-ionone ring is fixed in the protein.[53]

4.5 CONCLUSION

In this study the spectroscopic and biochemical data of opsin regenerated with 11-Z 11-methyl, 11-Z 12-methyl and 9-Z or 11-Z 11-methyl-13-desmethyl retinal are presented and discussed. It is demonstrated that studying artificial pigments provides insight into the structure-function relationships for the visual pigment. The modifications in the central part of the polyene that is actively involved in the isomerisation step have mixed effects on the regeneration efficiency, the generation of photointermediates and the G-protein activation properties. The low to moderate incorporation of the derivatives reflect a tight packing of the C11=C12 part of the retinylidene in the native Rho. Apparently, the tolerance of the binding pocket for an additional 10-, 11- or 12-methyl group is low, while removal of the 13-methyl can partially compensate for this effect. The delayed formation of intermediates that is observed in all derivatives also suggests that ligand-protein contacts hamper relaxation of the retinylidene and protein structure towards the spatial position in activated Meta-II. This corroborates recent inferences that a translational repositioning of the ligand is required for optimal binding of the G-protein.[57,58]

In addition, this study provides evidence that pronounced spatial perturbations of the ligand during isomerisation correlate with an increased ability to activate the receptor. In particular, it is tempting to conclude that an entropic effect in the vicinity of the E2 loop triggered by the relaxation of the distorted retinylidene in Batho may produce a more disordered protein that crosses the energy barrier towards the active receptor conformation more easily.[49,50] Such a concept would be in agreement with earlier experiments that indicate that the Meta-I↔Meta-II transition is entropy driven[54,55] and is in line with the disruption of the H-bonded network near the chromophore during activation.[51-53]

With respect to the formation of the Batho intermediate, the data suggest that interactions of the 11-methyl group with *e.g.* the neighbouring C9 methyl group or protein residues introduces additional torsions in the C10–C11 bond that suppress fast isomerisation. The quantum conversion of the 12-methyl pigment, in contrast to 11-methyl, indicates that fast rotation of the C11 hydrogen may be involved in the efficient isomerisation pathway and that counter rotation of the C11H and C12H elements may help to favour a H11-H12 *trans* position in Batho, possibly by steric interactions of these hydrogens with the protein.[45]

REFERENCES

(1) Mathies, R. A.; Lugtenburg, J. In *Handbook of Biological Physics, Volume 3*; Stavenga, D. G., DeGrip, W. J., Pugh Jr., E. N., Eds.; Elsevier Science: Amsterdam, 2000.
(2) DeLange, F.; Bovee-Geurts, P. H. M.; VanOostrum, J.; Portier, M. D.; Verdegem, P. J. E.; Lugtenburg, J.; DeGrip, W. J. *Biochemistry* **1998**, *37*, 1411-1420.
(3) Verdegem, P. J. E.; Helmle, M.; Lugtenburg, J.; De Groot, H. J. M. *J. Am. Chem. Soc.* **1997**, *119*, 169-174.
(4) Bifone, A.; De Groot, H. J. M.; Buda, F. *Pure Appl. Chem.* **1997**, *69*, 2105-2110.
(5) Cembran, A.; Bernardi, F.; Olivucci, M.; Garavelli, M. *J. Am. Chem. Soc.* **2003**, *125*, 12509-12519.
(6) Yan, E. C. Y.; Ganim, Z.; Kazmi, M. A.; Chang, B. S. W.; Sakmar, T. P.; Mathies, R. A. *Biochemistry* **2004**, *43*, 10867-10876.
(7) DeGrip, W. J.; Rothschild, K. J. In *Molecular Mechanisms in Visual Transduction, Volume 3*; Stavenga, D. G., DeGrip, W. J., Pugh Jr, E. N., Eds.; Elsevier Science: Amsterdam, 2000; Vol. 3, p 1-54.
(8) Kochendoerfer, G. G.; Verdegem, P. J. E.; Van der Hoef, I.; Lugtenburg, J.; Mathies, R. A. *Biochemistry* **1996**, *35*, 16230-16240.
(9) Wang, Y. J.; Bovee-Geurts, P. H. M.; Lugtenburg, J.; DeGrip, W. J. *Biochemistry* **2004**, *43*, 14802-14810.
(10) Verdegem, P. J. E.; Monnee, M. C. F.; Lugtenburg, J. *J. Org. Chem.* **2001**, *66*, 1269-1282.
(11) Verdegem, P. J. E.; Bovee-Geurts, P. H. M.; DeGrip, W. J.; Lugtenburg, J.; De Groot, H. J. M. *Biochemistry* **1999**, *38*, 11316-11324.
(12) Creemers, A. F. L.; Lugtenburg, J. *J. Am. Chem. Soc.* **2002**, *124*, 6324-6334.
(13) Lugtenburg, J. *Pure Appl. Chem.* **1985**, *57*, 753-762.
(14) Olive, J. L.; Mousserom, M.; Dornand, J. *Bull. Soc. Chim. Fr.* **1969**, 3247-&.
(15) Groesbeek, M. *Recl. Trav. Chim. Pay B.* **1992**, *111*, 149-154.
(16) Jansen, F.-J. H. M.; Kwestro, M.; Schmitt, D.; Lugtenburg, J. *Recl. Trav. Chim. Pay B.* **1994**, *113*, 552-562.
(17) Sato, K.; Mizuno, S.; Hirayama, M. *J. Org. Chem.* **1967**, *32*, 177-180.
(18) Friese, A.; Hell-Momeni, K.; Zundorf, I.; Winckler, T.; Dingermann, T.; Dannhardt, G. *J. Med. Chem.* **2002**, *45*, 1535-1542.
(19) Cooke, M. P. *J. Org. Chem.* **1986**, *51*, 951-953.
(20) DeGrip, W. J.; Van Oostrum, J.; Bovee-Geurts, P. H. M.; Van der Steen, R.; Van Amsterdam, L. J. P.; Groesbeek, M.; Lugtenburg, J. *Eur. J. Biochem.* **1990**, *191*, 211-220.
(21) DeGrip, W. J.; VanOostrum, J.; Bovee-Geurts, P. H. M. *Biochem. J.* **1998**, *330*, 667-674.
(22) Dartnall, H. J. A. In *Handbook of Sensory Physiology*; Dartnall, H. J. A., Ed.; Springer Verlag: Berlin, 1972.
(23) Liu, R. S. H.; Crescitelli, F.; Denny, M.; Matsumoto, H.; Asato, A. E. *Biochemistry* **1986**, *25*, 7026-7030.
(24) Hubbard, R.; Wald, G. *J. Gen. Physiol.* **1952**, *36*, 269-315.
(25) Clark, N. A.; Rothschild, K. J.; Luippold, D. A.; Simon, B. A. *Biophys. J.* **1980**, *31*, 65-96.
(26) DeLange, F.; Merkx, M.; BoveeGeurts, P. H. M.; Pistorius, A. M. A.; DeGrip, W. *Eur. J. Biochem.* **1997**, *243*, 174-180.
(27) Phillips, W. J.; Cerione, R. A. *J. Biol. Chem.* **1988**, *263*, 15498-15505.
(28) Fahmy, K.; Sakmar, T. P. *Biochemistry* **1993**, *32*, 7229-7236.
(29) Kuehn, H. In *Prog. Retinal Res.* 1984; Vol. 3, p 123-156.
(30) Bifone, A.; De Groot, H. J. M.; Buda, F. *J. Phys. Chem. B* **1997**, *101*, 2954-2958.

(31) Buda, F.; De Groot, H. J. M.; Bifone, A. *Phys. Rev. Lett.* **1996**, *77*, 4474-4477.
(32) Kim, J. E.; Pan, D. H.; Mathies, R. A. *Biochemistry* **2003**, *42*, 5169-5175.
(33) Pan, D. H.; Ganim, Z.; Kim, J. E.; Verhoeven, M. A.; Lugtenburg, J.; Mathies, R. A. *J. Am. Chem. Soc.* **2002**, *124*, 4857-4864.
(34) Pan, D. H.; Mathies, R. A. *Biochemistry* **2001**, *40*, 7929-7936.
(35) DeGrip, W. J.; Gray, D.; Gillespie, J.; Bovee, P. H. M.; Van den Berg, E. M. M.; Lugtenburg, J.; Rothschild, K. J. *Photochem. Photobiol.* **1988**, *48*, 497-504.
(36) Rothschild, K. J.; Cantore, W. A.; Marrero, H. *Science* **1983**, *219*, 1333-1335.
(37) Han, M.; Groesbeek, M.; Smith, S. O.; Sakmar, T. P. *Biochemistry* **1998**, *37*, 538-545.
(38) Rodieck, R. W. *The vertebrate retina, Principles of structure and function*; W.H. Freeman and Company: San Francisco.
(39) Sperling, W.; Rafferty, C. N. *Nature* **1969**, *224*, 591-594.
(40) Tsujimoto, K.; Shirasaka, Y.; Mizukami, T.; Ohashi, M. *Chemistry Letters* **1997**, 813-814.
(41) Liu, R. S. H.; Asato, A. E. In *Chemistry and Biology of Synthetic Retinoids*; Dawson, M. I., Okamura, W. H., Eds.; CRC Press: Florida, 1990, p Chapter 3.
(42) Palings, I.; Van den Berg, E. M. M.; Lugtenburg, J.; Mathies, R. A. *Biochemistry* **1989**, *28*, 1498-1507.
(43) Eyring, G.; Curry, B.; Broek, A.; Lugtenburg, J.; Mathies, R. *Biochemistry* **1982**, *21*, 384-393.
(44) Mathies, R.; Smith, S. O.; Palings, I. In *Biological Applications of Raman Spectrometry*; Spiro, T. G., Ed.; John Wiley & Sons: 1987.
(45) Okada, T.; Fujiyoshi, Y.; Silow, M.; Navarro, J.; Landau, E. M.; Shichida, Y. *Proc. Natl. Acad. Sci. U. S. A.* **2002**, *99*, 5982-5987.
(46) Liu, R. S. H.; Asato, A. E.; Denny, M.; Mead, D. *J. Am. Chem. Soc.* **1984**, *106*, 8298-8300.
(47) Sheves, M.; Albeck, A.; Ottolenghi, M.; Bovee-Geurts, P. H. M.; DeGrip, W. J.; Einterz, C. M.; Lewis, J. W.; Schaechter, L. E.; Kliger, D. S. *J. Am. Chem. Soc.* **1986**, *108*, 6440-6441.
(48) Wang, Q.; Kochendoerfer, G. G.; Schoenlein, R. W.; Verdegem, P. J. E.; Lugtenburg, J.; Mathies, R. A.; Shank, C. V. *J. Phys. Chem.* **1996**, *100*, 17388-17394.
(49) Craven, C. J.; Derix, N. M.; Hendriks, J.; Boelens, R.; Hellingwerf, K. J.; Kaptein, R. *Biochemistry* **2000**, *39*, 14392-14399.
(50) Rubinstenn, G.; Vuister, G. W.; Mulder, F. A. A.; Dux, P. E.; Boelens, R.; Hellingwerf, K. J.; Kaptein, R. *Nat. Struct. Biol.* **1998**, *5*, 568-570.
(51) Yan, E. C. Y.; Kazmi, M. A.; Ganim, Z.; Hou, J. M.; Pan, D. H.; Chang, B. S. W.; Sakmar, T. P.; Mathies, R. A. *Proc. Natl. Acad. Sci. U. S. A.* **2003**, *100*, 9262-9267.
(52) Birge, R. R.; Knox, B. E. *Proc. Natl. Acad. Sci. U. S. A.* **2003**, *100*, 9105-9107.
(53) Spooner, P. J. R.; Sharples, J. M.; Goodall, S. C.; Seedorf, H.; Verhoeven, M. A.; Lugtenburg, J.; Bovee-Geurts, P. H. M.; DeGrip, W. J.; Watts, A. *Biochemistry* **2003**, *42*, 13371-13378.
(54) Birge, R. R.; Vought, B. W. *Methods Enzymol.* **2000**, *315*, 143–163.
(55) Cooper, A. *FEBS Lett.* **1981**, *123*, 324-326.
(56) Jang, G. F.; Kuksa, V.; Filipek, S.; Bartl, F.; Ritter, E.; Gelb, M. H.; Hofmann, K. P.; Palczewski, K. *J. Biol. Chem.* **2001**, *276*, 26148-26153.
(57) Spooner, P. J. R.; Sharples, J. M.; Goodall, S. C.; Bovee-Geurts, P. H. M.; Verhoeven, M. A.; Lugtenburg, J.; Pistorius, A. M. A.; DeGrip, W. J.; Watts, A. *J. Mol. Biol.* **2004**, *343*, 719-730.
(58) Patel, A. B.; Crocker, E.; Eilers, M.; Hirshfeld, A.; Sheves, M.; Smith, S. O. *Proc. Natl. Acad. Sci. U. S. A.* **2004**, *101*, 10048-10053.

Chapter 5

General Discussion and Outlook

5.1 Introduction

In this thesis some aspects of the spatial and electronic structure that relate to the fast 11-Z to all-E isomerisation process of the retinylidene ligand in rhodopsin have been investigated. The ligand of rhodopsin is 11-Z retinal that is an achiral molecule in solution. The opsin apoprotein binds the ligand covalently to the ε-amino group of a lysine residue in a chiral 12-s-*trans* conformation.[1-3] Nonbonding interactions between the C13 methyl group and the C10 hydrogen that arise as a consequence of the 12-s-*trans* conformation lead to a nonplanar retinylidene.[4] The deviation from planarity leads to torsions distributed over the C10–C11=C12–C13 segment of the chromophore and configure the polyene for fast photoisomerisation.[4,5] A correlation between nonplanarity and efficiency was first illustrated by two examples: the decreased photoisomerisation rate of (i) isorhodopsin[6] and (ii) rhodopsin incorporated with the chemically modified 13-desmethyl retinal[7] (Figure 1.8).

In both examples the absence of intramolecular steric interaction within the respective isomerisation region of the chromphores strongly reduces the rate and efficiency of the photoreaction. To investigate the effect of steric modifications and the resulting torsion in the isomerisation region in more detail, it is useful to study rhodopsin incorporated with ligands that are modified in the isomerisation region, for example by addition of bulky methyl groups at the 11-, 12- and 20-positions of the retinal. The intra- or intermolecular interactions of such modified retinal derivatives may affect the torsion in the isomerisation region in a manner that changes the rate or efficiency of the rhodopsin photoisomerisation.

The electronic properties of the retinylidene chromophore also have an important role in preparing the ligand for efficient photoisomerisation.[8] The electronic properties of polyenes are well studied and it appears that part of the properties of the retinylidene chromophore is intrinsic to the polyene character of the ligand and another part is imposed by the protein environment, which presents charged and polar amino acid residues around the polyene.[9-11] The previous chapters have addressed both the electronic and spatial aspects of the retinylidene ligand in relation to the ultrafast and efficient isomerisation properties. In this final chapter the most relevant outcomes are discussed and an outlook to the future is presented.

5.2 Synthesis of retinal derivatives

The research into the spatial aspects crucially depends on the availability of chemically modified retinal derivatives. The synthesis of the 11-methyl, the 12-methyl and the 11-methyl-13-desmethyl retinal are described in Chapter 2 and 4. The synthesis of 12-methyl retinal is

straightforward and can be performed with the palette of organic chemical reactions that is commonly used in retinoid and carotenoid chemistry.[12-15] During the synthesis of 11-methyl retinal with Wittig or Horner-Wadsworth-Emmons (HWE) reagents, cyclohexadiene products were the major reaction products instead of the linear olefination products that are generally formed in the reaction of a carbonyl and a phosphorus reagent. It has been described that the reaction of a conjugated carbonyl compound with a conjugated phosphorus reagent can lead to a Michael addition followed by an acid-base reaction and subsequent internal Wittig/HWE reaction yielding cyclohexadiene products.[16-18] However, till now no method has been developed to prevent this unwanted reactivity in favour of the linear Wittig or HWE product. In Chapter 2 it is shown that by a rational modification of the reaction scheme the unwanted reaction pathway can be blocked to give the 11-methyl retinal precursor. In particular, the reaction progress of the formation of the cyclohexadiene can be blocked by inhibition of the acid-base reaction with a γ–substitution driving the reaction to the linear Wittig product exclusively. In addition, it appears that working under kinetically controlled conditions can sufficiently suppress the formation of the cyclohexadiene products and only yields the regular Wittig product. Although the Wittig and HWE reactions are often very reliable and successful these novel approaches are useful additions to the synthetic toolbox for unsaturated phosphorus reagents reacting with unsaturated carbonyl compounds.

A synthetic challenge that remains unsolved in Chapter 2 is the reaction between β-ionone and the phosphonate 4-(diethyl phosphono)-3-methyl-2-butenenitrile. It was observed that even at decreased temperature the reaction results in the formation of the cyclohexadiene product. It appears that the threshold temperature for elimination of the phosphorus oxide is too high, leading to a β-oxido adduct in equilibrium with the phosphonate anion and the ketone. In that case the competing Michael addition is not suppressed sufficiently at increased reaction temperatures. It is proposed that working under conditions far from equilibrium will overcome this problem, by analogy with the synthesis of *cis* olefins with Wittig reagents. Extensive research on Wittig reactions in the last 45 years has shown that the application of 'salt-free' conditions or *ortho* substituted Wittig salts leads to *cis* olefines with high selectivity since these methods exclude the epimerisation of the kinetically formed *erythro* adduct before the elimination of the phosphorus oxide.[19,20]

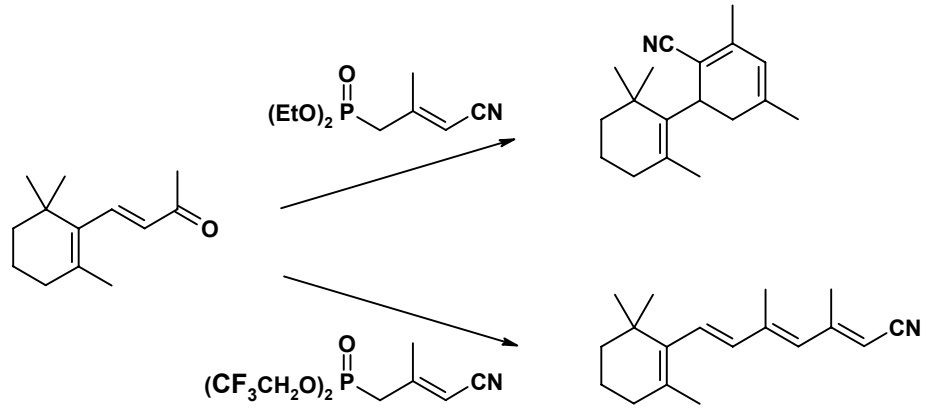

Scheme 5.2 Reaction of β-ionone with a more reactive phospohonate is more likely to lead to a linear product.

For phosphonates this would imply the use of phenyl, trifluoro ethyl or the recently proposed 2-*tert*-butyl phenyl side groups.[21-23] For instance, olefination of β–ionone at low temperature with the 4-(di*trifluorethyl* phosphono)-3-methyl-2-butenenitrile may result in a higher ratio of the linear olefination product 3,5-dimethyl-7-(2,2,6-trimethyl-cyclohex-1-enyl)-hepta-2,4,6-trienenitrile (Scheme 5.2 bottom) to the cyclohexadiene product (top).

5.3 Analysis of the rhodopsin analogues

The 11-Z 11-methyl retinal, 11-Z 12-methyl retinal and 11-Z and 9-Z 11-methyl-13-desmethyl retinal have been incorporated into opsin to form rhodopsin analogues. Photochemical and biochemical experiments have been employed to describe the effect of the methyl substitution pattern on the rate and efficiency of the photochemical reaction. In the past the bulky 11,19-ethano and 11,19-10,20-dimethano retinal have been shown to fit in the binding pocket of rhodopsin.[24,25] The 11,19-ethano rhodopsin that has the C9=C10–C11 part of the polyene locked shows virtually identical isomerisation properties as the native system,[25] which suggests that rotation of the C12H element is sufficient for isomerisation of this ligand. The 11-Z 11-methyl retinal should fit equally well in the protein binding pocket. However, the incorporation is much less efficient than for the ethano and methano derivatives, indicating that the steric interaction in 11-methyl rhodopsin strongly perturbs the conformation. Apparently, the steric interaction of the proximal C9 and C11 methyl groups induces unfavourable torsion in the retinylidene compared to ethano or mehtano ligand. The resulting pigment is irreversibly converted to its first photointermediate with Φ=0.28, much less efficient than for the native rhodopsin. Upon illumination the photointermediates form slowly and lead to a deprotonated

Meta-II-state only at pH<6.0 resulting in a low rate of receptor activation of 29 % of the native activation level.

Except for the increased ability to activate the G-protein, the results of 11-Z 11-methyl-13-desmethyl rhodopsin are comparable with 11-Z 11-methyl retinal. The absence of the 13-methyl group reduces the efficiency of the formation of the first photoproduct to Φ=0.18. The transducin activation approaches the native system to 70%. Compared to 13-desmethyl rhodopsin, the absence of the 13-methyl group is partly compensated during the receptor activation stage by the presence of the 11-methyl group. The results of 11-methyl-13-desmethyl isorhodopsin show an additional improvement of the ability to activate the G-protein, which is 110% with respect to rhodopsin. Generally, corresponding rhodopsin and isorhodopsin pigments exhibit the same activation ability, since the same relaxed all-E retinylidene bathorhodopsin is formed. Hence, the 11-methyl-13-desmethyl isorhodopsin is anomalous and the results indicate that the methyl group on C11 produces extensive disruption and structural rearrangement of the protein upon isomerisation, leading to a more active conformation of the receptor.

The incorporation of the 12-methyl ligand is moderately efficient. Optical and vibration spectroscopy and transducin activation experiments indicate that the Meta-I-like state does not convert into a stable Meta-II signalling state. In addition, the 12-methyl Meta-I-like state is unstable towards hydrolysis into opsin and free ligand. The ultrafast primary event of the isomerisation reaction in rhodopsin strongly depends on the rotation of the C12 hydrogen, which is substituted by a methyl group in the 12-methyl rhodopsin analogue.[26] This methyl group has a 15 times higher mass than a hydrogen atom and has at a ~40-45 % longer bond distance that results in an increase of the angular momentum for the rotation during the primary event of the isomerisation. A rough estimate shows that this increase is critical. For a point mass the energy of the rotation is $E=\frac{1}{2}\, I\cdot\omega^2$, where I is the moment of inertia and ω the angular velocity, since $I=m\cdot r^2$ the rotation of the methyl group takes ~30 times more energy. Interestingly, the quantum yield for the 12-methyl pigment is 0.54±0.08, which is close to the native system. It has been suggested that an efficient decay of the photoexcited rhodopsin takes place *via* a fast and coherent pathway over the excited state surface. It is expected that such a path is available only when bond extension of the C11=C12 bond is accompanied by fast torsional motion in the extended double bond. The data suggest that the fast rotation in 12-methyl rhodopsin is provided by the C11 hydrogen instead. It is therefore proposed that also for native rhodopsin the C11H element can be involved in a rotation during ultrafast isomerisation. Hence, 2×90° counter rotation of the C11 and the C12 hydrogens may lead to the required *trans* position of in the

HC11=C12H segment in Batho. The Raman spectra of rhodopsin and bathorhodopsin show intense reorganisation energies for the C11H and C12H moieties and steric constraints in the protein X-ray structure allow this mechanism to occur.

5.4 Electronic structure of the retinylidene in rhodopsin

The investigation presented in Chapter 3 demonstrates that the availability of a 10-fold ^{13}C-labelled retinal with labels in the tail end offers the opportunity to make a snapshot of the electronic structure of the polyene of the ligand. In previous work dedicated organic synthesis efforts and sample preparation followed by solid-state NMR experiments led to the measurement of the chemical shift of one specific atom in every set of experiments.[27] In particular the development of 2-D dipolar correlation spectroscopy in solid-state NMR made this tedious procedure obsolete, allowing the detection of many chemical shifts in one experiment.[28] Consequently, the synthesis of one multispin labelled ligand is sufficient to probe the electronic structure, which is a leap forward. The same procedure has been extended recently for rhodopsin and for the ligand of the histamine H-1 receptor.[3,29] Further development of solid-state NMR methods recently produced the first sequential assignment of small proteins, aided by specially designed specific labelling patterns.[30-32] For the research of receptor proteins this means that the discovery of essential information on binding properties of natural or artificial agonists or antagonists is possible in a much shorter time. The design of improved ligands for receptors aided by these NMR methods may lead to rational design of drugs, provided that synthetic routes to labelled or modify ligands are available.[33]

For the specific case of the retinylidene ligand in rhodopsin the NMR results help to resolve the mechanism of the ultrafast isomerisation reaction. Measurement of the chemical shift data in this study corroborated the prediction in theoretical calculations that a conjugation defect is present in the polyene.[26] The interpretation presented in this work indicates that, compared to the neutral and unpolarised reference compound 11-Z β–carotene, the positive charge that is formally located on the Schiff base nitrogen has moved into the polyene, in such a way that the C13 atom has the highest positive charge density, slightly higher than C15. It is shown that as much as +0.5 of the total of +1 charge of the protonated Schiff base is delocalised over the carbons in the retinylidene tail. The electron-phonon interaction is the main interaction in polyenes, which establishes a relationship between the electronic and spatial structure.[9,10] In particular, the bond lengths around a positive charge in a polyene exhibit a conjugation defect in which double bonds are extended and single bonds are contracted. This relationship provides a

link between the distances observed in DFT calculations and the chemical shift data. Hence the chemical shift data indicate that the extension of C=C bonds and contraction of C–C bonds takes place in the retinylidene chromophore with a conjugation defect at C13 as predicted by DFT.[26]

A linear relationship between the positive charge that is established at the odd numbered carbon atoms of the polyene during protonation of the Schiff base and the strength of the counterion was found in Chapter 3. These results indicate that the counterion of the protonated Schiff base in rhodopsin is very soft, in agreement with the complex counterion model.[34] A neat linearity indicates that the amount of positive charge on odd-numbered atoms of the retinylidene depends predominantly on the strength of the anion and that no other charges are in play. Recent work of Mathies *et al.* confirms that except for the Glu113 counterion the amino acid residues in the binding pocket close to the isomerisation region of the polyene are uncharged.[35]

Recent progress in the field of solid-state NMR offers the possibility to measure carbon-carbon distances accurately.[36] With this method the bond lengths can be estimated with an accuracy of 0.020 Å, which is accurate enough to observe the difference between single and double bonds and to measure the extent of the conjugation defect. Whereas in the all-E protonated Schiff base crystals the C11=C12 bond of ~1.32Å appears shorter than the C13=C14 bond at ~1.35 Å, in rhodopsin both these bonds are 1.37Å long.[36,37] The change in the C11=C12 bond is partly due to the configurational difference around the C12–C13 bond. At the same time the C–C bonds contract ~0.02 Å, except for the C14–C15 bond that extends slightly due an extended delocalisation. These results confirm that the defect has settled well into the polyene.

The chemical shift data in Chapter 3 reveal for the odd-numbered carbon atoms a strong correlation with the optical spectroscopic properties of the polyene and confirm that a soft complex counterion facilitates an extended charge delocalisation. In contrast, a correlation between the even-numbered carbons and the atomic charge density could not be established. Moreover, the chemical shift response to the delocalisation appears attenuated at the even numbered atoms. Unpublished results on the alternation of the scalar coupling in rhodopsin show a similar trend.[38] Here, the alternation of the coupling over the polyene single and double bonds is clearly present and increases going from the protonated Schiff base model to rhodopsin. However, the difference in the coupling over the double bonds within one species is insignificantly small. It appears that the double bonds are less sensitive to changes in chemical environment than the single bonds. This phenomenon is not yet understood and not consisted with the outcome of the DFT calculations. Further research into the mechanisms underlying the bond extension/contraction in relation with charge will be needed in the future.

Finally, it is concluded that the knowledge of the spatial and electronic structure of the retinylidene ligand in rhodopsin leads to a comprehensive view on the isomerisation mechanism. Future research on the electron-lattice interaction in the retinylidene polyene on the one hand and the ligand-protein interactions on the other hand may reveal the driving force of the fast isomerisation reaction. The tight packing and the specific arrangement of protein residues around C11 and C12 suggest that the protein pocket plays an important role in guiding the atoms of the chromophore to a *trans* position of the C11=C12 motif. In the future a more detailed structural description of the retinylidene chromophore and also the primary photoproduct bathorhodopsin may help to resolve these mechanistic aspects of the isomerisation. In addition, the structure and position of the ligand in Metarhodopsin-II may lead to better understanding of the structural rearrangements that occur during activation of rhodopsin and a general picture for activation of GPRCs may emerge. Ultimately, the combined approach of synthesis and spectroscopic techniques can reveal fundamental aspects of the interplay of the electronic properties and the spatial arrangement of the ligand and may ultimately allow a more profound understanding of the activation of GPCRs, in addition to knowledge about the ultrafast and efficient isomerisation of the retinylidene chromophore in rhodopsin.

REFERENCES

(1) Verdegem, P. J. E.; Helmle, M.; Lugtenburg, J.; De Groot, H. J. M. *J. Am. Chem. Soc.* 1997, *119*, 169-174.
(2) Spooner, P. J. R.; Sharples, J. M.; Goodall, S. C.; Bovee-Geurts, P. H. M.; Verhoeven, M. A.; Lugtenburg, J.; Pistorius, A. M. A.; DeGrip, W. J.; Watts, A. *J. Mol. Biol.* 2004, *343*, 719-730.
(3) Creemers, A. F. L.; Kiihne, S.; Bovee-Geurts, P. H. M.; DeGrip, W. J.; Lugtenburg, J.; De Groot, H. J. M. *Proc. Natl. Acad. Sci. U. S. A.* 2002, *99*, 9101-9106.
(4) Verdegem, P. J. E.; Bovee-Geurts, P. H. M.; DeGrip, W. J.; Lugtenburg, J.; De Groot, H. J. M. *Biochemistry* 1999, *38*, 11316-11324.
(5) Bifone, A.; De Groot, H. J. M.; Buda, F. *Pure Appl. Chem.* 1997, *69*, 2105-2110.
(6) Schoenlein, R. W.; Peteanu, L. A.; Wang, Q.; Mathies, R. A.; Shank, C. V. *J. Phys. Chem.* 1993, *97*, 12087-12092.
(7) Kochendoerfer, G. G.; Verdegem, P. J. E.; Van der Hoef, I.; Lugtenburg, J.; Mathies, R. A. *Biochemistry* 1996, *35*, 16230-16240.
(8) Michl, J.; Bonacic-Koutecký, V. *Electronic Aspects of Organic Photochemistry*; John Wiley: New York, 1990.
(9) Lu Yu *Solitons & polarons in conducting polymers*; World Scientific Press: Singapore, 1988.
(10) Su, W. P.; Schrieffer, J. R.; Heeger, A. J. *Phys. Rev. B* 1980, *22*, 2099-2111.
(11) Pople, J. A.; Walmsley, S. H. *Mol. Phys.* 1962, *5*, 15-20.
(12) *Carotenoids Volume 2: Synthesis*; Britton, G., Ed.; Birkhäuser Verlag: Basel, 1996.
(13) Creemers, A. F. L.; Lugtenburg, J. *J. Am. Chem. Soc.* 2002, *124*, 6324-6334.
(14) Lugtenburg, J. *Pure Appl. Chem.* 1985, *57*, 753-762.

(15) Lugtenburg, J.; Creemers, A. F. L.; Verhoeven, M. A.; van Wijk, A. A. C.; Verdegem, P. J. E.; Monnee, M. C. F.; Jansen, F. J. H. M. *Pure Appl. Chem.* 1999, *71*, 2245-2251.
(16) Dauben, W. G.; Ipaktsch.J *J. Am. Chem. Soc.* 1973, *95*, 5088-5089.
(17) Bohlmann, F.; Zdero, C. *Chem. Ber.* 1973, *106*, 3779-3787.
(18) Padwa, A.; Brodsky, L. *J. Org. Chem.* 1974, *39*, 1318-1320.
(19) Wang, Q.; El Khoury, M.; Schlosser, M. *Chem.-Eur. J.* 2000, *6*, 420-426 and references therein.
(20) Wang, Q.; Deredas, D.; Huynh, C.; Schlosser, M. *Chem.-Eur. J.* 2003, *9*, 570-574 and references therein.
(21) Still, W. C.; Gennari, C. *Tetrahedron Lett.* 1983, *24*, 4405-4408.
(22) Ando, K. *Tetrahedron Lett.* 1995, *36*, 4105-4108.
(23) Touchard, F. P. *Eur. J. Org. Chem.* 2005, 1790-1794.
(24) Personal communication P. H. M. Bovee-Geurts and W. J. DeGrip
(25) Sheves, M.; Albeck, A.; Ottolenghi, M.; Boveegeurts, P. H. M.; DeGrip, W. J.; Einterz, C. M.; Lewis, J. W.; Schaechter, L. E.; Kliger, D. S. *J. Am. Chem. Soc.* 1986, *108*, 6440-6441.
(26) Buda, F.; De Groot, H. J. M.; Bifone, A. *Phys. Rev. Lett.* 1996, *77*, 4474-4477.
(27) Smith, S. O.; Palings, I.; Miley, M. E.; Courtin, J.; De Groot, H. J. M.; Lugtenburg, J.; Mathies, R. A.; Griffin, R. G. *Biochemistry* 1990, *29*, 8158-8164.
(28) Bennett, A. E.; Ok, J. H.; Griffin, R. G.; Vega, S. *J. Chem. Phys.* 1992, *96*, 8624-8627.
(29) Ratnala, V. R. P.; Hulsbergen, R. B.; De Groot, H. J. M.; DeGrip, W. J. *Inflamm. Res.* 2003, *52*, 417-423.
(30) van Gammeren, A. J.; Buda, F.; Hulsbergen, F. B.; Kiihne, S.; Hollander, J. G.; Egorova-Zachernyuk, T. A.; Fraser, N. J.; Cogdell, R. J.; De Groot, H. J. M. *J. Am. Chem. Soc.* 2005, *127*, 3213-3219.
(31) van Gammeren, A. J.; Hulsbergen, F. B.; Hollander, J. G.; De Groot, H. J. M. *J. Biomol. NMR* 2004, *30*, 267-274.
(32) Castellani, F.; van Rossum, B.; Diehl, A.; Schubert, M.; Rehbein, K.; Oschkinat, H. *Nature* 2002, *420*, 98-102.
(33) De Groot, H. J. M. *Curr. Opin. Struct. Biol.* 2000, *10*, 593-600.
(34) Creemers, A. F. L.; Klaassen, C. H. W.; Bovee-Geurts, P. H. M.; Kelle, R.; Kragl, U.; Raap, J.; DeGrip, W. J.; Lugtenburg, J.; De Groot, H. J. M. *Biochemistry* 1999, *38*, 7195-7199.
(35) Yan, E. C. Y.; Ganim, Z.; Kazmi, M. A.; Chang, B. S. W.; Sakmar, T. P.; Mathies, R. A. *Biochemistry* 2004, *43*, 10867-10876.
(36) Carravetta, M.; Zhao, X.; Johannessen, O. G.; Lai, W. C.; Verhoeven, M. A.; Bovee-Geurts, P. H. M.; Verdegem, P. J. E.; Kiihne, S.; Luthman, H.; De Groot, H. J. M.; DeGrip, W. J.; Lugtenburg, J.; Levitt, M. H. *J. Am. Chem. Soc.* 2004, *126*, 3948-3953.
(37) Elia, G. R.; Childs, R. F.; Britten, J. F.; Yang, D. S. C.; Santarsiero, B. D. *Can. J. Chem.* 1996, *74*, 591-601.
(38) Lai, W. C.; McLean, N.; Verhoeven, M. A.; Gansmüller, A.; Antonioli, G. C.; Carravetta, M.; Duma, L.; Bovee-Geurts, P. H. M.; Johannessen, O. G.; De Groot, H. J. M.; Lugtenburg, J.; Emsley, L.; Brown, S. P.; Brown, R. C. D.; DeGrip, W. J.; Levitt, M. H., *submitted*.

List of abbreviations

1-D	one-dimensional
2-D	two-dimensional
Batho	bathorhodopsin
cGMP	guanosine-3',5'-monophosphate
CP	cross-polarisation
CW	continuous wave
Cys	cysteine
DCM	dichloromethane
DDM	dodecyl maltoside
DFT	density functional theory
DIBAl-H	diisobutylaluminium hydride
DTE	dithioerythritol
EDTA	ethylenediamine N,N,N',N'-tetraacetate
FID	free induction decay
FTIR	Fourier transform infrared
FTOA	Fourier transform optical absorption
GDP	guanosine-5'-diphosphate
Glu	glutamate
GPCR	G-protein coupled receptor
GTP	guanosine-5'-triphosphate
GTP-γ-S	guanosine-5'-(3-O-thio)triphosphate
HEPPS	3-[4-(2-hydroxyethyl)-1-piperazinyl]propanesulfonic acid
HOMO	highest occupied molecular orbital
HOOP	hydrogen-out-of-plane
HPLC	high performance liquid chromatography
HWE	Horner-Wadsworth-Emmons
LDA	lithium diisopropyl amide
Lumi	lumirhodopsin
LUMO	lowest unoccupied molecular orbital
Lys	lysine
MAS	magic angle spinning

Meta-I/II	Metarhodopsin-I/II
NMR	nuclear magnetic resonance
NOE	nuclear Overhauser effect
PDE	phosphodiesterase
PE	petroleum ether
Phe	Phenylalanine
Pipes	piperazine-1,4-bis(2-ethanesulfonic acid)
PSB	protonated Schiff base
QM/MM	quantum mechanics / molecular dynamics
SB	Schiff base
SSNMR	solid-state nuclear magnetic resonance
THF	tetrahydrofuran
Thr	threonine
TLC	thin layer chromatography
TPPM	two pulse phase modulation
UV-Vis	ultraviolet-visible
R^2	rotational resonance
RFDR	radio frequency driven dipolar recoupling
Rho	rhodopsin
RR	resonance Raman

Summary

Rhodopsin is the protein in the retina of vertebrates responsible for dim light or black and white vision. The protein functions as a light-driven molecular switch that sets off a cascade of biochemical reactions ultimately leading to a nerve pulse to the brain. Rhodopsin is a member of the superfamily of G-protein coupled receptors that play an important role in signalling processes in living organisms. Around 40 % of the prescription medicine used today intervene in pathways that involve G-protein coupled receptors, which indicates the importance of studying these receptors.

For its function rhodopsin relies on the co-factor 11-Z retinal (vitamin-A aldehyde) that is covalently bound to lysine residue 296 *via* a protonated Schiff base linkage. In its dark-adapted state this retinylidene chromophore has the 11-Z configuration, upon capture of a photon the *cis* C11=C12 bond of the retinylidene chromophore isomerises to a *trans* configuration leading to the transformation of rhodopsin to the photoproduct Bathorhodopsin. This isomerisation reaction is finished within 200 fs and occurs with a quantum efficiency of Φ=0.67. Electronic and spatial properties of the retinylidene chromophore have an important role in preparing the ligand for efficient photoisomerisation. For instance, the protein binds the ligand in the 12-s-*trans* conformation and subsequent nonbonding interactions between the C13 methyl group and the C10 hydrogen give rise to a nonplanar structure. The resulting torsions in the chromophore are thought to configure the polyene for fast photoisomerisation around the C11=C12 double bond. The electronic properties of the retinylidene chromophore are on the one hand intrinsic to the polyene character of the ligand and on the other hand imposed by the protein environment that presents charged and polar amino acid residues around the polyene. The aim of this thesis is to investigate and discuss the spatial and electronic properties of the retinylidene chromophore in relation to the fast and efficient photoisomerisation reaction of rhodopsin.

Chapter 2 deals with the synthesis of 11-methyl and 11-methyl-13-desmethyl retinal. During the synthesis of 11-methyl retinal a conjugated Horner-Wadsworth-Emmons reaction was observed leading to cyclohexadiene products in analogy with the previously described conjugated Wittig reaction. Two methods to suppress the formation of the cyclohexadiene products are investigated and described: (i) Methyl substitution of the γ-position with respect to the phosphorus atom in the Wittig or Horner-Wadsworth-Emmons reagent, which blocks the progress of the pathway to the cyclohexadiene product and (ii) execution of the reaction at low

temperature, which favours the product formation *via* a kinetic pathway and leads to the normal linear olefination reaction. The 11-Z and 9-Z isomers of 11-methyl and 11-methyl-13-desmethyl retinal have been prepared using these two methods.

Chapter 3 describes the electronic ground state of the retinylidene chromophore in rhodopsin. 11-Z-[8,9,10,11,12,13,14,15,19,20-$^{13}C_{10}$]-retinal has been incorporated in opsin to yield rhodopsin in its natural membrane environment. 1-D and 2-D correlation experiments with solid-state NMR have led to the assignment of the response from the 10-fold labelled chromophore. Comparison of the chemical shifts of 3 model compounds in solution with data for rhodopsin has resulted in an interpretation at various levels. In particular, evaluation of the chemical shift difference with a protonated 11-Z retinylidene Schiff base model reveals the effect of the protein environment on the chemical shift or 'opsin shift'. The results show that the protein environment presents an extremely soft counterion, resulting in an extended delocalisation of the positive charge into the polyene. Assessment of the chemical shift difference of rhodopsin compared to an unprotonated Schiff base shows the effect of protonation on the polyene. The positive charge that is formally located on the nitrogen is delocalised into the polyene leading to positive charge density on the odd-numbered atoms, while Coulomb interaction leads to negative charge on the even-numbered atoms. This leads to a pattern of carbon atoms with alternating positively and negatively charge density that is characteristic for charged polyenes. In the retinylidene the charge alternation is tapering off towards the ionone ring. The chemical shift difference between the retinylidene in rhodopsin and the uncharged and unpolarised model compound 11-Z β-carotene reveals that a charge defect is stabilised at the Schiff base end of the polyene, which confirms the prediction of this defect by *in silico* DFT experiments. This autolocalised defect appears to facilitate the fast isomerisation properties of the chromophore since it leads to bond extension and contraction of the double and single bonds, respectively close to the isomerisation region, which is necessary for isomerisation. The cumulative chemical shifts at the odd-numbered carbons of 11-Z protonated Schiff base models relative to the unprotonated Schiff base can be used to measure the extent of delocalisation of positive charge into the polyene. For a series of 11-Z protonated Schiff base models and rhodopsin it appears that the cumulative chemical shifts correlate linearly with the frequency of maximum visible absorption. Since the cumulative shift for rhodopsin is larger than for the model compounds the data contribute to existing and converging spectroscopic evidence for a complex counterion stabilising the protonated Schiff base in the binding pocket.

In Chapter 4 investigations about the protein-ligand interactions, photoisomerisation and receptor activation of the rhodopsin analogues resulting from incorporation of 11-Z 11-methyl, 11-Z 12-methyl and 11-Z and 9-Z 11-methyl-13-desmethyl retinal into opsin are described. UV-Vis and FTIR spectroscopy and a G-protein activation assay are used to resolve details of the ligand-receptor communication and photoactivation for the native pigment of the receptor and for its photointermediates. The results indicate that the formation of the first photointermediate is slowed down by the presence of an 11-methyl substituent, while for the 12-methyl substituent a bathorhodopsin-like intermediate is formed reversibly and with Φ=0.54±0.08, nearly as efficient as in the native pigment (Φ=0.67). These results suggest that counter rotation of the C11H and C12H elements of the polyene lead to the required *trans* position in bathorhodopsin, in contrast with a rotation of C12H only. In addition, the data in this study show that, compared to the native system 11- or 12-methyl modification of the retinylidene chromophore leads to a lower incorporation efficiency, delays the formation of the late photointermediates and finally yields a low activity state of the receptor (<30%). The removal of the 13-methyl group in 11-methyl-13-desmethyl rhodopsin partly compensates for these effects. The receptor activation data suggest that pronounced spatial perturbations of the protein in the vicinity of an extracellular loop triggered by the relaxation of the distorted retinylidene ligand produce a more disordered protein that crosses the energy barrier towards the active receptor conformation more easily.

Finally, the general discussion and outlook in Chapter 5 put the results and conclusions presented in this thesis in perspective with recent findings and discusses directions for future research.

Samenvatting

Staafjes en kegeltjes vormen de lichtgevoelige laag achter in het oog die verantwoordelijk is voor het omzetten van licht dat van een object afkomt naar informatie die in de hersenen een beeld van dat object vormen. Het oog bevat ongeveer 3 miljoen kegeltjes (3 megapixels) voor het waarnemen van kleur indien er voldoende licht is en 100 miljoen staafjes (100 megapixels) voor het waarnemen van zwart-wit beelden in de schemering. Rodopsine is het actieve bestanddeel in de staafjes en werkt als een lichtgevoelige schakelaar. Indien licht de schakelaar op 'aan' zet, wordt een cascade van biochemische reacties in werking gezet die uiteindelijk resulteert in een zenuwpulsje naar de hersenen. Dit proefschrift handelt over de interactie van het eiwit rodopsine met zijn ligand retinal die samen verantwoordelijk zijn voor de eerste stap van het zien.

Retinal (vitamine-A aldehyde) dat chemisch gebonden is aan rodopsine, is verantwoordelijk voor de activering van het eiwit. Rodopsine bindt retinal in de 11-Z-configuratie via een geprotoneerde Schiffse-base met een amine van het eiwit. Eén foton kan de op deze manier gevormde 11-Z-retinylideen-chromofoor isomeriseren naar de all-E vorm. Deze eerste stap vindt plaats binnen 200 femtoseconden en is met een kwantumopbrengst van Φ=0.67 één van de meest efficiënte reacties bekend in de natuur. Naast het onderzoek naar de specifieke eigenschappen van rodopsine, is het hier gepresenteerde onderzoek ook belangrijk, omdat deze receptor de meeste prominente vertegenwoordiger is van de familie van G-eiwit-gekoppelde receptoren. Deze groep van receptoren speelt een belangrijke rol bij het doorgeven van biochemische signalen in alle levende wezens. Het belang van het onderzoek aan rodopsine wordt onderstreept door het feit dat van alle voorgeschreven medicijnen ~40 % aangrijpt op G-eiwit-gekoppelde receptoren.

De elektronische en ruimtelijke eigenschappen van het retinylideen-ligand spelen een belangrijke rol bij het mogelijk maken van de snelle en efficiënte fotoreactie. Een voorbeeld hiervan is dat het eiwit het retinal-ligand bindt in de 12-s-*trans*-conformatie. Hierdoor onstaat in het ligand intramoleculaire sterische interactie tussen het waterstofatoom aan C10 en de methylgroep aan C13. Het gevolg van de sterische interactie is dat het koolstofframe wordt getordeerd rond de C11=C12-binding. Men denkt dat de aanwezigheid van deze torsies bijdragen aan de snelle en efficiënte isomerisatie. Het doel van dit proefschrift is om de rol van de elektronische en ruimtelijke eigenschappen van de retinylideen-ligand te onderzoeken en te bespreken in relatie tot de snelle en efficiënte isomerisatie.

Voor het onderzoek naar de ruimtelijke eigenschappen van het retinylideen-ligand in rodopsine is het van belang om te beschikken over chemisch gemodificeerde retinal-liganden. In Hoofdstuk 2 wordt de synthese van de 9-Z en 11-Z isomeren van 11-methyl en 11-methyl-13-desmethylretinal besproken. Tijdens de synthese van 11-methylretinal werd een geconjugeerde Horner-Wadsworth-Emmons-reactie waargenomen die leidt tot de vorming van een cyclohexadiëen-product, analoog aan de eerder waargenomen geconjugeerde Wittig-reactie. Twee methoden om de vorming van het cyclohexadiëen-product tegen te gaan worden besproken: (i) het aanbrengen van een methylsubstituent op de γ-positie van het Wittig- of fosfonaatreagens, hetgeen de vorming van het ongewenste cyclohexadiëen-product blokkeert doordat de noodzakelijk zuur-base-reactie niet kan plaatsvinden. (ii) het uitvoeren van de reactie bij lage temperatuur, waardoor de reactie verloopt onder kinetisch gecontroleerde omstandigheden, hetgeen leidt tot een normaal lineair Wittig-product.

Hoofdstuk 3 beschrijft 1-D en 2-D vaste-stof-NMR-experimenten aan rodopsine geïncorporeerd met 10-voudig gelabeld 11-Z-[8,9,10,11,12,13,14,15,19,20-$^{13}C_{10}$]-retinal. Deze experimenten geven een beschrijving van de elektronische grondtoestand van de retinylideen-chromofoor. Vergelijking van de chemische verschuiving van 3 modelverbindingen in oplossing met de data van rodopsine leiden tot een interpretatie op drie verschillende niveaus. Ten eerste tonen de verschillen in de chemische verschuiving tussen een 11-Z-geprotoneerde Schiffse-base model en rodopsine aan wat het effect van de eiwitomgeving is. Het blijkt dat het tegenion dat aanwezig is in het eiwit extreem zacht is. Dit resulteert in additionele delokalisatie van de positieve lading naar de koolstofatomen rond de isomerisatiegevoelige C11=C12 binding. Ten tweede wordt het effect van protonering van de retinylideen-polyeen duidelijk door vergelijking van de NMR-data van een ongeprotoneerde 11-Z-Schiffse-base met rodopsine. De positieve lading in rodopsine die formeel op de stikstof zit, wordt gedelokaliseerd over de oneven genummerde koolstofatomen, terwijl even genummerde koolstofatomen negatieve lading krijgen door Coulomb-interacties. Dit leidt tot een patroon van alternerend positieve en negatieve lading dat karakteristiek is voor geladen polyeenfragmenten. In rodopsine zwakt dit patroon af gaande van de Schiffse-base naar de iononering. Als laatste toont het verschil tussen de chemische verschuiving van het ongeladen en niet-gepolariseerde model 11-Z-caroteen dat er een conjugatiedefect aanwezig is in de chromofoor van rodopsine. Dit bevestigt het bestaan van dit defect dat eerder werd aangetoond met behulp van geavanceerde computerberekeningen. Er zijn sterke aanwijzingen dat de ultrasnelle isomerisatie vereenvoudigd wordt door de aanwezigheid van dit conjugatiedefect doordat het leidt tot contractie en extensie van de bindingen, hetgeen

essentieel is voor isomerisatie. De cumulatieve chemische verschuiving op de oneven genummerde koolstofatomen met als ijkpunt de ongeladen Schiffse-base, zijn een indicatie voor de mate van delokalisatie van positieve lading. Voor een serie van geprotoneerde Schiffse-basen met verschillende anionen in oplossing is de totale positieve lading in de polyeen evenredig met de verschuiving van het optisch absorptiemaximum. In het geval van rodopsine ligt de cumulatieve chemische verschuiving duidelijk buiten het gebied van de geprotoneerde Schiffse-basen in oplossing, waarmee wordt bevestigd dat een complex tegenion de positieve lading van de geprotoneerde Schiffse-base stabiliseert.

In Hoofdstuk 4 wordt het onderzoek naar de eiwit-ligandinteracties, foto-isomerisatiereacties en activering van de receptor van rodopsine-analoga beschreven. Met behulp van UV-Vis en Fourier-Transform IR-spectroscopie en G-eiwit-activeringsmetingen zijn rodopsine-analoga geïncorporeerd met 11-Z-11-methyl- en 12-methylretinal en 9-Z- en 11-Z-11-methyl-13-desmethylretinal onderzocht. De resultaten moeten een beeld geven van de interactie tussen het eiwit en het retinal-ligand in de bindingsholte en de manier waarop de activering van rodopsine plaatsvindt. Het blijkt dat de aanwezigheid van een methylgroep op de C11-positie de vorming van het eerste foto-intermediair vertraagt, terwijl in een rodopsine-analoog met een methylgroep op de C12-positie de vorming van een bathorodopsine-achtig intermediair reversibel plaatsvindt met een kwantumefficiëntie van Φ=0.54±0.08, dit is bijna even efficiënt als natief rodopsine (Φ=0.67). De resultaten doen vermoeden dat een tegengestelde rotatie van het C11H- en C12H-fragment van de retinylideen-chromofoor verantwoordelijk is voor het bereiken van de *trans*-positie in bathorodopsine, in tegenstelling tot een rotatie van enkel het C12H-fragment. Verder tonen de resultaten dat in dit hoofdstuk dat de modificatie op de 11- en 12-positie van de retinylideen-ligand leiden tot een lagere incorporatie van het ligand, een vertraagde vorming van de latere foto-intermediairen en uiteindelijk leiden tot een lagere G-eiwit-activeringscapaciteit (<30%). Het verwijderen van de methylgroep van de C13-positie in 11-methyl-13-desmethylrodopsine heft de waargenomen effecten gedeeltelijk op. De data van de receptor-activeringsexperimenten suggereren dat een hoge mate van verstoring van de interne eiwitstructuur in de omgeving van een naar binnengevouwen extracellulaire lus als gevolg van de relaxatie van de getordeerde ligand, leidt tot een eenvoudiger transitie van het eiwit naar de geactiveerde receptorvorm.

In Hoofdstuk 5 worden de resultaten van de voorgaande hoofdstukken nogmaals besproken en in perspectief geplaatst met recente ontwikkelingen in het veld. Tevens wordt een visie gepresenteerd op mogelijk toekomstig onderzoek.

List of publications

1. Lugtenburg, J.; Creemers, A. F. L.; Verhoeven, M. A.; van Wijk, A. A. C.; Verdegem, P. J. E.; Monnee, M. C. F.; Jansen, F., Synthesis of C-13-labeled carotenoids and retinoids. *Pure and Applied Chemistry* **1999,** 71, (12), 2245-2251.
2. Wang, Y.; Xu, X. Y.; van Lieshout, M.; West, C. E.; Lugtenburg, J.; Verhoeven, M. A.; Creemers, A. F. L.; van Breemen, R. B., A liquid chromatography-mass spectrometry method for the quantification of bioavailability and bioconversion of beta- carotene to retinol in humans. *Analytical Chemistry* **2000,** 72, (20), 4999-5003.
3. van Lieshout, M.; West, C. E.; Muhilal; Permaesih, D.; Wang, Y.; Xu, X. Y.; van Breemen, R. B.; Creemers, A. F. L.; Verhoeven, M. A.; Lugtenburg, J., Bioefficacy of beta-carotene dissolved in oil studied in children in Indonesia. *American Journal of Clinical Nutrition* **2001,** 73, (5), 949-958.
4. Verhoeven, M. A.; Creemers, A. F. L.; Bovee-Geurts, P. H. M.; DeGrip, W. J.; Lugtenburg, J.; de Groot, H. J. M., Ultra-high-field MAS NMR assay of a multispin labeled ligand bound to its G-protein receptor target in the natural membrane environment: Electronic structure of the retinylidene chromophore in rhodopsin. *Biochemistry* **2001,** 40, (11), 3282-3288.
5. Maeda, A.; Balashov, S. P.; Lugtenburg, J.; Verhoeven, M. A.; Herzfeld, J.; Belenky, M.; Gennis, R. B.; Tomson, F. L.; Ebrey, T. G., Interaction of internal water molecules with the Schiff base in the L intermediate of the bacteriorhodopsin photocycle. *Biochemistry* **2002,** 41, (11), 3803-3809.
6. Pan, D. H.; Ganim, Z.; Kim, J. E.; Verhoeven, M. A.; Lugtenburg, J.; Mathies, R. A., Time-resolved resonance Raman analysis of chromophore structural changes in the formation and decay of rhodopsin's BSI intermediate. *Journal of the American Chemical Society* **2002,** 124, (17), 4857-4864.
7. Petkova, A. T.; Hatanaka, M.; Jaroniec, C. P.; Hu, J. G. G.; Belenky, M.; Verhoeven, M. A.; Lugtenburg, J.; Griffin, R. G.; Herzfeld, J., Tryptophan interactions in bacteriorhodopsin: A heteronuclear solid-state NMR study. *Biochemistry* **2002,** 41, (7), 2429-2437.
8. Spooner, P. J. R.; Sharples, J. M.; Verhoeven, M. A.; Lugtenburg, J.; Glaubitz, C.; Watts, A., Relative orientation between the beta-ionone ring and the polyene chain for the chromophore of rhodopsin in native membranes. *Biochemistry* **2002,** 41, (24), 7549-7555.

9. van Lieshout, M.; West, C. E.; Van de Bovenkamp, P.; Wang, Y.; Sun, Y. K.; van Breemen, R. B.; Muhilal, D. P.; Verhoeven, M. A.; Creemers, A. F. L.; Lugtenburg, J., Extraction of carotenoids from feces, enabling the bioavailability of beta-carotene to be studied in Indonesian children. *Journal of Agricultural and Food Chemistry* **2003,** 51, (17), 5123-5130.
10. Carravetta, M.; Zhao, X.; Johannessen, O. G.; Lai, W. C.; Verhoeven, M. A.; Bovee-Geurts, P. H. M.; Verdegem, P. J. E.; Kiihne, S.; Luthman, H.; de Groot, H. J. M.; DeGrip, W. J.; Lugtenburg, J.; Levitt, M. H., Protein-induced bonding perturbation of the rhodopsin chromophore detected by double-quantum solid-state NMR. *Journal of the American Chemical Society* **2004,** 126, (12), 3948-3953.
11. Maeda, A.; Verhoeven, M. A.; Lugtenburg, J.; Gennis, R. B.; Balashov, S. P.; Ebrey, T. G., Water rearrangement around the Schiff base in the late K (K-L) intermediate of the bacteriorhodopsin photocycle. *Journal of Physical Chemistry B* **2004,** 108, (3), 1096-1101.
12. Spooner, P. J. R.; Sharples, J. M.; Goodall, S. C.; Bovee-Geurts, P. H. M.; Verhoeven, M. A.; Lugtenburg, J.; Pistorius, A. M. A.; DeGrip, W. J.; Watts, A., The ring of the rhodopsin chromophore in a hydrophobic activation switch within the binding pocket. *Journal of Molecular Biology* **2004,** 343, (3), 719-730.
13. Lai, W. C.; McLean, N.; Verhoeven, M. A.; Gansmüller, A.; Antonioli, G. C.; Carravetta, M.; Duma, L.; Bovee-Geurts, P. H. M.; Johannessen, O. G.; de Groot, H. J. M.; Lugtenburg, J.; Emsley, L.; Brown, S. P.; Brown, R. C. D.; DeGrip, W. J.; Levitt, M. H., Accurate measurements of ^{13}C-^{13}C J-couplings by double-quantum solid-state NMR reveal an electronic perturbation of the rhodopsin vhromophore, **2005,** *submitted*.
14. Verhoeven, M. A.; Bovee-Geurts, P. H. M.; Lugtenburg, J.; de Groot, H. J. M.; DeGrip, W. J., Methyl substituents at the 11- or 12-position of retinal profoundly affect photochemistry and function of rhodopsin, *manuscript in preparation.*
15. Verhoeven, M. A., Novel efficient synthesis routes to 11-methyl retinal isomers, *manuscript in preparation*
16. Verhoeven, M. A.; Carlyle, L; Haasnoot, J. G.; Reedijk, J., Study of defects in old masterpiece painting: ^{207}Pb Solid-state NMR on lead(II) carboxylates, *manuscript in preparation*
17. Verhoeven, M. A.; Haasnoot, J. G., Reedijk, J., Lead(II) acetate revisited: Crystal structure and ^{207}Pb Solid-state NMR on lead(II) acetate half hydrate, *manuscript in preparation*

Curriculum Vitae

Michiel Verhoeven werd geboren op 6 oktober 1972 te Malden. Na het behalen van het VWO diploma aan de Nijmeegse Scholengemeenschap Groenewoud begon hij in 1991 met de studie Scheikunde aan de Universiteit van Utrecht. In mei 1997 studeerde hij af in de Vakgroep Fysisch Organische Chemie onder begeleiding van Prof. dr. L.W. Jenneskens op de synthese en karakterisering van *host-guest crown ether*-complexen met een bijvak Enzymologie. In juni dat jaar werd aangevangen met het promotieonderzoek beschreven in dit proefschrift bij de groep Biofysische Organische Chemie onder begeleiding van Prof. dr. H.J.M. de Groot en Prof. dr. W.J. de Grip. De in dit proefschrift beschreven organische synthese is uitgevoerd bij de groep Bio-organische Fotochemie in samenwerking met Prof. dr. J. Lugtenburg.

De resultaten van het onderzoek werden in de vorm van posters gepresenteerd op de *8th International Conference on Retinal Proteins* op Awaji Island in Japan (juni 1998) en verschillende SON bijeenkomsten in Lunteren. Tevens werd het werk mondeling gepresenteerd bij de NMR-Discussiegroep van de KNCV bij DSM Geleen (oktober 2001) en op een HRSMC-bijeenkomst in Amsterdam (januari 2003).

Van september 2003 tot maart 2005 heeft de auteur bij de groep Coördinatie- en Bio-anorganische Chemie van Prof. Dr. J. Reedijk samen met Dr. J.G. Haasnoot gewerkt aan *Coördinatie chemie van loodzepen en -pigmenten in oude verflagen van meesterwerken* binnen het NWO prioriteitsprogramma De Mayerne. In het kader van dit werk werden mondelinge presentaties gegeven bij *11th International Conference on the Co-ordination and Organometallic Chemistry Of Germanium, Tin and Lead* in Santa Fe, New Mexico (juni 2004) en het *De Mayerne programma symposium* georganiseerd door NWO in Amsterdam (november 2004).